Chapter 2
Electrode–Electrolyte Interfacial Processes in Ionic Liquids and Sensor Applications

Xiangqun Zeng, Zhe Wang, and Abdul Rehman

2.1 Introduction

Electroanalytical methods or electrochemical sensors involve a group of quantitative and qualitative methods in which an electric excitation function is applied to an electrochemical cell and a response function is measured. Based on the properties of the applied excitation function, they are categorized as potentiometry, voltammetry, impedance spectroscopy, etc. All these methods require the use of electrodes where the electron-transfer reactions occur and an electrolyte, an ionically conducting medium, to transport charge within the electrochemical cells, to establish the electrochemical contact of all electrodes effectively, and to solubilize the reactants and products for efficient mass transport. Ionic liquids (ILs) are a class of compounds containing organic cations or anions that melt at or near room temperature. They represent a new type of nonaqueous and biphasic electrolytes that combine the benefits of both solid and liquid systems [1–7]. They are shown to have negligible vapor pressure, high ionic conductivity, wide potential window (up to 5.5 V), high heat capacity, and good chemical and electrochemical stability and have been demonstrated as media in electrochemical devices including super-capacitors, fuel cells, lithium batteries, photovoltaic cells, electrochemical and mechanical actuators, and in electroplating [8–10]. The liquid crystalline structure as well as the solvation properties of ILs has their own significance in many of these applications. In the past, ILs are regarded as completely nonvolatile, but the work of Earle et al. has shown that some ILs may be evaporated and recondensed [11]. However, generally speaking, most ILs have zero vapor pressure at room temperature; thus, there is no drying out of the electrolytes presenting many potential benefits for analytical methods and technique developments in comparison to traditional aqueous and nonaqueous electrolytes/solvents.

X. Zeng (✉) • Z. Wang • A. Rehman
Department of Chemistry, Oakland University, Rochester, MI 48309, USA
e-mail: zeng@oakland.edu

A.A.J. Torriero (ed.), *Electrochemistry in Ionic Liquids*,
DOI 10.1007/978-3-319-13485-7_2

It is well known that the maximum efficiency of electrochemical devices depends upon electrochemical thermodynamics, whereas real efficiency depends upon the electrode kinetics. To understand and control electrode reactions and the related parameters at an electrode and solution interface, a systematic study of the kinetics of electrode reactions is required. When ILs are used as solvents and electrolytes, many of the electrochemical processes will be different and some new electrochemical processes may also occur. For example, the properties of the electrode/electrolyte interface often dictate the sensitivity, specificity, stability, and response time, and thus the success or failure of the electrochemical detection technologies. The IL/electrode interface properties will determine many analytical parameters for sensor applications. Thus, the fundamentals of electrochemical processes in ILs need to be studied in order to have sensor developments as well as many other applications such as electrocatalysis, energy storage, and so on. Based on these insights, this chapter has been arranged into three parts: (1) Fundamentals of electrode/electrolyte interfacial processes in ILs; (2) Experimental techniques for the characterization of dynamic processes at the interface of electrodes and IL electrolytes; and (3) Sensors based on these unique electrode/IL interface properties. And in the end, we will summarize the future directions in fundamental and applied study of IL–electrode interface properties for sensor applications.

2.2 Fundamentals of Electrode/Electrolyte Interfacial Processes

Electroanalytical methods and electrochemical sensors are based on changes of electrode–electrolyte interface or the electrochemical reactions occurring at electrode/electrolyte interface for the detection of a specific analyte. The nature of electrode/electrolytic solution interfaces plays a central role in electrochemical surface science. A large number of important reactions take place at the interface between a metal and a solution: metal deposition and dissolution, electron- and proton-transfer reactions, corrosion, film formation, and electro-organic synthesis. If we want to understand and control these processes using ILs, it requires a detailed knowledge of the properties of the electrode/IL interface such as the adsorption of the ILs on electrode surfaces upon the variation of the electric potential, which acts as a driving force for all charge transfer reactions. As shown in Fig. 2.1, a study of electrochemical reaction at an electrode/solution interface is performed in an electrochemical cell. Typically, an electrochemical cell consists of three electrodes. The reference electrode establishes a constant electrical potential and the working electrode is where electrode reaction takes place. The electrical current is expected to flow between the working electrode and the auxiliary electrode, often also called the counter electrode. By holding certain variables of an electrochemical cell constant and applying an external electrical excitation function to the working electrode, information about the analyte can be obtained based on the measurement of how other variables change with the controlled variables. The common electrical

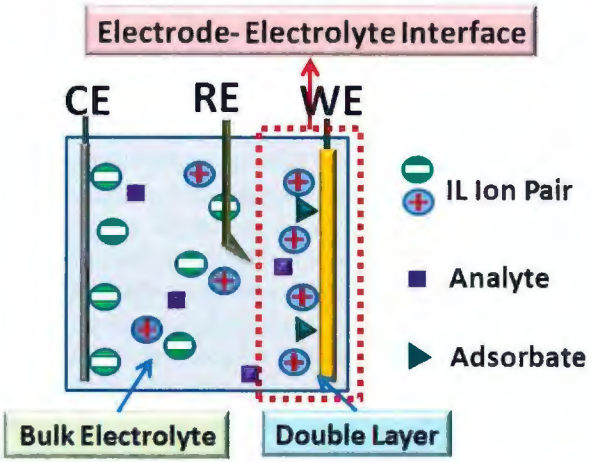

Fig. 2.1 Schematic of electrochemical cell containing the bulk electrolyte, interface and double-layer regions. *CE* counter electrode, *RE* reference electrode, *WE* working electrode

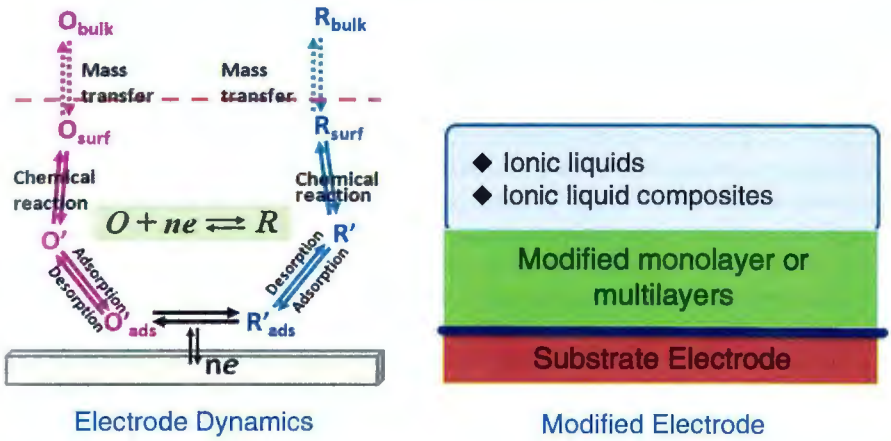

Fig. 2.2 Schematic of electrode processes at IL/electrode interface (*left*) and interfacial structure (*right*) for the electrochemical sensors at IL modified electrodes

excitation parameters are potential, current, and charge. Electrode kinetics for any electrochemical reactions can be controlled by the electrical excitation parameters (e.g., potential). As shown in Fig. 2.2, the electrode reactions typically involve three major steps: (1) Mass transport step (diffusion, diffusion-convection, and migration); (2) Heterogeneous step (charge transfer, adsorption and desorption, nucleation, crystal growth, and surface diffusion); and (3) Homogeneous step (chemical reactions in solution). The rate of an electron-transfer reaction occurring at the electrode/solution interface mainly depends on the electrical potential. However, other

physical processes may also contribute to the overall kinetics of any particular reaction creating complex electrolysis mechanism. The overall reaction rate will be limited by the slowest step. In particular, the mass transport process (i.e., the transport of the reactant molecules to the electrode surface and the removal of the reaction products from electrode interface when formed) plays significant roles for the kinetics of electrode reactions. Chemical reactions at the electrode or in the solution also affect the mechanisms and kinetics of electrode reactions. The chemical reactions involved in electrolysis mechanisms are not only occurring in the homogenous solution phase (e.g., if the products of the electrode reactions are not chemically stable), but a significant range of heterogeneously coupled chemical reactions can also occur. Furthermore, the chemical processes that occur at electrode/electrolyte interface can also be coupled to mass transport. Finally, electrode materials and properties influence electrochemical reactions. For example, the surface area and the geometry of an electrode could influence the current and may also affect the mass transfer process, as in the case of a rotating disk electrode [12] and an ultramicro electrode [13]. Another area of electrode/electrolyte interface is that an electrode can be modified by the immobilization of a layer of material on to its surface so that the surface character of the immobilized material can control the electrode's performance and can be explored for a wide range of applications. The modified surfaces can offer novel properties such as the ability to hold charge (as in battery), induce novel specific reactions, and act as organic semiconductors or chemical/biosensors. The modification of the electrode greatly expands the application of electrochemistry [14–16] such as the enzyme electrodes that are widely used in biosensors and bio-electrochemistry. Thus, electrode–electrolyte interface processes can be complicated, and understanding these processes will enable the selection of the electrode potential, current density, solvent, supporting electrolyte, solution pH, temperature, deliberate modification of electrode surface or addition of other reagents, etc., based on the requirements of a specific application including sensors. Below we will detail the most important processes at electrode/electrolyte interface.

2.2.1 Adsorption

Electrode surface conditions such as roughness and modification are related with the electrochemical active sites and the properties of the electrode/electrolyte interface. Electrode surface conditions also include their single crystal faces. ILs contain organic cations or anions that could adsorb specifically or nonspecifically on the electrode surfaces. The adsorption of organic substances at an electrode/solution interface is of fundamental importance for many chemical and electrochemical processes. For example, adsorption can affect and change the electrode reaction kinetics. Molecules that exhibit structure-sensitive chemisorption are expected to undergo structure-sensitive electrocatalytic reactions. The adsorption of electrochemically active materials could change the peak shape, peak potential, and peak current of a cyclic voltammogram [17]. Depending upon the site of adsorption, electrochemically

active species can be oxidized at different potentials. More complicated adsorption mechanisms exist when surface adsorbed species are not stable in either its charged or uncharged forms, or if they are desorbed during potential cycling. An IL's tremendous diversity in structural and chemical properties will allow various electrode–IL interfaces to be designed to unravel the IL–IL and IL–electrode substrate interaction. Typically, in the case of chemisorptions, the dominant IL–electrode interaction will be due to strong covalent or ionic chemical forces; in the case of physisorption, one often finds that the van der Waals force acting directly between the adsorbates dominates. In this case, the optimum adsorbate–substrate bonding geometry can be overridden by the lateral adsorbate–adsorbate interactions, yielding, for example, incommensurate structures in which the overlayer and the substrate have independent lattices. The IL–IL interactions will include electrostatic interactions, hydrogen bond interactions, orbital-overlapping interactions, and van der Waals interactions. These interactions may be attractive or repulsive depending on the properties of IL and the substrate electrode. Adsorption phenomena in IL–electrode interface are important for understanding the structure of the electric double layer (EDL) and for their various electrochemical applications.

2.2.2 *Electrical Double Layer*

The double-layer model is used to visualize the ionic environment in the vicinity of a charged surface which can be either a metal under potential control or a dielectric surface with ionic groups. It is easier to understand this model as a sequence of steps that would take place near the surface if its neutralizing ions were suddenly stripped away. The double layer formed, in turn, causes an electrokinetic potential between the surface and any point in the mass of the suspending liquid. This voltage difference is on the order of millivolts and is referred to as the often surface potential. The magnitude of the surface potential is related to the surface charge and the thickness of the double layer (Table 2.1).

Table 2.1 The molecular interaction forces present in IL solvents

Type of interaction	The energy equation
Ion–dipole	$U_{\text{ion-solvent}} = -(ze\mu \cos\theta)/(4\pi\varepsilon_0)r^2$
Dipole–dipole	$U_{\text{dipole-dipole}} = -(2\mu_1{}^2\mu_2{}^2)/(4\pi\varepsilon_0)3K_BTr^6$
Dipole-induced dipole	$U_{\text{dipole-induced dipole}} = -(\alpha_1\mu_2{}^2 + \alpha_2\mu_1{}^2)/(4\pi\varepsilon_0)r^6$
Ion-induced dipole	$U_{\text{ion-induced dipole}} = -(z^2e^2\alpha)/(4\pi\varepsilon_0)2r^4$
Dispersion	$U_{\text{dispersion}} = -(3\alpha_1\alpha_2)(I_1I_2)/(I_1+I_2)2r^6$

Symbols: z—the charge of the ion; θ—the dipole angle relative the line joining the ion to the center of dipole; e—electric charge of -1.602×10^{-19} coulomb; I—the ionization potential; ε_0—the vacuum permittivity; r is the separation distance between the charges; q—the charge (assuming equal value of charge on each side of the molecule); α—polarizability of the solvents; K_B—the Boltzmann constant; T—the absolute temperature; μ_i—permanent dipole moment of solvent

ILs are free of solvents; thus, electrostatic interaction is the predominating force between the electrode and IL electrolyte. The electrode may have interactions with dipole moments of the anion and cation functional groups due to the bulky anions or cations of ILs. Even though the IL–electrode interface structure has some similarity to traditional electrode–electrolyte double layer, the IL–electrified metal interface behaves differently from those described by Gouy–Chapman–Sterns double-layer model. The study shows a well-defined structural organization of IL at Au(111) electrode interface with three structurally distinct regions: the interfacial (innermost) layer composed of ions in direct contact with the electrode; the transition region over which the pronounced interfacial layer structure decays to the bulk morphology; and the bulk liquid region where structure depends on the degree of ion amphiphilicity [18]. The innermost layer which templates ion arrangements in the transition zone is much more structured where the ions form a single layer at the surface to screen the electrode charge [19]. AFM results on gold and graphite in various ILs showed that the double layer at IL–electrified metal interface is not one layer thick, thereby extending the transition zone up to five ion pair diameters from the interface [20, 21]. In addition to the Coulombic short range electrostatic interaction, the ions in ILs are often large in size, flexible, highly polarizable, and chemically complex with a number of interionic forces (such as dispersion forces, dipole–dipole interaction, hydrogen bonding, and pi-stacking forces). Steric effects will contribute to the IL–electrode interface structure as well. Moreover, adsorptions of anions and/or cations are likely to occur at the IL–electrode interfaces. The specific adsorption, ion structures and properties, and the applied potential all influence the structure and thickness of the double layer of ILs near metal surface. For example, multiple sterically hindered allylic functional groups could be incorporated to minimize IL–electrode interactions and maximize compressibility of the solvation layers [22–24]. It was reported that the adsorption and dissolution of gas molecules in the IL–electrified metal interface can lead to the change of the double-layer structure and thickness and the change of IL viscosity and the dielectric constant (i.e., less organized arrangement of ILs) [25, 26]. The molecular structure of ILs such as alkyl chain length influences the relative permittivity [27]. Capacitance at a fixed potential will depend on double-layer thickness and permittivity of the liquid at the interface. Consequently, varying the structure of IL anions or cations and applied potential can result in the rearrangement of ions and/or adsorbates that enables the modification of the double-layer structure at the IL–electrified metal interface (e.g., thickness and permittivity) [28–30] and subsequently the modification of the IL double-layer capacitance.

2.2.3 Chemical Reactions

An electron-transfer process at electrode/electrolyte interface can often have two types of chemical reactions. One is the electron-transfer reaction coupled with heterogeneous chemical reactions including those surface adsorption processes that

occur at electrode/electrolyte interface. Another is the electron-transfer reaction-coupled homogeneous reactions such as EC reaction: ($A+ne \leftrightarrow B$; $B \rightarrow$ product), ECE reaction: ($A+ne \leftrightarrow B$; $B \rightarrow C$, $C+ne \leftrightarrow D$), EC′ mechanism ($A+ne \leftrightarrow B$; $B+Y \rightarrow A+$product), where the prime (′) represents a catalytic process. Among these coupled chemical reactions, catalytic reactions are widely sought after since they often represent a clean and efficient method of enhancing chemical reactivity. The reaction mechanisms change with the solvents. In ILs, the electrophilic (Lewis acid) organic ions can be reduced electrochemically at the cathode or chemically by reducing agents ($Q+e \rightarrow Q^{\bullet-}$). On the other hand, many of the nucleophilic (Lewis base) organic ions can be oxidized electrochemically at the anode or chemically by oxidizing agents ($Q \rightarrow Q^{\bullet+}+e$). Here, $Q^{\bullet-}$ and $Q^{\bullet+}$ are radical anion and cation, respectively, and are extremely reactive if their charges are localized. However, if the charges are more or less delocalized, the radical ions are less reactive. The dynamic properties of ILs can have remarkable influences on the potentials of various types of redox couples and on the mechanisms of the electron-transfer processes that occur either heterogeneously at the electrode or homogeneously in the solution. For example, in high-permittive ILs, ILs can easily dissociate into ions. The anion or cation of ILs can form ion-pair complex with the radical cation or anion, respectively. With the decrease in permittivity of ILs, however, complete dissociation becomes difficult. Some part of the IL electrolyte remains undissociated and forms an ion pair ($A^+ + B^- \leftrightarrow A^+B^-$). Ion pairs contribute neither ionic strength nor electric conductivity to the solution. Since there is high concentration of anion and cations in ILs, the formation of triple ions ($A^+ + A^+B^- \leftrightarrow A^+B^-A^+$) and quadruples can also occur. ILs could also play roles as proton donors to lower the energy needed to oxidize the electroactive materials. In summary, the study of redox processes in ILs can be very complex requiring the adaptation of a diverse range of electrochemical and spectroscopic tools to characterize their properties and mechanisms during electron-transfer processes at electrode/electrolyte interface.

2.3 Techniques for Studying Interfacial Properties in ILs

The interfacial properties of IL/electrode interfaces are different from other media (i.e., aqueous or traditional nonaqueous media) because of the unique properties of ILs, especially the electrochemical properties. To understand the electrode/electrolyte interface chemistry for sensor research, the mechanisms of the electrochemical reactions, and the essential performance-limiting factors, both in the bulk and at the surface of the electrode materials need to be investigated, preferably in situ. In situ analysis is much desired due to the fact that ex situ measurements are usually not able to follow the fast kinetics at electrode interfaces. The past decades have been characterized by a spectacular development of in situ techniques for studying interfacial processes at metal electrodes. Radioactive tracer [31, 32], pulse potentiodynamic [33, 34], and galvanostatic methods [35] have been applied quantitatively to study the adsorption of organic compounds at solid metals. In the study of complex

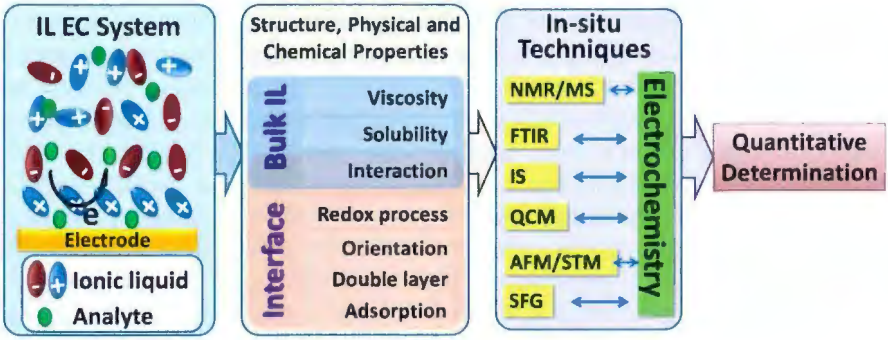

Fig. 2.3 Methods for characterization of IL–electrode interface

electrode reactions, vibrational spectroscopies, such as Raman [36–40], the infrared (IR) [41–43], and UV–vis spectroscopies [44, 45], have been used to identify adsorbed intermediates and the nature of the chemisorption bond [46]. And the electroreflectance spectroscopies [47] have provided information about the orientation of molecules in adsorbed overlayers. X-ray absorption spectroscopies [48, 49] were employed to determine the coordination numbers of adsorbed species and the substrate–adsorbate and adsorbate–adsorbate bond lengths. Ab initio-based computations on the property of electrode materials and continuum modeling have been incorporated to provide theoretical insights and predictions [50, 51]. Finally, the images of adsorbate-covered electrode surfaces have been obtained using scanning tunneling [52–54] and atomic force microscopies [53, 55].

As shown in Fig. 2.3, many of these techniques have also been used to study the IL/electrode interface properties. Baldelli et al. studied the surface structure at the IL–electrified electrode interfaces by SFG [19, 56–58]. And Endres' group use ATM and SPM to investigate the IL interface morphology and interaction force [59, 60]. As expected, their studies show that the IL/Pt electrode interface has a very thin double-layer structure where the ions form a single layer at the surface to screen the electrode charge. However, it is difficult to obtain high-resolution AFM and SFG and to obtain the dynamics of the interfacial structure of IL real time. Difficulties also exist in how to interpret the AFM, electrochemical impedance spectroscopy (EIS), and SFG results. Additionally, these studies were limited to the non-Faradaic region of the electrode where there are no electron-transfer reactions to occur. Below we will illustrate the principles of electrochemical techniques as well as spectroelectrochemical and microscopic methods that have been used for in situ characterization of the electrochemical processes at IL–electrode interfaces. Combining complementary characterization methods in situ can provide mechanistic understanding of interfacial structure, interfacial dynamics, interfacial chemical composition, etc., and enable the development of new analytical methods based on IL chemistry for the identification and quantitative determination of analytes.

2.3.1 Cyclic Voltammetry

Cyclic voltammetry (CV) is a widely used electrochemical technique to study electrochemical reaction mechanisms and the rates of oxidation and reduction processes. In CV, the current at the working electrode is plotted versus the applied potential to give the cyclic voltammogram traces of an analyte in solution. For studying an electrochemical process using CV, a stable supporting electrolyte and good solubility of analyte in the electrolyte is essential. ILs can offer benefits in both these aspects for CV characterizations. The solubility of the redox active materials in ILs would not be a problem due to the availability of a wide range of ILs with desired functionalities to choose from. ILs have high thermal stability. Most of ILs are stable up to 300 °C [61]. However, the electrochemical stability of an IL electrolyte is important for various electrochemical applications.

2.3.1.1 Electrochemical Stability (Electrochemical Potential Window)

The electrochemical stability of nonaqueous electrolytes is crucial for any electrochemical application. The electrolyte must be electrochemically stable up to the high voltage cutoff (the highest voltage at which cell is allowed to operate), and stable down to the lowest voltage cutoff. Typically, electrochemical potential window lies at a voltage range in which the electrolyte is not oxidized or reduced. The electrochemical potential window is a measure of the electrochemical stability of an electrolyte against oxidation and reduction processes. This value, on one hand, characterizes the electrochemical stability of ILs, i.e., the limits of the potential window correspond to the oxidation limits and the reduction limits of the electrochemical decomposition of the involved ions. On the other hand, the width of the electrochemical window governs the range of potentials available for studying the electrochemical processes that will not be affected by the electrolytes and/or the solvents. One of the important considerations in electrochemical characterization of the potential window is the cell design and reference electrode. In order to avoid contamination to the IL electrolytes due to the reference electrode filling solution (e.g., KCl), a quasi-reference electrodes often used are rather than the saturated Ag/AgCl or calomel electrode. The quasi-reference electrode often used is Ag, Au, or Pt thin film or wire. The quasi-reference electrode and the auxiliary electrode are placed far apart so that the product at the counter electrode will not diffuse to the reference electrode which can affect its stability. Compared with different reference electrodes in the same IL system, the width of potential window should be consistent. The change of reference electrode materials only affects the absolute value of potential in most of IL systems. And all of them can be calibrated by using stable redox couple, such as Fc^{+}/Fc. Thus, we can compare the potential windows reported using different quasi-reference electrodes.

The structures of ILs make them more electrochemically inert than other solvents such as H_2O and acetonitrile [62].The electrochemical window in ILs is much larger than that of most conventional aqueous and nonaqueous electrolytes [63].

Table 2.2 Potential windows of common RTILs

RTIL	Potential window (vs. Fc^+/Fc, ±0.2 V)
$[C_2mim][NTf_2]$	−2.6 to 3.0 V
$[C_4mim][CF_3SO_3]$	−2.6 to 2.2 V
$[C_4mim][BF_4]$	−2.8 to 3.2 V
$[C_4mim][PF_6]$	−2.5 to 3.0 V
$[C_4mim][HSO_4]$	−2.5 to 3.0 V
$[C_4mim][Cl]$	−2.5 to 1.5 V
$[C_4mim][NO_3]$	−2.5 to 2.0 V
$[P_{4,4,4,4}][NO_3]$	−2.3 to 2.0 V
$[N_{4,4,4,4}][NO_3]$	−3.5 to 2.0 V
$[N_{6,2,2,2}][NTf_2]$	−3.5 to 3.0 V
$[P_{14,6,6,6}][NTf_2]$	−3.4 to 3.0 V
$[P_{14,6,6,6}][FAP]$	−3.5 to 3.0 V
$[C_4mPy][NTf_2]$	−3.2 to 3.0 V

Table 2.2 lists the potential windows of some commercial ILs, obtained from references [64–67] and also from our own investigations. Here, the purities of all ILs are higher than 95 %. The electrochemical stability of ILs with cations of either quaternary ammonium structures or pyrrolidinium is better than that of imidazolium. However, anion stability is an issue. Halides can be easily oxidized; thus, halides-based ILs have lower electrochemical stabilities. Additionally, the high chemical activity of halides may result in side reactions during the analyte redox process. The fluorine-containing anions (BF_4^- and PF_6^-) are not as stable and can be decomposed in the presence of trace amounts of water producing HF under electrochemical process, although this reaction usually isn't observable during electrochemical study for short time testing, since both B–F and P–F bonds are weaker than C–F bond [68]. Additionally, for most organic anions, the negative charge is delocalized which increases their stability. It denotes that the electrochemical potential window is sensitive to impurities. Schröder and coworkers have reported that ILs such as $[C_4mim][BF_4]$ can rapidly absorb atmospheric water and that the presence of water has a profound effect on cyclic voltammetric experiments with platinum electrodes [69–71]. Any other impurities such as moisture residues from preparation could give an electrochemical signal during CV characterization. Since the purity of ILs affects the accuracy of the potential window measurement, the potential window obtained experimentally can be regarded to have some uncertainty. Theoretically potential window of ILs was basically dominated by the stability of ions. A general trend for the magnitude of the electrochemical oxidative limit is observed as follows: $[P_{14,6,6,6}]^+ > [N_{6,2,2,2}]^+ > [C_n mim]^+ \approx [C_4mPy]^+$ and $[FAP]^- \approx [NTf_2]^- > [BF_4]^- > [PF_6]^- > [MeSO_4]^- > [NO_3]^- > [CF_3SO_3]^-$ [61, 62]. The anodic "breakdown" is presumed to be due to the oxidation of the anionic component of the ILs. In most cases, the stability of the anion determines the anodic potential limits, and stability of the cation determines the cathodic potential limits. But in the practical measurement, the predicted values depend also on the electrode material and current density.

2.3.1.2 Mass Transport

The mass transport of electroactive species plays significant roles in electrode kinetics. The electroactive species can move by diffusion, convection, and migration. The measured mass transport is a combination of these three processes:

1. Migration: movement of charged species under the influence of an electric field.
2. Diffusion: movement of species because of their concentration gradient.
3. Convection: movement of species under the influence of a physical disturbance.

Typically, the contribution of the charged electroactive species which is often in very low concentration to migration process is much smaller than the contribution of inert electrolyte. In conventional electrolyte solutions, ions exist in the form of solvent complexes, and consequently, the solvent molecules are parts of moving ions. As a result, in addition to the flux of ions, there is also a flux of the solvent. This flux leads to the formation of a concentration gradient between the cathodic and anodic compartments during the electrochemical reaction. In the ILs, there is no solvent. ILs can be considered as an excess of inert ions carrying the current; thus, migration of electroactive species can be neglected. In an IL electrolyte, the ionic conduction is related to both the anion and the cation mobility and their transference number. The total cation and anion transference numbers is equal to unity.

$$t_+ + t_- = 1 \tag{2.1}$$

where t_+ and t_- are the transference numbers, depicting the portion of charge carried by cations or anions, respectively. Since ILs have much higher viscosities than common electrochemical supporting electrolytes, they have an effect on the diffusion coefficients of species. A previously reported study compares the diffusion coefficients of a neutral molecule and the radical cation produced after an electrochemical reaction in an IL and acetonitrile. The diffusion coefficient of the cation radical was consistently about half that of the value of the neutral molecule. In contrast, in acetonitrile, the ratio of the diffusion coefficients was nearly 60 % or higher [72], providing an indication that viscosity and charge have considerable effects on the transport of diffusing species in ILs [73–75]. We can consider that mass transport is mainly governed by the diffusion process. In this case, the diffusion coefficients, for both the reduced and oxidized forms of the redox species, can be calculated from the slope of the dependence of the peak current i_p on the square root of the scan rate, according to the Randles–Sevcik equation [76]:

$$i_p = 0.446nFA\left(\frac{nF}{RT}\right)^{1/2} CD^{1/2}v^{1/2} \tag{2.2}$$

The Stokes–Einstein equation [77] is generally applicable for molecular liquids and ILs, at least semi-quantitatively, for analyzing the diffusion coefficient D. Water is ubiquitous in the environment. It was shown that water induced accelerated ion diffusion compared to its effect on neutral species in ionic liquids [78]. We also observed that IL conductivity is significantly increased when [Bmim][BF_4] is

exposed to normal atmosphere for 24 h with 0.25 % wt moisture since fewer cycles are needed to reach a fully conductive polyvinyl ferrocene film [79]. Because of its high molecular weight, the diffusion coefficient of an IL is typically smaller than that of analytes regardless of the medium. However, despite the presence of an additional interaction between the functional group in IL and analytes, this behavior contrasts with the case of a small anion or radical anion; ion-pair formation leads to a marked decrease in the diffusion coefficient.

2.3.1.3 Charging Current in CV

As mentioned before, ILs have a unique double-layer structure, and the double-layer capacitance can be measured by both cyclic voltammetry and EIS. Our studies and others have shown that the capacitance of IL/electrode interface is potential dependent, and the adsorption of gas on the IL/electrode interface will decrease the double-layer capacitance under a specific DC bias potential [80]. In contrast to the EDL typically observed in dilute aqueous or nonaqueous electrolytes, the ions of ILs are strongly oriented near the electrode into an ordered layer structure with local ion density at maximum possible value [81, 82]. Multiple ion pair layers form at the interface of IL and metal electrode. Due to this heterogeneity, the lattice formation at the interface and the subsequent capacitance variations are not monotonic as described by the Gouy–Chapman–Stern's model [83–85]. Additionally, the hysteresis effects of an IL, where the double-layer capacitance depends on the scan direction of the DC potential, contribute to the slow pseudocapacitive process at the IL–electrode interface [86–88]. Since the change of IL orientation due to applied potential is a very slow process, the resulted charging currents only can be observed at a slow scan rate. Figure 2.4 shows that the small CV peaks related to heterogeneous IL orientations were observed in CV at slow scan rates (e.g., 20 mV/s) in the most of studied ILs. These small peaks will contribute to some uncertainty for the current measured, especially for the Faradaic process, under slow scan rates. Consequently, the double-layer charging current will increase the complexity of CV results. In order to obtain accurate Faradaic current measurement, it is recommended that the peak current of electrochemical processes should be measured under the high scan rate in CV study. The double-layer capacitance measured under this condition can be considered the average capacitance instead of the potential-dependent value.

2.3.1.4 Scan Rate Effects on the IL Double-Layer Charging Currents

In an EC redox process, the Faradaic current depends on the concentration of the analyte and increases monotonically with analyte concentrations. Numerous studies by others and our lab show that the structure and dynamics of the electrochemical double layer in room temperature of ILs are very different from the traditional

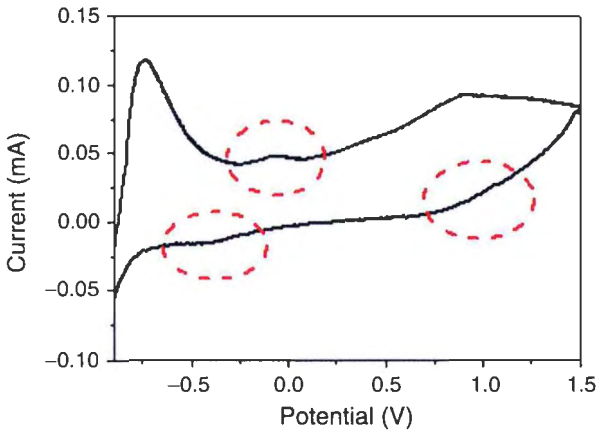

Fig. 2.4 CV of $[C_4mPy][NTf_2]$ at 20 mv/s on Pt under air condition. The small peaks (*red circles*) are presenting charging current by the IL orientation during the potential scanning

aqueous and nonaqueous electrolytes. For example, in two separated studies, Gore and Druschler et al. [86, 89] have reported the hysteresis effects in the potential-dependent double-layer capacitance of room temperature ionic liquids at either a Pt electrode or a gold electrode. They explained this hysteresis effect due to the slow pseudocapacitive processes in a frequency range below 10 Hz. We have also observed a similar behavior in our study [90]. It is well known that the first potential cycle is critical to target analyte concentration profile for a Faradaic process in aqueous solutions. However, it is unpredictable in ionic liquid since its pseudocapacitance is scan rate related, and thus the value is highly dependent on the potential and the history of electrode conditions in the IL [91–93]. Currently, there is no method that can obtain the accurate value of pseudocapacitance in an IL consistently. As we know, increasing the scan rate in cyclic voltammetry allows one to decrease the thickness of the diffusion layer, and the pseudocapacitive process caused by the slow orientation of the IL will be negligible. Thus, the hysteresis of the IL double layer will be minimized using higher scan rate. This can help to obtain the reproducible and accurate current values for sensor application. High scan rate could facilitate a steady state of the IL–electrode double layer to be established during the multiple potential cycling. As shown in Fig. 2.5, for the methane-oxygen system [94], the difference of peak currents of methane oxidation (0.9 V) and oxygen redox (−1.2 V/0.9 V) processes in the 6th cycle and 20th cycle at 500 mV/s, is less than 0.2 μA, confirming that the methane and oxygen concentration profile in ionic liquid is reproducible and the double-layer charging current is relatively constant. Thus, electrochemical measurements based on redox processes in IL should be characterized at the high scan rate, and peak current of first cycle should not be used for the analyte quantification.

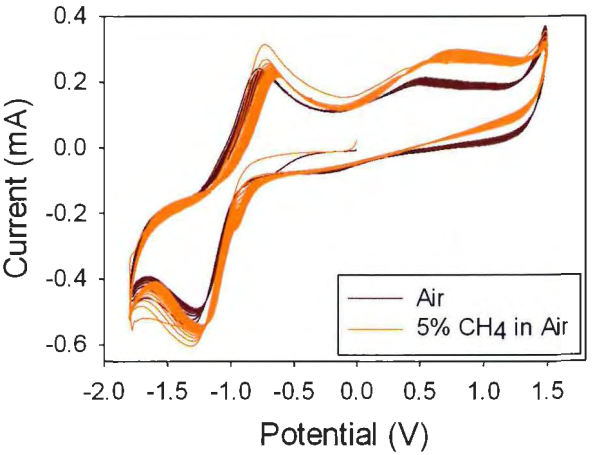

Fig. 2.5 Cyclic voltammograms of 5 % methane and dry air in $[C_4mPy][NTf_2]$ (500 mV/s scan rate)

2.3.1.5 Electrolyte Conductivity

Compared to the conventional aqueous electrolyte, the conductivity of the ILs is at least one order of magnitude smaller. In contrast to the conventional aqueous electrolyte, the higher the concentration of the ILs, the smaller the conductivity of the solution due to their high viscosity. This is expected. At high salt concentrations, all solvent molecules are called "solvent in salt solution," in which the ions primary shell is more complex, and the resulting system shows different properties at the low concentration salt solution [95–97]. In such a case, the conductivity increases with the increasing amount of salt, goes through a maximum, and decreases with a further increase of the salt concentration. However, most of the molecular liquids have relatively low viscosity, and therefore, the dilution of the viscous neat IL with molecular diluents decreases the viscosity of the mixture [98]. Table 2.3 lists the dynamic viscosity (η) and specific conductivity (κ) values of common solvents and RTILs [66, 99]. In an IL system, the solution resistance (R_u) is high due to higher viscosity and slow ion mobility of ILs. Typically, the solution resistance was calculated from conductivity of the ILs and electrode geometry. In most ILs, the dynamic voltage drop (IR-drop) would not be negligible and can affect the accuracy of the applied electrode potential. The IR-drop is the voltage loss (drop) when current flows through a resistor. IR-drop occurs in most of the electrical circuits and electrochemical systems. In ILs, the solution resistance R_u could be measured by both AC and DC techniques. In most electrochemical systems, IR-drop could be estimated to be lower than 10 mV. However, in some high capacitance systems and high Faradaic current systems, such as supercapacitor and fuel cell, IR-drop is significant. Although many commercial electrochemical instruments have the capability to compensate IR-drop, it still has to be considered in some analysis of an electrochemical process [100, 101].

Table 2.3 A comparison of dynamic viscosity (η) and specific conductivity (κ) for a representative selection of molecular solvents and nonhaloaluminate RTILs

Solvents	Viscosity (cP)	Conductivity (mS/cm)
N,N-Dimethylformamide	0.794	4.0[a]
Acetonitrile	0.345	7.6[a]
Ethanol	1.074	0.6[a]
Dimethylsulfoxide	1.987	2.7[a]
$[C_2mim][NTf_2]$	28	8.4
$[C_4mim][NTf_2]$	44	3.9[b]
$[C_6mim][NTf_2]$	59	
$[C_8mim][NTf_2]$	74	
$[C_2mim][BF_4]$	43	13.0
$[C_2mim][PF_6]$		5.2
$[C_4mim][PF_6]$	275	1.5
$[N_{6,2,2,2}][NTf_2]$	167	0.67
$[N_{6,4,4,4}][NTf_2]$	595	0.16
$[C_3mPy][NTf_2]$	63	1.4
$[C_4mPy][NTf_2]$	85	2.2

Unless otherwise stated, $T = 25$ °C
[a]Conductivity for organic solvent containing 0.1 M tetrabutylammonium perchlorate at 22 °C
[b]20 °C

2.3.2 *Potential-Step Methods (Chronoamperometry)*

Potential-step method is an electrochemical technique in which the potential of the working electrode is either held at constant or stepped to a predetermined value, and the resulting current due to Faradaic processes and double-layer charging processes occurring at the electrode (caused by the potential step) is monitored as a function of time. Especially for practical electrochemical sensor in real-world application, chronoamperometry is preferred due to its simplicity and low cost of instrumentation. Besides its wide use in most electrochemical sensor systems, chronoamperometry has been used in the understanding of the kinetics of the electrochemical processes as well.

2.3.2.1 Kinetics Study for Electrochemical Process

Chronoamperometry was used to determine the electron-transfer kinetics and it could provide information regarding the dynamic model of an electrochemical process. In chronoamperometry, the current is integrated over relatively long time intervals; thus, it gives a better signal to noise ratio in comparison to other voltammetric techniques. The Faradaic current, which is due to electron-transfer events and is

most often the current component of interest, decays as described by the Cottrell equation [77] in planar electrodes.

$$i(t) = id(t) = \frac{nFAD_O^{1/2}C_O^*}{\pi^{1/2}t^{1/2}} \tag{2.3}$$

In most electrochemical cells, the decay of Faradaic current vs. time is much slower than that of double-layer charging current; however, electrochemical systems with no supporting electrolytes are notable exceptions. ILs are more viscous than traditional organic solvents, thus slowing the diffusion of the electroactive species leads to transient behaviors. While the current behavior in the ILs system could be interpreted using the continuum model, it was recognized that the mechanisms by which an IL–electrode interface responds to an applied electrical field are quite different from a traditional, polar solvent. In the latter, solvent molecules re-orientate, whereas in an IL the molecules must move relative to each other. These differences must impact upon the overall observed rate of electron transfer, even if the free energies of activation are similar. That is, while inner-sphere electron-transfer rates might be expected to be very similar in ILs compared to polar organic solvents, outer-sphere electron transfers will be very different due to the screening response mechanisms [102, 103]. In order to possibly minimize the effect of "IR drop" and "capacitive charging" on the estimation of the heterogeneous electron-transfer rate constant, the microelectrode, scanning electrochemical microscopy (SECM), and other techniques have been used in many investigations by Mirkin, Bard, and Compton [104–107].

2.3.2.2 Faradaic Current Determination

Chronoamperometry (or potential step) can be regarded as an extreme fast potential sweep of CV which is especially beneficial for the practical IL-based sensor development due to its unique double-layer structure as discussed in the earlier section. However, as with all pulsed voltammetric techniques, chronoamperometry generates high charging currents, which decay exponentially with time as in any Randles circuit. As shown in our early work [90], the time-dependent oxygen reduction currents, $i(t)$, in ILs, can be described as the sum of the Faradaic current for EC reaction, i_f, and the double-layer charging current, i_c, on the electrode as shown in Eq. (2.4):

$$i(t) = i_f + i_c = i_\infty + \frac{C_{dl}\mathrm{d}V_{dl}}{\mathrm{d}t} + \frac{C_{bulk}\mathrm{d}V_{bulk}}{\mathrm{d}t} \tag{2.4}$$

In this expression, C and V represent capacitance and electrode potential, with "dl" and "bulk" denoting double layer and bulk solution, respectively. The Faradaic current (e.g., due to oxygen reduction) ordinarily decays much more slowly than the charging current (cells with no supporting electrolyte are notable exceptions). Typically the cell time constant $\tau = R_u C_d$, where R_u is the uncompensated resistance and C_d is the double-layer capacitance, is very useful to determine the timescale of

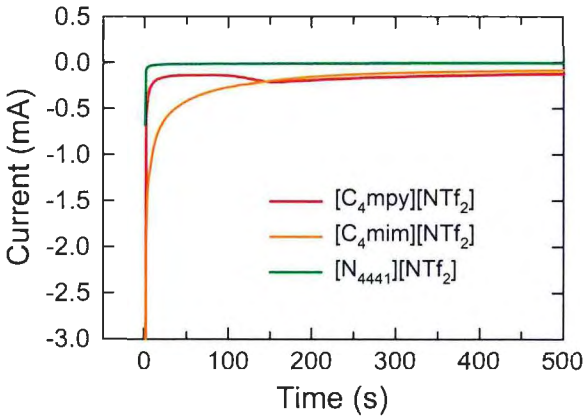

Fig. 2.6 Potential step experiment from 0 V to −1.2 V at 100 % air in three ILs. Time constant τ=6 s and 50τ is about 300 s

a potential step method. As such, it is important that analysis is applied over a sufficiently broad time interval in order to assure the reliability of the results. The charging current can be considered insignificant when current is sampled at times exceeding $5R_uC_d$. As shown in Fig. 2.6, the time constant obtained from potential step experiment (step from 0.0 V to −1.2 V in 100 % air) is τ=6 seconds (the time required for current decays to 37 % maximum current). Thus, in order to minimize the large double-layer charging current of IL, we measured the current at the 300th second which is 50τ. The current can be mainly attributed to the Faradaic current of oxygen reduction, and the double-layer charging current is negligible after 300 s, which is much longer than that in aqueous electrolytes (lower than few seconds). And the double-layer capacitance is also potential-dependent [80], because under different potentials the orientations of IL are different and the values of relative capacitances vary as well. Thus, cell time constant τ is not a constant and varies in different systems. The value of τ is related to the IL structure. Thus, chronoamperometry is not an efficient method to study the dynamic interfacial process in an IL system. For practical electrochemical applications, the significant conditioning process or preconditioning step (>50τ) is required to establish a constant IL–electrode interfacial boundary layers. Obviously, in different ionic liquids, the interface relaxation processes due to potential step vary and these processes have not been fully investigated so far.

2.3.3 *Electrochemical Impedance Spectroscopy*

In CV and potential step, the electrode surface reaction is studied through large perturbation on the system to drive the electrode to a condition far from equilibrium and observe the response. Typically in EIS, the electrochemical reaction is perturbed

with an alternating signal (e.g., potential) of small magnitude and the way in which the system follows the perturbation in steady states is measured. The use of low amplitude perturbation in EIS allows the application of a linear model to interpret the results which can yield useful information about the physicochemical properties of the system. Analysis is generally carried out in the frequency domain, although measurements are sometimes made in the time domain and then Fourier transformed to the frequency domain. For the analytical application, EIS is a powerful, informative, and noninvasive method, which can be used to study the interfacial events and trace the blocking behaviors (as complexation and adsorption) or diffusion effects at modified electrodes and serve as a transducer [108], especially in the electrochemical system. EIS has been used to measure the resistance of an electrolyte solution, grain boundary resistance, and interfacial capacitance. The Nyquist plot (Z_{im} vs. Z_{Re}) at high frequency (near 100 kHz) is determined by the solution resistance (R_s) and the electrode capacitance. However, for a specific electrochemical process and physical status, EIS is by no means limited to the measurement and the analysis of data at the impedance level (e.g., impedance vs. frequency) but may involve any of the four basic immittance levels; thus, most generally, IS stands for immittance spectroscopy. The signal of the whole system can be equivalent to a combination of certain electric components described by an "equivalent circuit."

2.3.3.1 Randles Circuit

An ideal electrode–electrolyte interface with an electron-transfer process can be described using Randle equivalent circuit shown in Fig. 2.7. The Faradaic electron-transfer reaction is represented by a charge transfer resistance R_{ct}, and the mass transfer of the electroactive species is described by Warburg element (W). The electrolyte resistance R_s is in series with the parallel combination of the double-layer capacitance C_{dl} and an impedance of a Faradaic reaction. However, in practical application, the impedance results for a solid electrode/electrolyte interface often reveal a frequency dispersion that cannot be described by simple Randle circuit and simple electronic components. The interaction of each component in an electrochemical system contributes to the complexity of final impedance spectroscopy results. The EIS results often consist of resistive, capacitive, and inductive components, and all of them can be influenced by analytes and their local environment, corresponding to solvent, electrolyte, electrode condition, and other possible electrochemically active species. It is important to characterize the electrode/electrolyte interface properties by EIS for their real-world applications in sensors and energy storage applications.

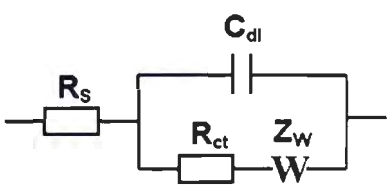

Fig. 2.7 The typical Randle's circuit

2.3.3.2 Proposed Equivalent Circuit in ILs

The typical IL system could be considered as a solvent-free system, in which it can simplify the EIS analysis significantly which spurs its wide use in the characterization of the IL–electrode interface. However, due to low mobility of ions in an IL and multiple molecular interactions present in an IL, more time is needed to reach to a steady state of IL–electrode interface structure and arrangement, when a potential is applied. Furthermore, the electron-transfer process in ILs is different from that in traditional solvents containing electrolytes. Thus, the interfacial structures of IL are more complex than other systems. Even the electrode geometry could affect the EIS results of IL systems. It is noted that the bulk ILs could not be simply described by a resistor (R_s) as in classic electrochemical systems. And the electrode double layer in IL electrolyte couldn't be simply depicted as a capacitor. So the Randle equivalent circuit is not sufficient to describe an IL system. Significant efforts have been made to illustrate the properties of diffusion layer and the bulk ILs with equivalent circuits. However, currently there is no general equivalent circuit model to describe the interface of an IL system.

2.3.3.3 EIS Measurement in IL

For practical EIS characterization of IL system, the purity of IL used, the hysteresis effect of IL, and the different experimental measurement conditions can all contribute to the variability of EIS results. Thus, for the EIS measurement: (1) A significant conditioning time for IL–electrode interface is required to minimize the hysteresis effect so that the interfacial boundary layer of IL is at a steady state for each measurement; (2) The electric field applied to the working electrode should be parallel. For sensor applications, the field effect transistor electrode structure in which the voltage applied across the gate and source terminals or the interdigited electrode structure is considered as better electrode designs for IL system using EIS testing. Additionally, EIS has the ability to monitor the ion movement and orientation in real time. However, the presence of the Faradaic process increases the complexity of results; because of the large capacitance of double layer, it is hard to analyze the contributions due to electron-transfer process or the charge transfer processes based only on impedance result. Combining impedance with spectroscopic methods is often used to obtain conclusive results.

2.3.4 Infrared Spectroscopy

Spectrometric methods are based on the interactions of electromagnetic radiations with the atomic and molecular species. Among them, IR spectroscopy (with wavenumbers ranging from about 12,800 to 10 cm^{-1} or wavelengths from 0.78 to 100 μm) is mostly used to obtain structural information about the molecular species.

IR absorption, emission, and reflection spectra for molecular species either in solid, liquid, or gas phases arise mostly from various changes in energy due to transitions of molecules from one vibrational or rotational energy state to another. The frequency or wavelength of this energy transition is characteristic of the specific chemical bond vibration and/or rotation in the molecule which are determined by the molecular structure, the masses of the atoms, and the associated vibrational energy coupling. Attenuated total reflectance (ATR) and reflection-mode of IR in conjunction with electrochemical methods allow samples to be examined directly in the solid or liquid state without further preparation and are widely used in the characterization of electrode–electrolyte interface properties. Most of ILs are IR-active molecules. Since ILs are stable and chemically inert, the IR characterization can be easily performed on the IL-based system directly.

2.3.4.1 IR Signal from IL

ILs have negligible vapor pressure making them not volatile, and this property permits in situ IR characterization of IL systems at various timescales without considering solvent loss generated uncertainties. High solubility of analytes in the ILs enables accurate characterization of their IR spectra in ILs. On one hand, the usage of ILs can eliminate the effect of water, and on the other hand, the signal from IL functional group can complicate the interpretation of Fourier transform infrared spectroscopy (FTIR) results. For example, hydrogen bonding is barely present in highly hydrophobic ILs, and as a result, the relative band shifts caused by the hydrogen bonding are negligible when analyzing the IR results in ILs [100, 109–111]. For those high purity IL systems, the IR spectra could be considered as the sum of the spectra of anion and cation and other species. Most of the methods used for studying the traditional ionic compounds such as ionic melts can be applied to the study of ILs. It is also noted that the IR response in liquid states of IL is different from the one obtained in a crystalline IL, predominantly because of lower energy conformations of the molecules in liquid states. For example, the IR spectra of $[NTf_2]^-$ in crystalline $[C_4mim][NTf_2]$ shows intensive bands at 649 and ~600 cm^{-1} (Fig. 2.8). Therefore, one may conclude that the anion is in *cis* conformation in this crystal. Furthermore, the intensity of both bands gradually decreases in the premelting region due to the predominance of the *trans* conformation in the liquid state. But they are still detectable [112–115]. Those conformation differences are present in the fingerprint region of IR (under 1,000 cm^{-1}), whereas most variability comes from anions. $[NTf_2]^-$ has O=S=O (1,100 cm^{-1} and 1,400 cm^{-1}) and C–F bonding (1,000 cm^{-1}) [112–115]. B–F of BF_4 is located at 924 cm^{-1} and 1,312 cm^{-1}, and P–F of PF_6 is about 843 cm^{-1} [116–119]. For cations, the bands are located in the rest of the regions and address the IL structure, such as C–C (around 1,450 cm^{-1}), C=C (around 1,600 cm^{-1}), and C–N bonding (around 1,450 cm^{-1}). Only C–H bonds around 3,000 cm^{-1} and 1,200 cm^{-1} are highly sensitive to their chemical environment. Typically, the addition of an analyte will change the C–H vibration and hydrogen bonding as well (Fig. 2.8).

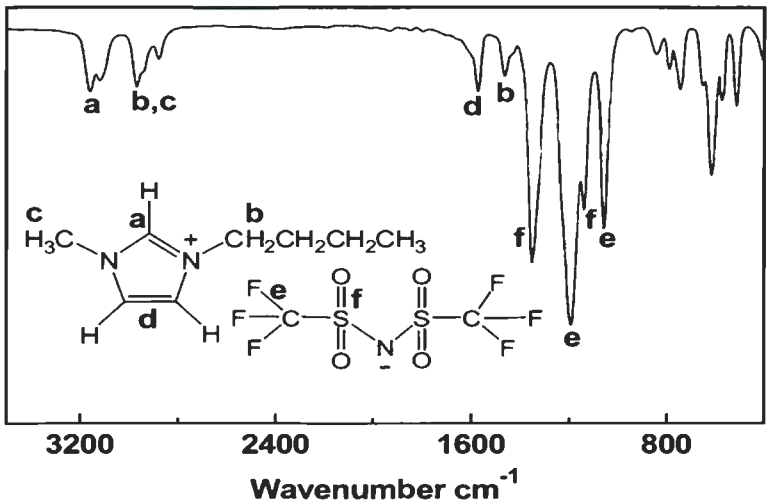

Fig. 2.8 FTIR spectra of $[C_4mim][NTf_2]$ under a nitrogen atmosphere

Table 2.4 Main IR bands (cm^{-1}) assigned C–H in ILs

Wavelength of the band (cm^{-1})	Vibration
3171, 3124	ν(C–H) aromatic, strong
2933, 2939, 2878	ν(C–H) aliphatic, strong
1575, 1467	ν(ring), strong, sym
1431, 1386	MeC–H, asym
1170	Ring, strong, sym

A comparison of IR spectra of acidic and basic ILs reveals only a small distortion of the aromatic ring, which is not of such extent as in the case of a salt with a smaller cation. This means that the hydrogen bond between the hydrogen on the carbon atom and a chloride ion is very weak or absent. This kind of bond is seen in the case of $[C_4mim][Cl]$, where there is a band at 3,088 cm^{-1}, and the peaks at 3,100 cm^{-1} are considerably smaller [120–123].The weak absorption from 2,500 cm^{-1} to 2,850 cm^{-1} may be attributed to the formation of hydrogen bonds between the aromatic protons and the halide ions. In basic ILs, the extent of hydrogen bond acceptor Cl^- is limited. Hydrogen bonds are weak or even not present. Other anions such as $[PF_6]^-$, $[BF_4]^-$, and $[NTf_2]^-$ are weakly complexing anions and not expected to participate in strong hydrogen bonding. Indeed, even $[C_4mim][PF_6]$ shows no hydrogen bonding bands in the region 3,000–3,100 cm^{-1} where C-H...Cl^- interactions on imidazolium chloride were observed previously. Therefore, IR results are consistent with a lack of hydrogen bonding within weakly complexing anions [124]. This means that cation–anion coulombic attraction is driving the overall structure, with local steric effects influencing the final orientation of ions. Table 2.4 lists the IR response of C–H bond in ILs [112–119].

2.3.4.2 Effects on Dissolved Analytes (Peak Position and Width)

ILs could provide a highly purified environment to monitor the interface reactions, and the species of interests can be localized near the interface because of the high viscosity of the ILs. Both these effects can enhance the observed IR signals. The p-type polarized IR is considered best as the light source for measuring IR-active species through bulk IL. However, typically the strength of signals is attenuated due to the long optical path in ILs.

Inorganic ILs such as the halogen salts of alkali metals provides strong ionic environment. The strong interaction between the analyte and the salt is manifested by peak shift from its position in gaseous state or liquid state of itself. For example, ν_3 of CO_2 was found with about 150 cm^{-1} shift from its position in gaseous state. The shift of ν_2 of CO_2 is about 40 cm^{-1}confirming this fact [125–128]. In an organic-based IL, this effect is not that strong. The position of this band for CO_2 dissolved in IL is very close to that of CO_2 dissolved in glassy polymers, such as poly(methyl methacrylate) (PMMA). The blue-shift is lower than 30 cm^{-1} [129–132]. However for H_2O the polar molecule structure and hydrogen bonding make this effect amplified. The presence of two bands corresponding to the antisymmetric and symmetric stretching modes of water indicated that molecules of water are present in the "free" (not self-aggregated) state bound to the basic anion via H-bonding [133–135]. The blue-shift of the antisymmetric stretching band has been used to correlate the relative strength of the interaction between water and RTILs with different anions. The strength of H-bonding increases in the order $[PF_6]<[SbF_6]<[BF_4]<[ClO_4]<[CF_3SO_3]<[NO_3]<[CF_3CO_2]$ [110, 111, 136–139].

Another effect is on the IR peak width of the analyte. Since most of the anions in IL are Lewis acids, the IR signal of dissolved analyte could be increased by the interaction. For example, the anions could act as weak Lewis bases, and CO_2 appears to be a useful probe to sense the extent of their basicity. The width of the ν_2 mode, measured as an effective average width of the split band (the average width represents the width of the doublet at the half maximum of the absorbance), is an estimate of the strength of the interaction of CO_2 with the Lewis bases: the width increases with the increase of the strength of the interaction [113, 130, 140]. This could also be a result of the strength of interaction decreasing with the increase of anion size. Thus, the strength of these interactions cannot be solely responsible for the solubility of CO_2 in these ILs, and, presumably, a free volume contribution in the IL plays a significant role. The strength of anion–cation interaction in the IL affects the available free volume, and one would anticipate that a weaker interacting anion leads to more free volume being available. It makes the result more complex.

2.3.4.3 Interface Signal

For the study of electrochemical processes, the interfacial information is even more important. However, due to the strong bulk absorption of IL, the transmission mode was limited to the electrode design. Using ATR mode may partially eliminate

interference from ILs, ATR–IR spectroscopy overcomes some of the limitations inherent to other techniques when the objective is to gain spectra of molecules dissolved in highly absorbing media. And also the interface information could be collected using the reflection mode as well. But the IR signal is limited by the thickness of the liquid film. The signal/noise ratio is another issue that should be considered. Typically, these methods are limited to verify the products during the electrochemical processes and are not able to provide the information regarding interfacial structure and dynamics. To understand the dynamical electrochemical process in IL and to obtain detailed molecular level information on the interface, the surface-enhanced spectroscopic techniques have to be applied since the bulk adsorption of IL is relatively strong. Among many surface enhanced spectroscopy techniques, SFG has been explored to characterize the electrode–IL interface. The nonlinear laser spectroscopy SFG method has long been recognized as an important tool for deducing the composition, orientation distributions, and some structural information of molecules at gas–solid, gas–liquid, and liquid–solid interfaces without interference from the bulk electrolyte. Thus, the interface is probed in situ, while the electrode potential is changed. Currently, SFG is the most efficient method to directly obtain the interfacial structure from the electrode surface.

SFG measurements of metal/aqueous electrode surfaces have been conducted on Au, Ag, and Pt electrode surfaces. The most extensive studies have been conducted with platinum single-crystalline and polycrystalline surfaces [141–143]. Using a free electron laser, Guyot-Sionnest and Tadjeddine demonstrated the first use of Vibrational Sum Frequency Spectroscopy (VSFS) to study ionic adsorption at an electrified metal/aqueous electrolyte interface [144–146]. Conboy et al. used it to determine the orientation of the imidazolium cation at the RTIL/SiO_2 interface, as well as the structure of the interfacial water molecules [147–149]. Baldelli et al. extended it to investigate the metal/IL interface. It provides solid evidences on the potential-dependant double layer of IL [19, 150]. SFG could determine the ion's location and orientations on the metal surface under variable applied potential via measuring the tilt of the terminal alkyl $-CH_3$ group on the cation. The results can be compared with those in situ EIS results to obtain an in-depth understanding of IL/solid interface [151, 152].

2.3.5 *In Situ EQCM Methods*

Electrochemical quartz crystal microbalance (EQCM) is a powerful analytical technique for probing electrode–electrolyte interfacial processes by using a quartz crystal electrode. Figure 2.9 shows an integrated EQCM electrode fabricated on a monolithic quartz wafer. AT-cut quartz crystals oscillating in a shear thickness mode exhibit extraordinary high sensitivity to potential-induced changes in the mass at electrode–electrolyte interface via the change of its resonance frequency. In addition to that, the monitoring of the mechanical state of the viscoelastic coatings at a quartz crystal electrode via a change in their shear storage and loss modulus is

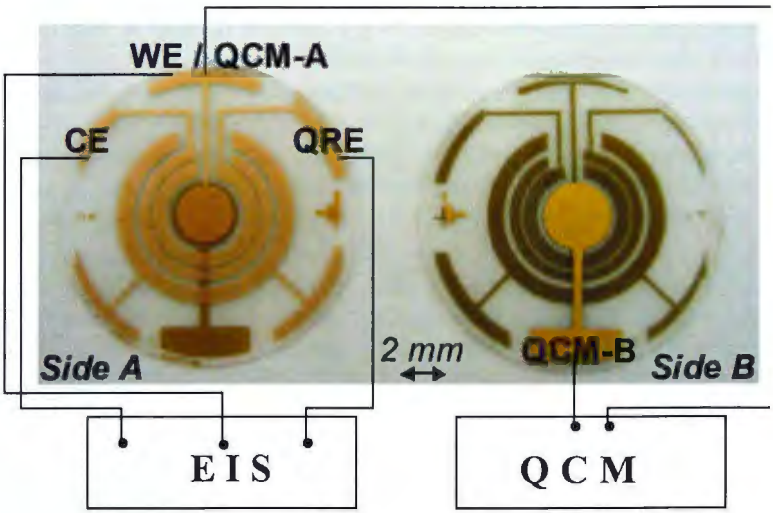

Fig. 2.9 Demonstration of the microfabrication of EIS–QCM electrode chip that was made on a 10 MHz AT cut quartz crystal formed EIS. It has a 2.5 mm disk-working electrode on both sides of 10 MHz AT cut quartz. Ring-shaped counterelectrodes (CE) and quasi-reference electrodes (QRE) are patterned around the circular working electrodes on one side and narrow gaps between disk and ring electrodes to support EIS and QCM

possible. When the coating on the quartz crystal electrode remains rigid, the major component of the QCM depends on the hydrodynamic interactions between the film on the electrode and the contacting electrolyte solution due to potential-induced volume and surface roughness changes in the coating. However, in the case of viscoelastic coatings, there are a variety of ways in which oscillation energy of the coated crystal may dissipate, and a large number of factors affect the change of the resonance frequency which are the indicators of the nature of the physicochemical processes behind the charging processes in the electrode coatings, requiring a careful analysis of the potential dependencies of both resonance frequency shift and resonance bandwidth. In some modern instruments, this damping of the oscillation is expressed through a quantity called dissipation. For a detailed understanding of these quantities and their effects, the readers can be directed to a recent review [153] presenting the main concepts of EQCM in context of its historical development, focusing on the exceptional sensitivity of the method. As described therein, its dynamic capability allows for the real-time monitoring of minute mass changes during electrochemical reactions in electroactive polymers and the accompanying viscoelastic changes [153]. Thus, a QCM used with electrochemistry methods such as EIS and CV allows real-time in situ measurement of the mass changes in the nanogram range during the electrochemical perturbation of the electrode solution interfaces.

ILs are highly viscous media thereby having large viscoelastic effects. Therefore, whether they are used as thin films for absorption–desorption-based phenomena or

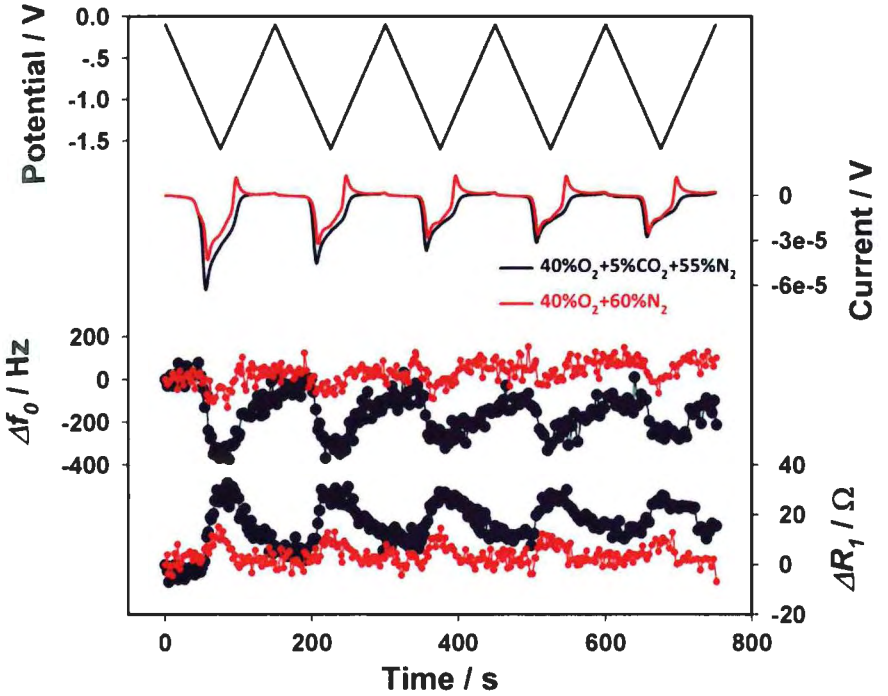

Fig. 2.10 Comparison of five-cycle-CV EQCM responses for O_2 (vol. 40 %) electrochemical reduction in the absence and presence of CO_2 in $[C_4mPy][NTf_2]$. Scan rate: 20 mV/s

more conventionally used as electrolytes for various electrochemical applications, in situ EQCM technique is quite powerful for characterizing the interfacial phenomena in ILs. For example, we have shown that in situ EQCM enables to answer several very important questions regarding the IL and electrified metal interfaces that have not been addressed before: what are the mechanisms of electrode oxidation and reduction reactions in ILs? Is the adsorption of ILs potential dependent? Is the adsorption of IL specific or nonspecific under potential control? What are the double-layer structure changes when the electrode changes from a metal to its oxide? These capabilities of EQCM methods facilitate the understanding of the structure/property relationships of electrode reactions in IL electrolytes. For instance, the electrochemical reactions of O_2, CO_2, and their mixture were investigated in three structurally different ILs by in situ EQCM [154]. Compared with electrochemical method only, the QCM integrated with the electrochemical method was shown to be significantly more sensitive and powerful for the characterization of the subtle differences (mass change or viscoelastic change) at IL/electrode interface as depicted in Fig. 2.10 showing current, frequency, and resistance responses obtained simultaneously. This led to the conclusion that the CO_2 reduction in ILs is irreversible and forms $CO_2^{\bullet-}$ adsorbate at electrode interface. With increasing concentrations of CO_2, the reduction

of oxygen is switched from a one electron process to the overall two-electron process, and forms adsorbed $CO_4^{\bullet-}$ intermediate species. Even though the mechanisms of electrochemical reaction between CO_2 and electrochemical-generated superoxide radical ($O_2^{\bullet-}$) in three structurally different ILs are found to be similar, the simultaneous EQCM experimental results show that the different cations in three ILs can modify the kinetics of the electrode reactions of O_2 and CO_2 due to a competition between the ILs' cation and CO_2 to react with $O_2^{\bullet-}$. The reactivity of $O_2^{\bullet-}$ toward CO_2 follows the order of the stability of the ILs' cation under $O_2^{\bullet-}$ attack. Understanding of such adsorption of redox intermediate at an electrode/electrolyte interface during CO_2 reduction is of fundamental importance for many chemical and electrochemical processes. In this way, EQCM technique can be used for the study of various gaseous molecules' redox processes in ILs in order to characterize the dynamics of the electrode reactions at an electrode and IL interface for a broad range of applications such as electrochemical synthesis, supercapacitor, Li-ion battery solid electrolyte interface, electrochemical conversion, fuel cells, and sensors.

EQCM has also been used to explore the ion–solvent coupling mechanisms in a redox polymer, polyvinylferrocene (PVF) in ILs, and their solutions. From the data of frequency and current values, the mass changes and the moles of electrons transferred can be calculated which can be plotted against each other to obtain very useful information as shown in Fig. 2.11. This study showed that the unique solvation and ionic properties of ILs significantly affected the break-in process and the ion–solvent transport mechanisms of PVF redox switching which is indicated in the form of difference for the significant difference of mass changes during first and fifth cycle of the redox reaction. Due to the existence of strong IL–polymer interaction, not only the anions but also the IL molecules interacted with the PVF matrix. The cations were later removed from the PVF matrix to balance the excessive positive charge in PVF oxidation. This also confirmed that IL was not only an electrolyte but also a

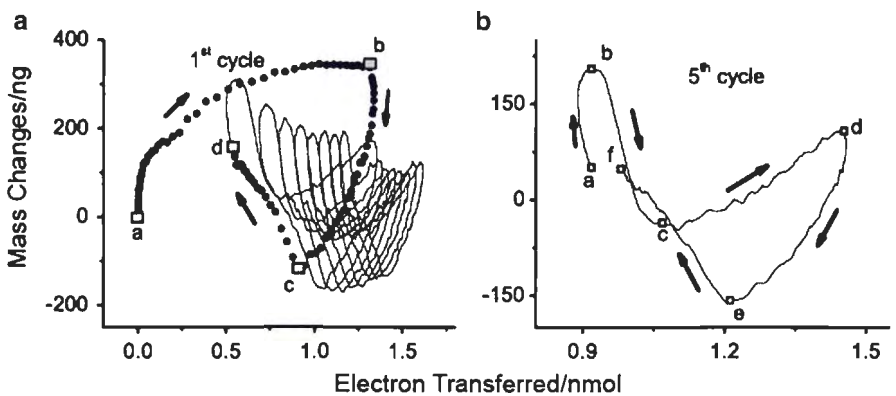

Fig. 2.11 Mass changes vs. electron transferred during PVF conditioning with $[C_5mPyr][NTf_2]$ as measured by EQCM. Potential scan rate: 50 mV/s. Scan range: 0–0.6 V. (**A**) The *dots* and the *arrows* correspond to the first potential sweeping cycle and the *solid line* to the following cycles. (**B**) The mass changes during the fifth potential sweeping cycle

solvent in PVF redox switching processes. Various types of interactions between PVF and the IL, including dispersion, dipole induction, dipole orientation, hydrogen bonding, or ionic/charge-charge interactions, could significantly change the PVF redox dynamics. The strong IL–polymer interaction in certain ILs, e.g., methanesulfonate ILs, may change even the polymer sublattice structure. This property was being utilized by preconditioning the PVF films with suitable ILs, such as *N*-alkyl-*N*-methylpyrrolidinium bis(trifluoromethanesulfonyl)imides, which allows PVF film to relax to a state compatible with reversible glycylglycylglycine peptide (GGG^-) doping/undoping. In contrast, ILs with structures and properties highly divergent from the target GGG^- failed to properly condition PVF to a compatible state [155]. These examples further confirmed that IL's tremendous diversity in structural and chemical properties and their distinctive properties offer an excellent opportunity to explore IL–polymer interactions and to dynamically control the conductive polymer relaxation processes and their redox switching mechanism for various applications.

Another new direction of EQCM-based exploration of ILs is by using in situ admittance mode of EQCM [156] which can characterize the changes in the composition of the ionic part of the EDL during charge/discharge of high surface area electrodes, such as activated carbons. Reliable dynamic information on the rather complicated charging processes in meso- and microporous carbon electrodes can be obtained by the measurement and analysis of the change in the bandwidth of the resonance. It has been shown that EQCM is able to monitor ionic and solvent fluxes [157, 158], and at the same time can reflect the mechanical status of composite activated carbon electrodes, with high sensitivity. The use of this technique provides excellent opportunities for designing new porous electrodes, for the optimization of already existing supercapacitor devices, and for developing effective desalination cells for capacitive deionization (CDI) of water. In situ EQCM frequency–potential responses have also been used for understanding the mechanism of the redox reaction of $[Au(III)Cl_4]^-$ at the Pt electrode in $EmimBF_4$ [159]. The results show that a series of $2e^-$ and $1e^-$ reductions occurs at the Pt electrode. Once metallic Au was formed on the Pt electrode surface, the subsequent reduction of $[Au(III)Cl_4]^-$ could occur on the Au deposit with a lower over-potential for electrodeposition. In addition, in situ EQCM experiments proved that the Au deposited was produced by the disproportionation of $[Au(I)Cl_2]^-$ to $[Au(III)Cl_4]^-$ and Au metal. The dissolution of the Au deposit was also investigated in this work by in situ EQCM method using Pt-QCM, thereby proving it to be a very powerful method in elucidating electrochemical surface phenomena accompanying mass changes in ILs.

2.3.6 *In Situ Electrochemical–Scanning Probe Microscopy*

STM and AFM are powerful tools for the in situ studies of the structure and morphology of electrode interface and have been used to characterize IL electrode interface as well [60]. These techniques are known to routinely achieve atomic resolution images in high vacuum conditions [160] and even in air. However, in situ

measurements in liquids tend to be less well resolved owing to inhibited cantilever resonance and a vast increase in noise [161]. When it comes to ILs, AFM imaging is quite a complicated process, not only in terms of cell designs [162] and arrangement but also in terms of image acquisition [18, 60]. Even for the aqueous and organic electrolytes, electro-viscous effect is quite evident. The viscosity of these solutions when in contact with the electrode increases more than twofold under the influence of an electric field [163]. Compared to other electrolytes, the excellent stability of ILs provides suitability for the long time operation. Moreover, their high purity can make it possible to investigate the molecular level information in IL at the interface. However, an IL represents a dense system of cations and anions with no solvent, so that the individual interactions between neighboring ions create an extraordinary viscosity effect [164]. In addition to this high viscosity, the adsorption of moisture by the ILs also creates challenges for the practical measurements. However, despite these challenges, some fundamental studies have been done in IL systems which can form the basis of new and more relevant discoveries. For instance, AFM measurements have been done to reveal that ILs are strongly adsorbed on solid surfaces and that several layers are present adjacent to the surface [124, 165]. This is consistent with X-ray reflectivity measurements [166] and the proposed theoretical models [167, 168]. But as expected from the diversity of features in ILs, the functional groups as well as the chain lengths can significantly affect the adsorption strength. Study of Atkin and Endres et al. [124] showed that $[C_4mPy][NTf_2]$ and $[C_2mim][NTf_2]$ behave quite differently on Au(111). Both liquids are adsorbed at the open circuit potential, but the first one adsorbed approximately four times more strongly than the latter. This adsorption of ILs on a solid surface is not at all surprising as water and organic solvents can also be adsorbed [169]. However, the force to rupture IL layers is one order of magnitude higher than for aqueous/organic solvents. Such a strong adsorption must influence the image quality in an in situ STM experiment [170], especially under electrochemical control thereby affecting the electrochemical reactions. This work also emphasizes that ILs should not be regarded as neutral solvents which all have similar properties, particularly regarding the differences in interfacial structure (solvation layers) on metal electrodes which is a function of ionic liquid species. Conventional double layers do not form on metal electrodes in IL systems. Rather, a multilayer architecture is present. The number of these solvation layers is determined by the IL species and the properties of the surface and up to seven discrete interfacial solvent layers are present on electrode surfaces. In a recently published paper [171], the structure and dynamics of the interfacial layers between the air- and water-stable IL $[C_4mPy][FAP]$ and Au(111) were investigated using STM, CV, EIS, and AFM measurements. In situ STM measurements reveal that the Au (111) surface also undergoes a reconstruction, forming a "herringbone" superstructure at −1.2 V. AFM force–distance profiles also showed that IL becomes more structured at higher cathodic potentials with an increase in both the solvation layers and the push-through effects. EIS measurements showed a capacitive process at the IL/Au (111) interface which is considerably slower than electrochemical double-layer formation and seems to be related to the reconstruction of Au(111). In another work from the same group, the anodic regime for the same IL system $[C_4mPy][FAP]$ and Au(111) was studied. It was again shown that structures form on the nanoscale

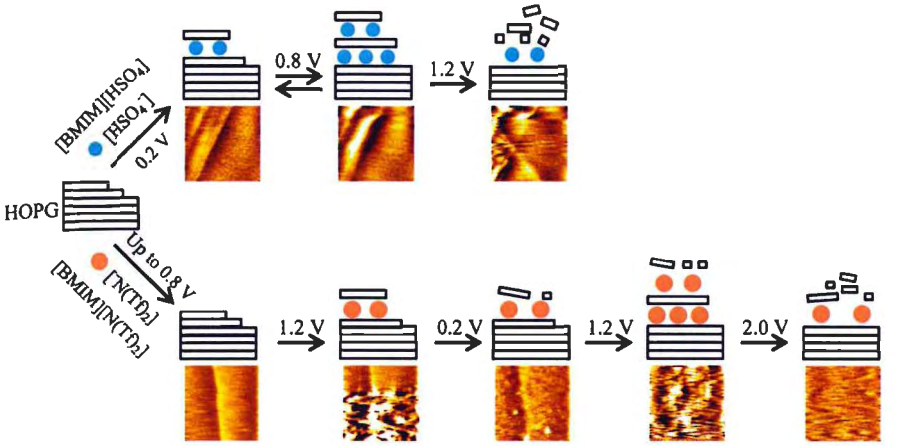

Fig. 2.12 Summary of the EC-AFM investigation of electrochemical intercalation–deintercalation of the anions into HOPG in pure $[C_4mim][HSO_4]$ and $[C_4mim][NTf_2]$

for electrode potentials of up to +2 V which disappear when the electrode potential is returned to the open circuit potential, and the original surface is recovered. Thus, these observed processes on the surface are reversible. Interestingly, the work done in our group has indicated that this heterogeneity of the double-layer structure posed by different ILs and at different potentials is extremely beneficial for designing sensing interfaces. Therefore, the information gathered by the EC-AFM and sole AFM studies can significantly enhance the sensor development process.

Heterogeneity in IL's structure can also influence their interaction with substrate electrodes as well, during the electrochemical reactions and such interaction can also be studied by EC-AFM. Again by understanding these phenomena, more stable and innovative electrochemical systems can be designed both for sensors and fundamental electrochemistry. We have studied [172] such interaction of ILs with highly oriented pyrolytic graphite (HOPG) electrodes using EC-AFM, as summarized in Fig. 2.12. It was observed that electrochemical intercalation–deintercalation processes in pure ILs have caused the morphological changes in HOPG. Such changes due to electrochemical intercalation–deintercalation of ions during electrochemical processes are a common phenomenon occurring in graphite electrodes. HOPG has been widely studied as a model to understand the processes during electrochemical intercalation–deintercalation of ions into graphite. According to the model proposed for aqueous electrolytes, solvent (H_2O) molecules play an important role during the oxidative reactions on HOPG. Therefore, studying the intercalation–deintercalation process in ILs which are composed entirely of ions is of primary significance. Being composed entirely of ions, morphological changes in HOPG will be mostly due to the intercalation–deintercalation of ions in ILs. Thus, the ionic sizes can have strong influence on intercalation into HOPG. The hydrophobic character of the ILs can also affect the intercalation of the ILs with the hydrophobic HOPG surface. However, these effects may play smaller roles compared to the anionic size effect. Our data proved that these morphological changes are reversible for intercalation and deintercalation,

which are strongly dependent on the anionic size of the ILs used. It was also possible to get the quantitative estimate of the amount of thickness changes on the HOPG surface during the intercalation–deintercalation process. And above a certain voltage, degradation of the steps on the HOPG surface occurs to form carbon nanoparticles. Furthermore, STM results can reveal the relationship of the electrochemical properties and the strength of this interaction. The results of these measurements are used to find out the symmetry and interatomic distances of metal atoms under potential control. Surface diffusion of metal atoms in contact with IL electrolytes has also been explored because of its close relation to the reactivity of the atoms on the surface. Such studies provide a key to understand many kinds of electrochemical processes at an electrode–electrolyte interface, such as anion desorption, electrodeposition, corrosion, and surface alloying with a deposit.

As discussed earlier, high viscosity of ILs leads to a complicated situation in terms of AFM measurements that result in much higher signal-to-noise ratios. In order to obtain better spatial resolution in such a scenario, a new EC-AFM technique has been developed which involves independent control of the AFM tip and working electrode substrate and is named as frequency-modulated AFM (FM-AFM) [173]. FM-AFM measures tip–sample interaction very sensitively by detecting changes in the resonant frequency of the oscillating cantilever. This allows the tip–sample interaction stiffness and tip deflection to be monitored simultaneously, providing the atomic resolution images. By utilizing this technique for ILs, not only the topography of the substrate can be accurately ascertained at very high resolution, but the energy dissipation curves for oscillating cantilever can be obtained. Thus, the microscopic information regarding the electrical double layer at the electrode surface can also be attained by the assessment of energy dissipation curves.

2.4 New Approaches for Sensor Development Using IL Interface

Following the 1980s PC revolution and the 1990s Internet revolutions, recent decades have experienced a revolution in sensor research which promises to have a significant impact on a broad range of applications including national security, health care, environment, energy, industry and food safety, and manufacturing. The parameters important in the evaluation of sensors can be thought of as the "five S's" of sensor characterization, and include *Sensitivity, Selectivity, Speed of response, Stability*, and *Size/shape/cost*. The unique properties of ILs and IL interface enable a systematic design process across all design layers, with judicious choices in sensing materials, sensing chemistries, and transducers to uniquely overcome all performance challenges, especially those related to sensing capability and miniaturized sensor system implementation. As summarized in Fig. 2.13, (1) ILs' remarkable dissolution properties for organic and inorganic substances enable analyte preconcentration and sensitivity enhancement for the detections; (2) various molecular noncovalent interactions between ILs and the analytes contribute in increasing reversibility; (3) synthetic flexibility of ILs enables selective sensing by

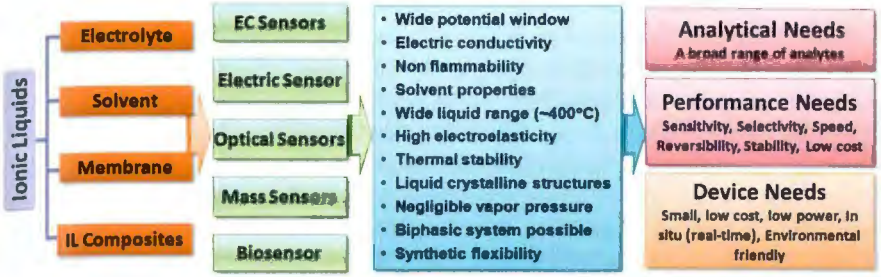

Fig. 2.13 Multifunctional character of ILs as related to different sensing platforms using their highly unique and diverse properties. All these properties help in improving one or more of the performance evaluation parameter of the sensors

constructing ILs' sensor arrays; (4) the high viscosity of ILs allows the formation of stable thin films for mass-based sensors; (5) high thermal stability of ILs enables high-temperature detection; (6) ILs' negligible vapor pressure and nonflammable nature provides stability to the sensing film; (7) ILs' negligible vapor pressure, wide potential windows, high ionic conductivity, and good solubility enable their uses as new electrolytes for many improved electrochemical sensor systems [90, 174–180]; (8) ILs can also serve as a medium or a solvent for dyes and fluorescent compounds to form stable optical matrices, which can be the basis of accurate optical detection systems; (9) ILs can be incorporated into conventional matrices, such as biopolymers, cellulose, carbon nanotubes (CNTs), metal nanoparticles, and sol–gel-based silica matrices [181, 182], to form stable composite materials. These composite materials amalgamate multifunctional properties of materials involved in preparing the composites, thereby enhancing both their utility and their performance for a variety of sensing applications. Moreover, the unique properties of ILs and their miscibility/immiscibility with other solvents can be easily controlled by changing the anions and cations, thereby providing unlimited options for their applications designs, and especially for sensors where cross functionalities are essentially required. In the following sections, we will discuss examples of ILs that have been successfully explored in multiple ways for their chemical and biological sensing capabilities. We will also illustrate the principles of some of the modifications in order to obtain good sensor interfaces which can then generate different types of sensor systems based on ILs.

2.4.1 *ILs as Electrolytes for Electrochemical Sensors*

Most electroanalytical methods are based on the measurements of electrochemical cell potential, current, charge, or impedance at a fixed or controlled external applied function to the electrochemical cell. There are three main types of electrochemical sensors based on either the measurement of a redox current (amperometry), the potential (potentiometry), or the impedance or capacitance (impedance spectroscopy)

at the electrode/electrolyte interface of interests. Both electrode materials and electrolytes play significant roles in the performance of the interface. The analytical detection properties (e.g., sensitivity, selectivity, response time, drift, stability, and interference) are largely determined by the electrode/electrolyte interface properties for all electroanalytical methods. Notably, a majority of the electrochemical sensors developed to date employ aqueous-based electrolytes that suffer from solvent volatility leading to the exhaustion of solvent in a reaction batch. The other option is the nonaqueous electrolyte. Typically, there are three kinds of nonaqueous electrolytes: aqueous salts that could be dissolved in organic solvents (e.g., lithium perchlorate, and other perchlorate compounds, which have good solubility and ionization in particular organic solvents, such as CH_3CN), organic compounds with charged ion center (e.g., tetra-*n*-butylammonium perchlorate) or polyelectrolytes (e.g., perfluorosulfonate [183, 184] and Nafion ionomers [185, 186]), and ILs. However, some of the aqueous electrolytes could not be dissolved in the organic solvents or cannot be ionized. The dielectric constants of organic solvents are usually smaller than the aqueous solvents too, which affects the conductivity a lot. So for a certain organic solvent, there are only some particular electrolytes used for a certain kind of solvent. Because of their nonvolatility and much higher ionic conductivity, ILs have the ability to replace almost all conventional electrolytes in all types of electrochemical sensors [174, 175, 187, 188]. Here, we will discuss the principles and examples of the most important analytical applications of ILs where they are used as electrolytes and solvents in electrochemical sensing.

2.4.2 Sensory Design Based on the Potentiometry

Potentiometry is a method in which the electrochemical cell potential is measured at equilibrium at which the current is zero. The properties of the interface region differ from the bulk properties. A potential is established at the phase boundaries, e.g., between the solution and the electrode surface. The potential of electrochemical cells is the sum of all interface potentials including electrode/electrolyte interface and liquid/liquid interface (i.e., the two electrolyte solutions of different compositions that are in contact with each other). Ideally the measured potential should depend only on the potential between the interfaces of interest for analytical purpose. This is typically accomplished by keeping all other interfaces constant through a suitable electrode construction. Potentiometric sensors (e.g., ion selective electrodes) usually consist of a membrane that contains ion exchangers, lipophilic salts, and plasticizers, and the transmembrane potential gives the activity of the analyte ion in solution.

2.4.2.1 Sensing Based on the Liquid Junction Potentials

ILs have a broad range of polarity and can be used to design the interface between two immiscible ILs such as water/organic solvent interface to detect ions that are not redox active. The transfer of ions across the interface, as opposed to electron

exchange at solid electrodes, generates a potential which is directly related to the concentrations of the ions of interest. ILs have been explored as an alternative water-immiscible solvent phase for sensing at the liquid/liquid interface by the detection of ions transferring across liquid/liquid interfaces as described in an excellent review by Samec and Kakiuchi [189]. The main advantage of this type of sensing compared to sensing in conventional electrolytes is that the IL is usually pre-saturated with water, so any differences in humidity in the environment will not affect the overall sensor response. The group of Kakiuchi in collaboration with Mirkin has recently reported [105] the kinetics of ion transfer at the IL/water nanointerface. The interface was formed at the tip of a nanopipette, and the transfer of tetrabutylammonium from water to the hydrophobic IL trihexyl(tetracdecyl) phosphonium bis(nonafluorobutylsulfonyl)[$P_{14,6,6,6}$][C_4C_4N] was reported. Although this work was not specifically related to sensing, this could have implications in the field due to the use of very small (nano) interfaces that give rise to lower ohmic drop and higher current density, which is highly beneficial for sensing applications. The same group has also highlighted the ultraslow relaxation of the electrical double layer in ILs at millimeter-sized interfaces [190], which may lead to the self-inhibition of the charge-transfer step across the IL–water boundary, limiting the performance of a sensor that relates charge transfer to analyte concentration. More research in this area is needed to understand the impact of the ultraslow relaxation on sensor responses and behavior, using smaller sized interfaces.

2.4.2.2 Ion-Selective Electrodes with ILs

Ion selective electrodes (ISEs) are electrochemical sensors that allow the potentiometric determination of the activity of an analyte ion in the presence of other interfering ions. An ion-selective membrane consists of four major constituents: ionophore [ion carrier, e.g., valinomycin (selective to K^+ over Na^+)], lipophilic salt as ion exchanger [e.g., K^+R^- (where R^-=lipophilic anion)], plasticizer [e.g., 2-nitrophenyloctylether (NPOE)] as organic solvent, and polymeric substrate matrix such as Polyvinyl chloride (PVC). The different potential response has, as its principal component, the Gibbs energy change associated with permselective mass transfer across a phase boundary. The ionophore in membrane can selectively complex the target ions at membrane interface that causes the interfacial charge separation. The measured potential differences of ISEs are linearly dependent on the logarithm of the activity of a given ion in solution as described in Nicolsky-Eisenman equation (Eq. 2.5).

$$E_i = E_i^0 + s_i \log\left[a_i + \sum_{i \neq j} K_{i,j}^{\text{pot}} \left(a_j\right)^{z_i/z_j} \right] \tag{2.5}$$

E_i: electromotive force (potential) of the cell assembly; E_i^0: cell constant; a_i: activity of primary ion **I** in sample solution; a_j: activity of interfering ion **J** in sample solution; z_i, z_j: charges of **I** and **J**, respectively; and $K_{i,j}^{\text{pot}}$: potentiometric selectivity coefficient of primary ion $\mathbf{I}^{z_i}$ against interfering ion $\mathbf{J}^{z_j}$. An ideal selective electrode would show all $K_{i,j}^{\text{pot}} = 0$.

ILs possess high ion concentration, high conductivity, and good electrochemical stability. So they seem to be natural candidates for liquid ion exchanger membrane electrodes. For these reasons, they have been employed as alternatives to plasticizers and ion exchangers in membranes of ISEs. Most charged carriers applied in conventional ISEs are ion exchangers that do not exhibit specific interactions with the ions to be sensed. As a result, selectivity is determined by the free energy of hydration of the ions and corresponds to the so-called Hofmeister series [191]. However, ILs can be designed by modifying cations such as imidazolium or pyridinium and pendant alkyl groups with functionality; thus increased selectivity or even specificity for a given set of ions can be obtained. This new type of IL-based membrane electrode could be smaller, more portable, and less expensive, with the possibility of conducting simultaneous and continuous analysis of multiple analytes. It is also possible to provide real-time output and higher sensitivity and selectively. Since no sample preparation is required and no secondary labels are needed, these ISEs are very user friendly. For example, low melting ionic solids, i.e., the ILs that melt slightly above room temperature, can be used in ISEs for the potentiometric determination of salicylate, perchlorate, thiocyanate, and iodide ions in water. Three of such ILs $[N_{6,6,6,6}][BSB]$, $[N_{8,8,8,8}][BSB]$, and $[N_{8,8,8,1}][BSB]$ were proved as suitable salts for both liquid-contact and solid-contact ISE membranes, and $[N_{8,8,8,8}][BSB]$ was chosen as the most suitable because of its lowest melting point. A Nernstian response was observed over the range 10^{-5} M to 10^{-1} M for the four chosen analyte ions, with good reproducibility and reversibility and a fast response time of <10 s. Peng et al. [192] also reported a sulfate ion sensor based on a PVC membrane containing either one of the two ILs $[C_8mim][Cl]$ or $[P_{14,6,6,6}][Cl]$ as both an anion exchanger and plasticizer, and sulfate ionophore I (1,3-[Bis(3-phenylthioureidomethyl)]benzene). Both membranes exhibited ideal Nernstian responses to sulfate over the range 10^{-5} M to 10^{-1} M and were successfully applied for the analysis of sulfate in drinking water samples. We used two imidazolium-based ILs, 1-butyl-3-methyl-imidazolium bis(trifluoromethanesulfonyl)imide $[C_4mim][NTf_2]$ and 1,3-dibutylimidazolium bis(trifluoromethanesulfonyl)imide $[C_4C_4im][NTf_2]$, to construct PVC liquid membrane electrodes for the detection of $[NTf_2]^-$. As shown in Fig. 2.14, the ISEs we made have improved selectivity and sensitivity as compared to anion-sensitive electrodes based on organic ammonium salts, but we also observed less than Nernstian response due to the partial solubility of the two imidazolium-based ILs in aqueous solutions. The uptake of water is expected for IL membranes being in contact with aqueous samples. The wide potential window is regarded as one of the most important advantages of ILs when they are used as pure electrolytes [189, 193]. This is not the case for IL–modified electrodes used as ISE, because they operate mostly in contact with aqueous solution. Similar to our observation, IL $[P_{14,6,6,6}][Cl]$/PVC membrane-based potentiometric sensor also suffered from severe potential instability due to the tendency of the IL to absorb water, but this was improved by the addition of carbon nanotubes (CNTs) to the membrane, resulting in a stable Nernstian response over the concentration range 10^{-5} M to 10^{-1} M [194]. Thus, hydrophobic ILs and low melting ionic solid are choices for IL-based new type of ISEs. The solubility of hydrophobic ILs in

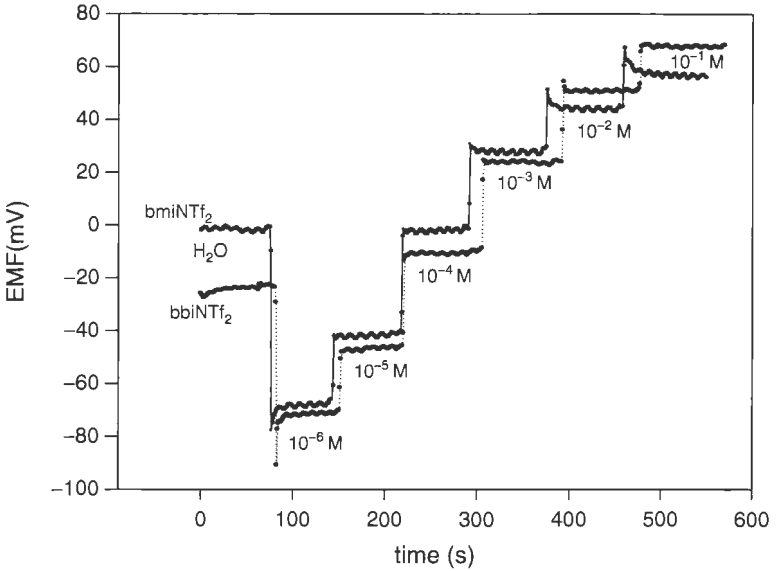

Fig. 2.14 EMF time profile of the $[C_4mim][NTf_2]$ and $[C_4C_4im][NTf_2]$ PVC membrane at various $Li[NTf_2]$ concentrations

water is much smaller than the solubility of water in IL and in some cases is much below the fraction of percent. This property is crucial from the point of view of stability of IL membrane electrodes, because of the possibility of microliter-sized liquid deposit dissolution in few milliliters of the surrounding aqueous electrolyte. However, IL–membrane electrodes are reported to be stable at least in electrochemical timescale indicating slow dissolution in the case of more hydrophilic ILs. For example, Nishi et al. [195] used the hydrophobic IL methyltrioctylammonium bis(nonafluorobutylsulfonyl)imide $[N_{8,8,8,1}][C_4C_4N]$ containing the ionophore dicyclohexano-18-crown-6 (DCH18C6) for the potentiometric detection of K^+ in water. Facilitated ion transfer was reported for K^+ and the two-phase system was used for the potentiometric determination of K^+. A Nernstian response to K^+ (59 mV per decade) was observed over the concentration range 10^{-5} M to 10^{-1} M with a response time of 20 min. It is clear from these reports that ILs have the ability to be used in membranes of ISEs. However, the long-term stability of such sensors may be restricted by the leaching of IL ions from the membrane into the water phase. At present, the ILs available may not be sufficiently lipophilic to serve as suitable replacements for components in conventional ISEs (e.g., ion exchangers in PVC membranes). This has prompted the researchers to use IL composites in ISEs. For example, polymer/IL/multiwalled CNT composite electrode was developed [194] as an all solid-state potentiometric sensor for various anions (SO_4^{2-}, Cl^-, NO_3^-, SCN^-, and ClO_4^-). Moreover, a potentiometric Er(III) sensor consisting of a multiwalled CNT/$[C_4mim][BF_4]$ carbon paste electrode containing 5-(dimethylamino) naphthalene-1-sulfonyl-4-phenylsemicarbazide (NSP) as the sensing material was

also constructed. A Nernstian response of 19.8 mV per decade was observed in the range 10^{-7} M to 10^{-1} M with a detection limit of 5×10^{-8} M for Er(III). This shows that the use of IL as a binder demonstrated improved performance compared to mineral oil (paraffin), and the combination of the three sensing materials gave better sensitivity, selectivity, response time, and stability compared to traditional Er(III) carbon paste sensors. Thus, this strategy is going to be more useful in preparing ISEs until new highly lipophilic ILs are synthesized.

2.4.2.3 Nonclassical Potentiometry

In ISE, the equilibrium potential change of the electrode is inversely proportional to the charge of the analyte being detected. Thus, it is not feasible for its use for detecting large, highly charged molecules, due to the very small sensor response to highly charged macromolecules. However, in 1990s, several research groups demonstrated a nonclassical potentiometry [196] for the detection of different macromolecular polyions, including heparin, protamine, carrageenan, and DNA. The response mechanism of nonclassical potentiometry is fundamentally different, employing nonequilibrium, steady-state conditions to generate a useful sensor response. Ionic liquids have also been used in the nonclassical potentiometric electrode fabrication. Langmaier and Samec [197] employed a thin microporous membrane impregnated with valinomycin and the hydrophobic IL $[N_{12,12,12,1}][TFPB]$ for the facilitated amperometric detection of K^+ and Na^+. The use of IL in the membrane in this case provided enhanced stability and selectivity compared to conventional K^+ ISEs. A similar strategy can be applied with the addition of a water-soluble crown ether (18-crown-6) to the aqueous phase, in order to make it possible to distinguish the voltammetric waves of various alkali metal cations (K^+, Na^+, Li^+, and Mg^{2+}), and the promising results suggest that the IL membrane may be suitable for application in an amperometric ISE for K^+. The work of Silvester and Arrigan [198] is quite important in this regard who reported the transfer of several common ions across the interface between water and a commercially available hydrophobic IL $[P_{14,6,6,6}]$ [FAP] with a melting point of <–50 °C. This was the first report of voltammetry at an *array* of water/IL microinterfaces, rather than at a single interface or porous polymer-supported interface. The interface array was formed within the micropores of a silicon chip membrane (30 pores and 23 μm diameters) and provided advantages of micron-sized interfaces such as radial diffusion, higher current densities, and lower iR drop, but with larger currents for sensing low concentrations of redox-inactive ions. This work has shown that sensing of various ions is possible at the water–IL interface, but it was limited to the ions that transfer at potentials less negative than the IL anion (e.g., $[FAP]^-$) transfers to water. As a result, the synthesis of ILs with extremely hydrophobic cations and anions which are not yet available in the liquid form is required in order to extend the potential windows to those similar to organic solvent/supporting electrolyte systems (e.g., 0.9 V). If this is made possible, this should allow for the observation of species that have been detected at the positive potential limit in water/organic solvent systems, e.g., important biomolecules such as lysozyme and hemoglobin.

It is already known that the contamination of IL with water shrinks potential window to that exhibited in aqueous electrolyte solution [78]. This is also the case of most hydrophobic ILs composed of large 1-alkyl-3-methyl-imidazolium cations and homologs of [NTf_2] anions. Therefore, the uptake of water is expected for IL deposit being in contact with aqueous electrolyte in the nonclassical potentiometry.

2.4.2.4 Sensing Based on Voltammetry

Voltammetry is a powerful suite of tools that enables qualitative and quantitative information about the analytes to be obtained by the measurement of the current as a function of applied potential. The technique can be applied to any species that can undergo redox transitions on solid electrodes, or any ion that can be transferred across interfaces (in the case of liquid/liquid interface). The analyte species diffuses through the electrolyte to be detected at the working electrode surface. It was also used to monitor the diffusion coefficients of species in solution and to understand their behaviors and electrochemical reaction mechanisms. Voltammetry typically takes place with two- or three electrodes that are connected through an electrolyte medium (e.g., water or organic solvents containing a background electrolyte). There has been a lot of work focused on understanding the reaction mechanisms, kinetics, and thermodynamics of electrochemical reactions in ILs. However, ILs have recently shown much promise as stable and nonvolatile electrolytes, especially in amperometric gas sensors. A typical amperometric gas sensor consists of three electrodes connected through an electrolyte, which is covered by a gas-permeable membrane. The gas passes through the membrane, diffuses through the electrolyte, and is detected at the working electrode. Most commercially available amperometric sensors of gases (e.g., O_2, CO, SO_2, H_2S, NO_2, and Cl_2) currently employ conventional solvents (e.g., H_2SO_4/H_2O mixtures, or organic solvents such as acetonitrile or propylene carbonate) that cannot survive drastic temperature changes or extremely dry or humid conditions. The "lifetime" of a sensor is often determined by how quickly the electrolyte dries up and the solvent often has to be replaced every few days/weeks in the most extreme conditions. ILs possess negligible volatility and high chemical stability, making them ideal electrolyte media in robust gas sensors for potential application in more extreme operating conditions (e.g., up to 300 °C), with no possibility of solvent evaporation or degradation. This, combined with the intrinsic conductivity (no need for supporting electrolyte), wide potential windows (to investigate compounds that may have been inaccessible otherwise), and, in some cases, increased gas solubility in ILs, makes them ideal electrolyte media for gas detection. Furthermore, ILs can stabilize the radical cation or radical anions which enables new redox chemistry of many analytes that are quasi reversible. However, the high viscosity of ILs often results in slow and less reproducible response [199] that have limited their direct use in practical sensors regarding the response time and sensitivity. To increase response speed and circumvent the high viscosity of ILs, we introduced an innovative electrochemical cell (Fig. 2.15) with a porous Teflon membrane as the support for ILs that facilitate diffusional transport through the pores and provide two levels of selectivity (i.e., the size of the pore and the IL membrane) [90]. Analytes entering from the back side

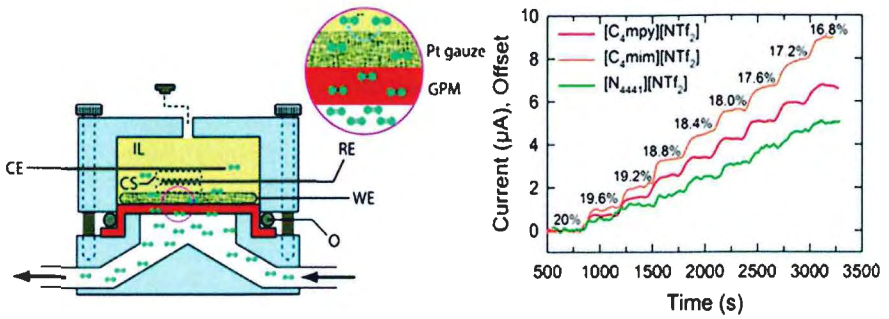

Fig. 2.15 Schematic diagram (not to scale) of the Clark-type oxygen sensing cell with the analyte flow from the back side to circumvent the high viscosity of ILs, and the current transients recorded at −1.2 V for different oxygen concentrations using three different ILs. Nitrogen was used as the carrier gas

were able to quickly reach the electrode/electrolyte interface without passing through the IL diffusion barrier, reducing response time to mere seconds. Figure 2.15 also shows the amperometric response of three $[NTf_2]$-based ILs to oxygen and illustrates a strong dependence on the choice of cation, as desired. High sensitivity, complete reversibility, long-term stability (less than 0.3 % potential shift over 90 days), rapid response, and strong selectivity (selectivity coefficient ~0.01 % for CO_2, NO, NO_2, SO_2) of this IL oxygen sensor were observed.

Recent advances in voltammetry-based gas sensing involving ILs have been reviewed by Rogers et al. [200] who describe the electrochemistry of various gases including oxygen, carbon dioxide, hydrogen, ammonia, hydrogen sulfide, sulfur dioxide, and nitrogen dioxide in ILs. From these studies, it appears that the most logical step forward in this area is to employ thin IL layers to overcome the slow diffusion often associated with viscous ILs. This may result in decreased response times, on the order of minutes or seconds, which is ideal for most gas sensor device requirements. Microelectrodes fabricated on a silicon chip can be an important advancement in this regard as shown by Compton's group [179]. The use of small (micron-sized) working electrodes can minimize any iR/Ohmic drop limitations that are often associated with voltammetry in highly resistive ILs on larger electrodes (larger currents). Also from these studies, the electrochemical reaction mechanisms of carbon dioxide, hydrogen sulfide, and chlorine gas in ILs can be explored. For example, the electrochemical reduction of CO_2 in the RTIL [C_4mim][Ac] was studied on a Pt microelectrode using cyclic voltammetry. CO_2 undergoes a chemically irreversible one-electron reduction to the radical anion $CO_2^{\bullet-}$ and subsequent followup chemistry including interaction/complexation with the IL. The behavior was found to be irreversible due to strong absorption of CO_2 in the IL, suggesting that this system may not be suitable for real-time sensing of CO_2; however, the high solubility (>1.5 M) of CO_2 in [C_4mim][Ac] suggests a method for sequestration of the greenhouse gas. We have also used voltammetry in ILs in combination with QCM technique [154] as described in in situ EQCM section

proving that the CO_2 reduction in ILs is irreversible and forms $CO_2^{\bullet-}$ adsorbate at electrode interface. In the presence of O_2 and with increasing concentrations of CO_2, the reduction of oxygen is switched from a one-electron process to overall two-electron process, and forms adsorbed $CO_4^{\bullet-}$ intermediate species. Such information about the mechanisms of the reaction is highly beneficial for the development of the sensor systems.

2.4.2.5 IL Redox Chemistry Enabled Reliable Voltammetric Sensing

Study focusing on understanding the reaction mechanisms and comparing behavior to that in conventional electrolyte systems is an active research area and always establishes the foundation of reliable sensing before the actual sensing protocols are developed. In some cases, reactions and mechanisms have been found to be the similar in ILs as those in conventional solvents, however, in some cases, notable differences and unusual behavior have also been observed. It is extremely important to understand the atypical behavior in ILs before they can be employed as direct replacements for conventional molecular solvents (containing supporting electrolytes) in sensor devices. Compton's group [201], for example, has reported the two-electron reduction of 100 % chlorine gas to chloride on a Pt microelectrode in a range of ILs ($[C_2mim][NTf_2]$, $[C_4mim][NTf_2]$, $[C_4mPy][NTf_2]$, $[C_4mim][BF_4]$, $[C_4mim][PF_6]$, $[C_4mim][CF_3SO_3]$, $[N_{6,2,2,2}][NTf_2]$, and $[C_6mim][Cl]$). The behavior of the voltammetry at various scan rates was highly unusual, with limiting currents observed to decrease with increasing sweep rate. This intriguing observation was assigned to a mechanism of adsorption of chlorine gas on the Pt electrode surface. The adsorbed chlorine itself cannot be reduced, but must undergo desorption before the electron-transfer step. At slower scan rates with longer timescales, there is more desorption resulting in more surface available for electron transfer, thereby resulting in higher currents at slower scan rates. The large voltammetric currents observed suggest that Cl_2 has a very high solubility (1–10 M) in ILs, making these solvents attractive for the purposes of Cl_2 gas sensors. The authors did not report the effect of varying concentrations of Cl_2 on the current response, but this seems like the next logical step especially given the unusual adsorption mechanism. If the current scales linearly with concentration, ILs may prove to be a useful medium for robust Cl_2 gas sensing.

Although IL electrolytes provide partial selectivity, the primary selectivity of an IL–electrochemical sensor comes from the redox properties of the analyte observed using amperometric methods, wherein the electrical current generated by reaction of an analyte at an electrode at a fixed or variable potential is measured [22]. We have shown redox chemistry that occurs only in ILs and can be exploited to enhance sensor performance [202]. As shown in Fig. 2.16, we discovered that at platinum electrode in $[NTf_2]$-based ionic liquids (ILs), facile methane electro-oxidation is observed suggesting a unique catalytic Pt-$[NTf_2]$ interface for electron-transfer reaction of methane at room temperature. Little methane electro-oxidation signals are observed in ILs with other anions. In this experiment, an oxygen reduction process

was included; as a result, the incomplete methane oxidation product CO was fully oxidized to CO_2 in the presence of superoxide ions, since superoxide can quickly adsorb on the electrode surface to form the active species, and $[C_4mPy][NTf_2]$ is one of the best solvents to stabilize superoxide. In contrast to many methane oxidation systems reported, there are no incomplete oxidation products such as CO or COOH detected and the final methane oxidation products in $[C_4mPy][NTf_2]$ are confirmed to be CO_2 and water by in situ infrared spectroscopy and electrochemistry. The electrochemical oxidation of methane at Pt/$[C_4mPy][NTf_2]$ interface depends on the methane concentration linearly (from 1 % to 10 vol% methane concentration). As shown in Fig. 2.16, taking advantage of the unique coupled chemical reactivity of superoxide with the methane electrode oxidation product CO_2 that takes place in $[C_4mPy][NTf_2]$ at room temperature, we introduce an innovative internally referenced electrochemical method for methane detection that increases the reliability of the measurements by determining these two ambient gases within a single sample matrix in real time, with cross-validation occurring for a single sensory element. The coupled reactions facilitate the complete oxidation of methane to CO_2 and water in $[C_4mPy][NTf_2]$ and the in situ generated CO_2 was used as an internal standard for oxygen detection which addresses the fundamental limitations to accuracy and the long-term stability and reliability in chemical analysis. We have validated this ionic liquid-based methane sensor employing both conventional solid macroelectrodes and flexible microfabricated electrodes using single- and double-potential step chronoamperometry and the analytical parameters [202]. Figure 2.16 shows the amperometric response of a methane sensor with the IL $[C_4mPy][NTf_2]$, as methane concentration is increased and oxygen concentration is decreased. Both analytes can be selectively quantified by alternating the bias potential. Oxygen can be reduced to superoxide radical which was used for oxygen sensor development (−1.2 V) as shown in Fig. 2.16. High sensitivity, complete reversibility, long-term stability (less than 0.3 % potential shift over 90 days), rapid response, and strong selectivity (selectivity coefficient ~0.01 % for CO_2, NO, NO_2, and SO_2) of this IL oxygen sensor were observed. The simplicity of detection using low-power and low-cost potential step chronoamperometry and microfabricated electrodes provides strong foundation for their easy integration with engineering advancements such as portable electronics, networked sensing, and next-generation monolithic implementation for autonomous, maintenance-free sensor operation with a long lifetime for the detection of methane with high sensitivity and specificity using smaller, inexpensive, and low-power transducers for their applications for monitoring the methane emissions.

2.4.3 *Electrified IL/Electrode Interface and Related Sensor Based on Impedance Technique*

EIS, which involves the application of a sinusoidal electrochemical perturbation (potential or current) over a wide range of frequencies, allows for the measurement of impedance changes in the forms of double-layer capacitance and the

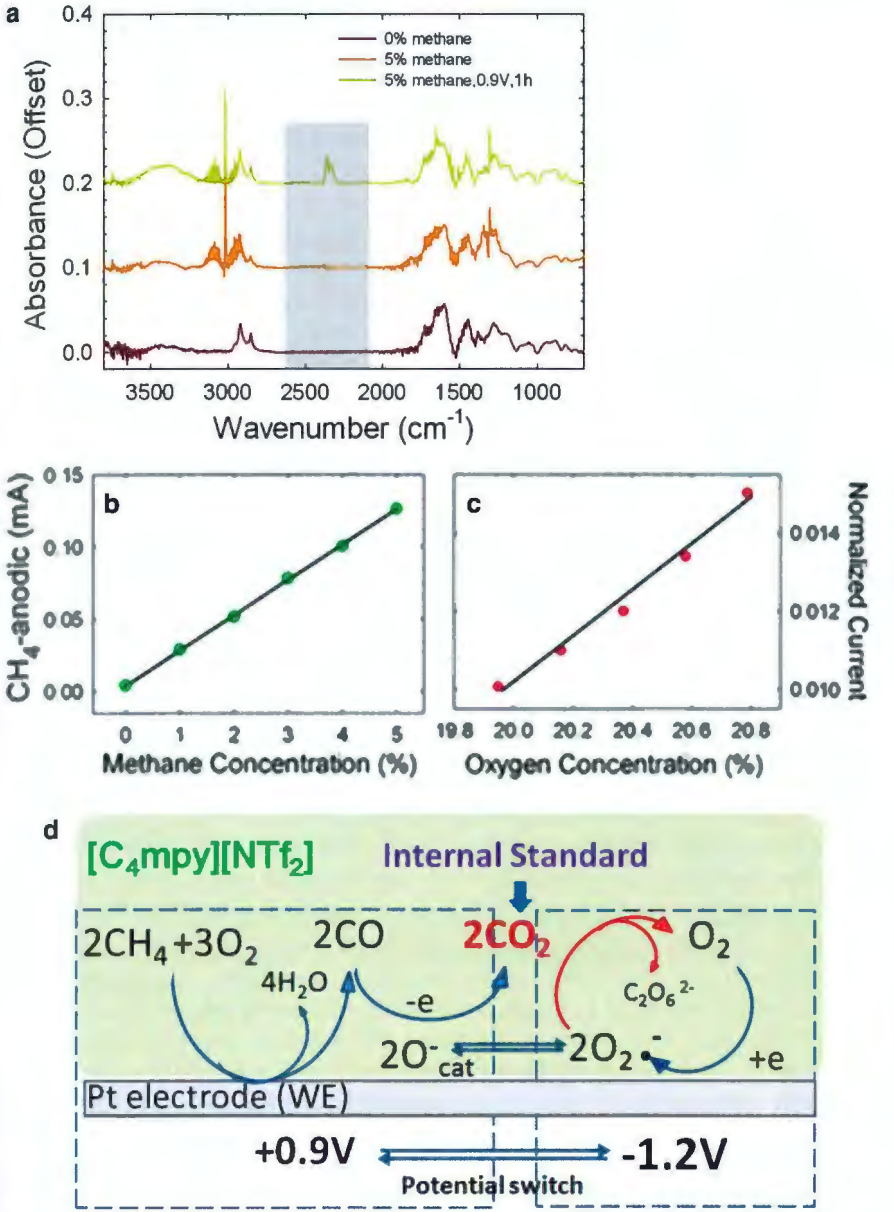

Fig. 2.16 (**a**) In situ FT-IR study of methane oxidation in $[C_4mPy][NTf_2]$; (**b**) plots of methane anodic currents at 0.9 V applied vs. methane concentration and (**c**) plots of normalized oxygen reduction currents at −1.2 V vs. oxygen concentration. (**d**) Scheme of methane oxidation and coupled oxygen reduction in $[C_4mPy][NTf_2]$

charge-transfer conductance that originate from the change of polarization of IL–electrode interface. The current signals and the impedance signals are all related to the active area of the electrodes. Thus, EIS-based sensors not only provide orthogonal detection modes to amperometric sensors but they also permit self-monitoring of the sensor's stability and automated calibration for drift mechanisms. We have demonstrated an innovative capacitance sensor based on the change of the surface charge at IL–electrified metal interfaces either due to the change of ion or electron transport in ILs resulted from the redox process of analyte or the polarization reaction due to adsorption/dissolution of analyte in ILs [80]. At room temperature, ILs have high viscosity, and the diffusion and conductivity of ions are normally lower in ILs than in aqueous electrolyte solutions. Thus, they can be regarded as a solid and liquid interface simultaneously. As a result, ILs are ideally suited for applications that require a thin or intensely concentrated layer of ionic charge, such as capacitance sensor development. Compared with molten salts at room temperature, the ions comprised of ILs are often large, flexible, highly polarizable, and chemically complex with a number of interionic forces (such as dispersion forces, dipole–dipole interaction, hydrogen bonding, and pi-stacking forces) in addition to coulombic forces present. Additionally, adsorption of anions and/or cations is likely to happen at the interfaces with ILs. Specific adsorption of IL on solid surface depends on the chemistry of the ions and applied potential. Varying the applied potential can result in the rearrangement of adsorbed ions which allows the modification of the IL double-layer capacitance. Capacitance at a fixed potential will depend on double-layer thickness and permittivity of the liquid at the interface. Ion size and applied potential influences the double-layer thickness, and alkyl chain length influences the relative permittivity. Consequently, varying the structure of IL anions or cations and applied potential enables the modification of the double-layer structure at the IL–electrified metal interface (e.g., thickness).

The double-layer structures in ILs are highly dependent on IL physicochemical properties and the applied potential. When exposed to an analyte especially small gaseous molecules, the molecular interaction events that occur at the IL interface can lead to polarization reaction at interface via redox reaction, binding, or dissolution of the analyte in ILs. For example, the analyte can displace or rearrange the IL order in the double layer to a new orientation. Removing analyte allows the IL double layer return to its original orientation. For example, the IL $[C_4mPy][NTf_2]$, which has a double-layer structure favoring small gas molecule adsorption, can sensitively and selectively measure concentrations of CH_4 (Fig. 2.17) using EIS with a −0.3 V DC bias [80]. Figure 2.17c also clearly shows that the sensor returns to its baseline value when the analyte is removed, demonstrating the reaction is fully reversible with less than 0.1 % drift. The selectivity comes from the unique highly ordered arrangement of ions in the innermost layer of IL–electrode interface which is potential dependent. The degree of ordered structure at IL–electrode interface can be tuned by the applied bias (e.g., −0.3 V for CH_4) and by the unique molecular structure of the IL ions. The high viscosity of ILs that is usually considered a limitation to practical electrochemical applications due to slow rate of mass transport is an advantage in capacitance [203] measurement due to a more ordered

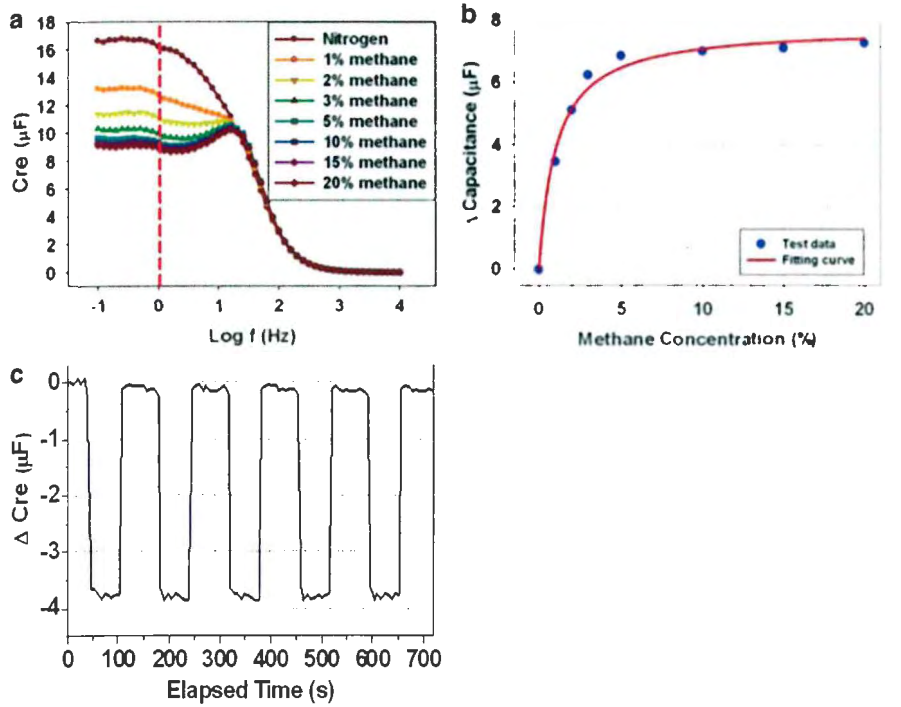

Fig. 2.17 (**a**) Plots of real part of complex capacitance at different methane concentrations. (**b**) Change of real part of complex capacitance (C_{re}) at 1 Hz vs. methane concentrations. [C_4mPy][NTf_2] is the IL and DC bias is –0.3 V; (**c**) C_{re} measured over five cycles of alternate exposure to 5 % methane (N_2 carrier gas at 200 sccm). DC potential is –0.3 V vs. Au quasi reference electrode. AC frequency is at 1 Hz

and concentrated double layer. Thus, impedance measurements provide an orthogonal detection mode to amperometric measurement, enhancing measurement sensitivity and improving sensor robustness.

2.4.4 *IL Electrochemical Microarrays*

For real-time multiple analyte monitoring, a group of sensors must be brought together, typically in an array format. We have demonstrated small arrays of IL sensors using both amperometric and impedance approaches. An array of four IL-coated glassy carbon electrodes was tested for the voltammetric detection of DNT and TNT, and a correlation (with 100 % classification accuracy) between the redox properties and the physiochemical parameters of the species involved was revealed (Fig. 2.18) [204]. Detection limits in liquid phase of 190 nM and 230 nM for TNT and DNT, respectively, and a linear range up to 100 μM were obtained.

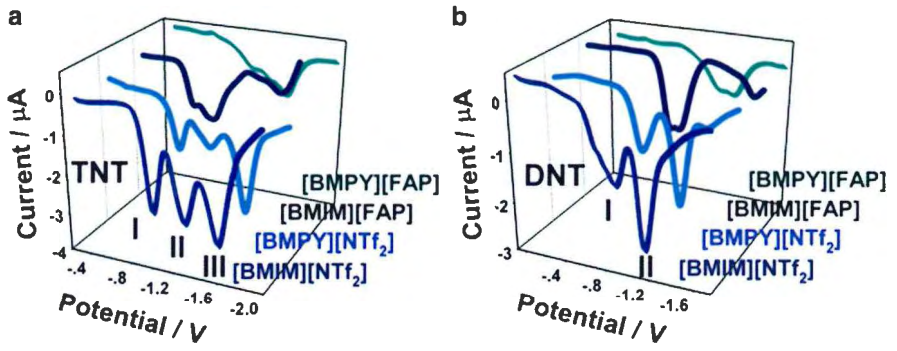

Fig. 2.18 Square wave voltammograms of 0.1 mM of TNT and DNT in four different ILs

Interference from water was eliminated by calibrating with a redox peak that was not proton related. Gas phase analysis showed strong redox signals for TNT and DNT and demonstrated that ILs serve as a preconcentrator to improve the sensitivity of very low vapor pressure analytes. These examples demonstrate that the combination of IL materials and electrochemical transducers overcomes many obstacles in forming an effective sensor system. IL–electrochemical sensors are also well suited for miniaturization and can be fabricated with very low cost. In contrast to nonspecific transducers such as a surface acoustic wave device, arrays of amperomertic and EIS transducers allow a secondary perturbation (e.g., potential) that enhances selectivity and increases analytical information content without increasing the number of physical sensor elements.

2.4.4.1 Microarray Fabrication

To improve current density and to overcome iR/Ohmic drop common in resistive ILs, small-sized working electrodes and eventually "lab-on-a-chip" type systems are being investigated. Microfabrication technologies, particularly thin film deposition of microelectrodes and formation of microfluidic channels, have been widely applied to analytical systems [205, 206]. Electrode arrays, both macro- and microscale, are now commonly fabricated using thin film metal deposition and photolithography [207–210]. For example, Fig. 2.19 shows an interdigitated electrode (IDE), which was fabricated using thin film deposition of gold on porous Teflon. Figure 2.19 also shows the data using this electrode for the measurement of oxygen concentrations. These miniaturized sensors yield similar sensitivity to results shown before. Similar fabrication techniques can be applied to optimize electrodes for the sensor interfaces developed within this project and design array structures. As fabrication of these electrodes relies on photolithography, the size and geometry of the electrode can easily be varied to meet the needs of the sensor interfaces, and different electrode configurations can be utilized within the same array to improve analytical performance.

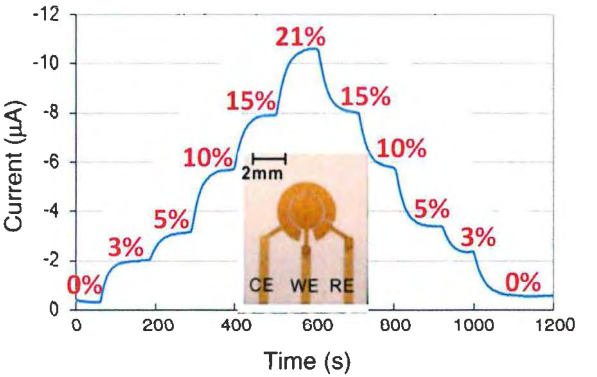

Fig. 2.19 Amperometric sensing of oxygen using (inset) micro-fabricated concentric ring disk electrode on porous Teflon

An ethylene gas sensor employing a thin layer of the IL $[C_4mim][BF_4]$ on a "lab-on-a-chip" sensor was proposed by Zevenbergen et al. [177] The sensor consisted of a 1-mm diameter Au working electrode surrounded by a Pt ring-shaped quasi-reference electrode and a Pt rectangular counter electrode. CV curve of ethylene in the IL revealed an oxidation peak before the onset of gold oxidation. Interestingly, the ethylene oxidation peak was only visible when water was present in the IL; no response was observed with humidity levels less than 20 %. As a result, the authors studied the dependence on humidity and observed larger responses when the humidity level was higher. A detection limit of 760 ppb and a linear response (current vs. concentration) up to 10 ppm were achieved. This suggests that amperometric ethylene detection in ILs is possible; however, it is limited only to environments with sufficient humidity levels (more than 40 %), which limits the application of such a sensor in extremely dry environments.

2.4.5 *IL as Component for New Electrode Materials*

Besides using ILs as electrolytes for electrochemical sensor development, their low melting points and low tendency to crystallize, realized by the combination of large, usually asymmetric cation and smaller anion, make them good candidates for electrode modifications that can lead to a diverse set of applications in sensing fields. These modifications can be done in many different ways as shown in Fig. 2.20; however, the choice of modification is entirely based on the application requirements. For example, IL/CNT-based composite materials, consisting of highly electroactive carbon nanotubes and fluid electrolyte, can be utilized for a wide variety of electrochemical applications, such as sensors, capacitors, and actuators. In electrochemical biosensors, these composite materials can also be used as an immobilizing matrix to entrap proteins and enzymes, which provide a favorable microenvironment

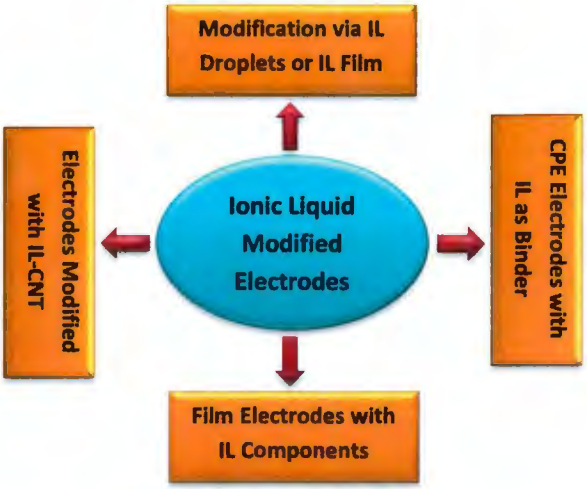

Fig. 2.20 Most common modes of the electrode modifications using ILs for different sensing applications

for redox proteins and enzymes to retain their bioactivity and perform direct electrochemistry and electrocatalysis. In the following sections, we will discuss some of the most common modifications for IL-based electrodes for sensing applications.

2.4.5.1 Electrodes Modified with IL Droplets or IL Films

Among many different types of electrode modifications possible for sensor applications, electrodes modified with IL droplets or films are the most commonly employed. In this method, electrodes are prepared by direct deposition of IL on the electrode surface [211] or from its diluted solution in volatile solvent [212]. These two procedures may provide different geometry of the deposit. Thin liquid film geometry is most important for sensors which can be enforced by surface coverage with porous Teflon membranes. The preparation of IL–modified electrode in situ by the adsorption of IL from aqueous solution has also been reported [213]. The appropriate selection of electrode substrate and IL is important in this case to obtain stable liquid deposit in contact with aqueous solution. Although research on IL–modified electrodes started from electrode substrate covered by droplets or liquid film, in the absence of other film components, now the focus has been shifted to film electrodes with organic or inorganic polymers, nanoparticles, nanotubes, and other micro- or nano-objects as other components. Their complexity ranges from simple ones as polymer film plasticized with IL to multicomponent films. The electrodes consisting of polymer membrane saturated with IL-based ionophore solution exhibit ion selectivity and were applied as ion-selective electrode. By using similar strategy with Ag/AgCl substrate, reference electrodes can be prepared. In particular, gel composed of poly(vinylidene fluoride-co-hexafluoropropylene) and viscous IL

(1-methyl-3-octylimidazolium bis-(trifluoromethyl-sulfonyl)imide) allows to obtain solid state and easy to miniaturize devices.

In many of these cases of direct modification, ILs, especially the imidazolium based, can also be appended to demonstrate functionalities which are related to their immobilization onto the electrodes to generate different types of modified electrodes. These functionalities include self-assemblies of IL on the electrode surface, covalent bonding of IL to the electrode surface, IL functions that can be used for the preparation of IL-based polymer (PILs) films, and IL used for the functionalization of conductive elements of the film. When the electrode is ready, the counter ions are electrostatically attracted to positively charged functionalities and they can be exchanged after immobilization on the electrode surface. Such small modifications can be highly suitable for incorporating the desired characteristics to the electrode materials. But most importantly, the electrodes modified by any of these methods can then be utilized for various sensing applications. For example, Ng et al. [214] employed a nanocomposite gel consisting of a three-dimensional graphene material and the IL $[C_4mim][PF_6]$ for the amperometric detection of nitric oxide (NO). A linear response of current vs. concentration over the range 1–16 μM NO was observed, with a fast response time of less than 4 s and a low detection limit of 16 nM. The improved response of this modified electrode is attributed to the porous graphene material that has a high specific surface area and superior conductivity which generated a 3-D graphene/IL nanocomposite to provide a novel platform for sensitive NO detection.

Although the generic combinations of IL with other electrode materials as shown in case of NO sensing have proven quite useful for sensing applications, the results are again generic in most cases with much less selectivity than required. Therefore, the focus is now shifting to use more task-specific ILs in the electrode modifications. Lu et al. [215] have shown that a task-specific IL in combination with bismuth oxide (Bi_2O_3) can be used for the electrochemical detection of heavy metal oxides including cadmium oxide (CdO), copper oxide (CuO), and lead oxide (PbO). The IL contained an $[NTf_2]^-$ anion and a tetraalkylammonium cation with one carbon chain functionalized with a carboxylic acid group. The presence of the acid group allowed for the solubilization of metal oxides into the IL. The IL was coated as a thin layer onto a surface containing three indium tin oxide (ITO) printed electrodes and acted as the selective solubilization medium and electrolyte. It is envisioned that more analyte species may begin to be detected by employing newly synthesized ILs with specific functional groups.

2.4.5.2 Carbon Paste Electrodes with IL as Binder

The high viscosity of ILs can also be employed to enhance the performance of the modified electrodes, for example, ILs as binders in carbon paste electrodes (CPE) which can then be used as sensing materials as well. In most cases, hydrophobic ILs are used for IL-based carbon paste electrodes (IL-CPE). Contrary to classic CPEs, their binder is composed of charged species and exhibits ionic conductivity which

enhances the electrochemical sensing capabilities of these modified electrodes. Typically, IL-CPEs are prepared as classic CPEs by mixing or grinding the graphite particles with IL and placing the mixture in a cavity of the polymer or glass tube. After polishing, the electrode is ready to use. The IL/graphite particles ratio has to be optimized from the point of view of not only mechanical stability but also capacitive current, resistance, and specific electrode process, and 7:3 graphite-to-IL ratio has become a popular composition. Imidazolium-type ILs also tend to form physical gel when ground with SWCNTs by physical cross-linking of the nanotube bundles, mediated by local molecular ordering of ILs. Recently, ILs have been found to be efficient binders in the preparation of carbon composite/carbon paste electrodes. They are prepared by mixing or grinding graphite particles with the IL, followed by the transfer of this mixture into a cavity of a polymer. Higher currents (both Faradaic and capacitive) are often observed at IL-CPEs compared to traditional CPEs. This is believed to be due to the larger electroactive area for electron transfer in the IL-CPEs due to the conductive IL medium. In traditional oil-based CPEs, electron transfer can only take place at the carbon/aqueous electrolyte interface. Other reasons for the higher currents may also be due to the changes in paste morphology, better solubility of polar analytes in the IL (compared to the binder), or the presence of additional interface where transfer across the liquid/liquid interface can occur.

From all this discussion, it is quite clear that ILs can be easily employed as a modifying component of the electrodes, and in whatever way it is done, they come up with good responses for analyte detection in synthetic and real-world samples. In particular, the higher currents at IL-CPEs compared to oil-CPEs have huge advantages for sensing applications. Task specificity renders high selectivity, if employed in this modification. Otherwise, many of the sensing performance parameters are enhanced up to certain extents, even if the ILs are used randomly. The ease of preparation and the low cost of such sensing systems suggest that this could be a very active field for future sensing of species in the food/drink industry and for environmental monitoring of soil/water samples.

2.4.6 Adsorption and Absorption-Based Chemical Sensing Using IL Thin Films

In contrast to electrochemical sensor, the high viscosity of ILs is beneficial for adsorption based sensor since they can be cast into a thin film which makes them suitable for many chemical sensing applications. Being highly volatile, solvents are seldom used as sensing elements. In contrast, ILs have no significant volatility, allowing chemical processes to be carried out with essentially zero emission of toxic organic solvents and enabling their utilization as recognition elements. In these applications, ILs behave as both solid and liquid interfaces simultaneously, thus overcoming the issues associated with the interchangeable use of solid and liquid phases and the requirement of solvents to generate these phases. Depending on the physical phenomenon involved for the solvation of analytes in ILs, a coating

of IL can swell, shrink, or undergo a viscosity change. The solvation in ILs is controlled by the variable contributions of adsorption-desorption and partition phenomena depending upon IL and analyte properties to furnish additional selectivity, thus opening up excellent opportunities to design different arrays of chemically selective IL films. Such characteristics make these ILs suitable for the detection of analytes in liquid or atmospheric environments via mass sensing approaches such as Quartz Crystal Microbalance (QCM) or MEMS.

2.4.6.1 IL-Based QCM Mass Sensor

QCM is a mass sensing transducer, the key component of which is quartz that functions for signal transduction and substrate for sensing materials. Applying alternating current to the gold electrodes coated on the quartz wafer induces mechanical oscillations modifiable by interfacial mass changes according to the Sauerbrey's equation:

$$\Delta f = -\frac{\Delta m f_0^2}{A\sqrt{\mu_q \rho_q}} \tag{2.6}$$

Here Δf=frequency shift, Δm=mass changes, f_0=fundamental frequency, A=electrode area, μ_q=quartz shear modulus, and ρ_q=quartz density. This principle assumes that the foreign mass is strongly coupled to the resonator making it quite straightforward for gas phase operations, where the added mass binds tightly to the surface, and the films are stiff and thin. However, density and viscosity strongly impact the nonrigid systems such as ILs, for which the following expression is used:

$$\Delta f = -f_0^{3/2}\left(\frac{\eta_L \rho_L}{\pi \mu_q \rho_q}\right)^{1/2} \tag{2.7}$$

Here η_L=viscosity and ρ_L=density of the liquid in contact with the crystal. ILs form stable layers just like the polymer matrices; however, being liquids, they bound firmly but not rigidly. QCM is capable of measuring the change of mass as well as the energy dissipation properties of thin films simultaneously, upon analyte adsorption/desorption or partition processes in thin films, thus providing rich information of the dynamic processes occurring during the adsorption–desorption events as depicted in Fig. 2.21. Dai and coworkers [216] first developed a sensor for organic vapors based on QCM using ILs as sensing materials. When analytes were dissolved in an IL, the viscosity of this IL changed rapidly which generated a frequency shift of the QCM device. The response of the QCM depended on the nature of both the analyte and the IL. Some of these ILs also have strong affinities for selected chemical species. Sensors comprising multiple of these sensors, each with a different IL coating, thus can not only detect target analytes but also help identify chemical speciation. In most of these cases, ILs are solely used as sensing films which interact with targets through ion and dipole forces, hydrogen bonding, and

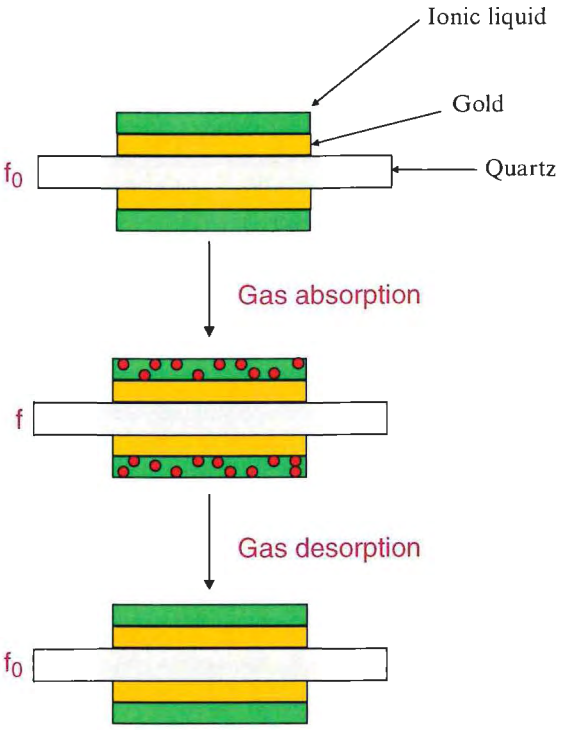

Fig. 2.21 Schematic illustration of the mechanism of frequency responses obtained in a QCM sensor

van der Waals interactions on various spatial and temporal scales. All these interactions depend upon variations in ionic composition and structure of ILs, thereby generating a criterion for selective incorporation and interaction of analytes. In addition, great solvation ability of ILs enables the rapid and reversible incorporation of gases, as shown in the work done by our group for detecting different explosive gases [176]. We have also shown that the very different solubilities of ILs for specific reactant gases create a membrane-like selectively to enhance or suppress (preconcentrate) the transport of specific reactants and provide a mechanism for selectivity [90]. Using this principle, we have successfully classified four volatile organic compounds (benzene, hexane, methylene chloride, and ethanol) via seven IL film-based mass sensors, where the unique selectivity of the ILs results from strong hydrogen bond basicity and significant capacity for dipole-type interactions with the analytes [217].

2.4.6.2 IL-Thin Film Formation

For the sorption-based sensor too, thin films on the electrodes are usually formed by employing the methods in the electrode modification sections. However, the effectiveness of most thin film-based sorption sensors relies on high sensitivity and specificity of the detection interface. The obvious approach to increase the sensitivity of

QCM sensors is to increase the thickness/amount of the sensing material. Pure ILs inherently possess certain limitations in this regard, especially for low molecular weight analytes, where sensitivity enhancement by thicker IL films can substantially influence the reproducibility through temperature-controlled variations in IL-layer thickness and the spreading out effects. Nonrigidity of thicker films makes the Sauerbrey's equation invalid in addition to slower responses, requiring a strategy to achieve higher IL loading while maintaining the IL-film integrity. For these situations, IL composite films are usually employed. Several approaches have been developed for fabricating IL-composite sensing films. In one such example, ILs are trapped as nanodroplets into the cylindrical cavities of solid alumina matrix, thus avoiding liquid wetting and softness [218]. Although this matrix can hold more IL than planar gold surface, the detection limits were not low enough for selected analytes. Contrarily, conducting polymers (CPs) and polyelectrolytes have charges, which make them ideal template materials to make IL-composite films. The proof of the concept was provided with the example of methane [219], a highly inflammable gas with very low molecular weight, and hence an evidential candidate for higher sensitivity in mass sensing devices requiring abundant total absorption/partition into the films. An ideal template for this purpose should be a porous and stable scaffold that can be modified to generate the required surface area and wettability for IL immobilization. Polyaniline (PAN) can provide this dimensionality. Four different oxidation states of PAN including the doped and undoped ones can be tested for the analytical response with an IL, e.g., 1-ethyl-3-methylimidazolium camphorsulfonate [C_2mim][CS], which can form hydrogen bonds through the sulfonate group; however, the doped PAN showed the highest sensitivity being highly charged, facilitating IL wettability through electrostatic interactions, in addition to hydrogen bonding. This increased IL surface area exposed to the analyte. The IL distribution into the nanosized channels of the PAN film helped to increase the response owing to the increase of IL film coverage. UV–vis and FT–IR data in this case confirmed [220] the formation of hydrogen bonds between camphorsulfonate and the nitrogen sites of protic acid-doped PAN. These bonds force the anions to align along the polymer backbone in a comb-like manner so as to enhance the long-range π-orbital conjugation. The interacting methane molecules can fit into these comb spaces and thus an enhanced sensitivity was observed. The enthalpy and entropy of the dissolution were shown to be higher than those in pure IL or PAN which further supported the existence of methane inside the composite generating a more ordered structure. Molecular mechanics simulation agreed with these results as well. This example and others indicate that CPs often have fairly rigid structures with tunable porosity and charge states, which can promote the rational development of the CP/IL interface alongside the IL-controlled parameters. The chemical selectivity can be provided by varying the oxidation states of CP and ionic structure of IL.

Besides this, many useful approaches are available for IL-composite formation both for their use in QCM sensors, biosensors, and even for their electrochemical sensing applications. The most widely used techniques include direct mixing, casting and rubbing, physical adsorption, electrodeposition, layer-by-layer assemblies, and sol–gel encapsulation. Physical adsorption of the IL onto a solid support is most

often used to prepare the sensing films, which is based on binding forces including ionic interactions, hydrogen bonds, van der Waals forces, hydrophobic interactions, and so on. However, the more sophisticated methods for this immobilization are electrodeposition, sol–gel encapsulation, and layer-by-layer assembly. In electrodeposition, a clean electrode is immersed in a bath containing the supporting electroactive material and corresponding IL which are then electrochemically deposited onto the electrodes [221, 222]. Electrodeposition of metal nanoparticles onto IL/CNT is another well-studied technique to prepare AuNP/IL/CNT nanocomposite-based sensors [223]. In sol–gel encapsulation, an IL–silica sol is synthesized which is then mixed with different types of interesting molecules to form the films [224], whereas in layer-by-layer method, a sequential deposition of multiple layers is achieved [225], one being the IL and the other one that is supporting material, onto the electrode surface by electrostatic, van der Waals, hydrogen bonding, and charge transfer interactions. From all these approaches, merits and demerits can be identified for any of them; however, the selection is highly related to the particular application in which the approach is going to be applied.

2.4.6.3 IL High Temperature Sensor

We have also demonstrated that the IL sensors show great promise for high-temperature gas sensing [226]. For that purpose, a polar IL, trihexyl(tetracdecyl) phosphonium dodecylbenzenesulphonate [$P_{14,6,6,6}$][DBS], was prepared via the alcohol-to-alkyl halide conversion method and coated onto QCM from its ethanol solution. This sensor was studied for the exposure of both polar (ethanol, dichloromethane) and nonpolar (heptane, benzene) vapors even at 200 °C showing linear response pattern and clear signals as shown in Fig. 2.22. As expected thermodynamically, the sensor signal decreased with increasing temperature, but still we could achieve a 5 % detection limit, which is encouraging because most solid surfaces are unable to adsorb vapors at temperatures that much higher than their boiling points. Additionally, there was an excellent reversibility for adsorption–desorption processes, requiring no experimental manipulation for sensor regeneration. The data for the damping resistance showed that physiochemical parameters such as Henry's constant can be more accurately determined at higher temperatures because of the lowered viscosity of the ILs.

2.4.6.4 IL Solvation and Other Sensing Platform

Although in many mass sensing applications, IL films play the role of solvents to dissolve the target analytes thereby having a partition coefficient, their roles as solvating species can be best described from the examples of optical sensing. Here, they dissolve many important optical substances to form stabilized optical matrices. For instance, Oter et al. reported [227] an optical CO_2 sensor using the ILs ([C_4mim][BF_4] or [C_4mim][Br]) as the matrix with 8-hydroxypyrene-1,3,6-trisulfonic acid

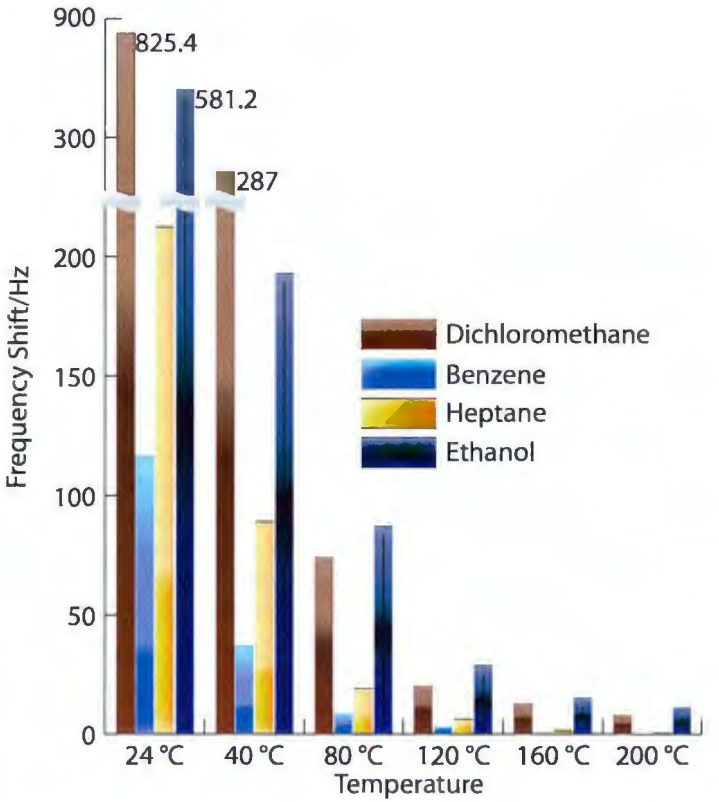

Fig. 2.22 Responses shown by IL-sensors from ambient to elevated temperatures for different volatile organic compounds (VOCs)

trisodium salt (HPTS). The detection of CO_2 is based on the fluorescence signal change of HPTS when pairing to CO_2. More recently, the same group reported [228] that IL modification of an ethyl cellulose matrix extended the detection range to 0–100 % pCO_2. In comparison to conventional solid matrix or liquid optical sensors, which have leaching problems, short life times because of evaporation of solvents, and poisoning issues from the ambient air and interfering gases, IL-based sensor showed much better performance due to IL's unique properties and better CO_2 adsorption than polymeric materials. Similar principles have been applied for temperature sensors, in which temperature indicators are dissolved in IL matrix to monitor temperatures in microregions, such as in case of microfluidics [229]. A hybrid electrochemical-colorimetric sensing platform for detecting explosives was also developed [230]. The product of the electrochemical reaction was detected by a colorimetric device. A thin layer of $[C_4mim][PF_6]$ played an important role in this platform: the IL coating selectively preconcentrated explosives by its solvation power and quickly transported them to the electrodes, and it facilitated the formation of reduction products.

2.4.6.5 Detection of Explosives and Chemical Warfare Agents

Although many of the new developments in this area can be covered by one of the previous headings, it seems appropriate to give this topic a separate section to highlight the importance of this area. With the increasing need of sensors for explosive materials at airports and security installations which may be at risk from improvised explosive devices, the interest in developing electrochemical and absorptive sensors for the detection of explosives is growing rapidly, and in the past few years, there have been several reports on the detection of explosive and toxic materials using ILs as solvent/supporting electrolytes. ILs are conductive and have low volatility, allowing them to be deployed in many types of extreme environments (e.g., hot/dry/arid conditions) where other sensor electrolytes would fail. In the prospects of such huge importance, the researchers have even used a combination of different sensing methodologies for these detections. For example, Forzani et al. proposed a hybrid electrochemical-colorimetric sensing platform for the detection of explosive trinitrotoluene (TNT) vapors [230]. A thin layer of the IL $[C_4mim][PF_6]$ was found to selectively preconcentrate the explosive materials and quickly transport the analytes to the electrodes. The explosive vapors were detected by electrochemical (cyclic voltammetry) and colorimetric (absorbance change) methods at the working electrode. The observed currents and distinct color changes provide a fingerprint for the identification and quantification of TNT. The same group later employed a conducting polymer nanojunction that was sensitive only to the reduction products of TNT and was able to discriminate from other redox-active interferents found in ambient air. The sensor simultaneously measured the current for the reduction of TNT and the resulting conductance change of the polymer, such as poly(ethylenedioxythiophene) (PEDOT). A linear response (current vs. concentration) was observed at concentrations of 30 pM to 6 nM TNT and the sensor was capable of detecting extremely low levels of TNT within 1–2 min.

Carbon materials have got a real interest in this sense, as they possess high surface area which can enhance the IL distribution in the film as well as help in improving the sensitivity which is critically required for explosive detections. Graphene is even special and, in conjunction with ILs, has been employed for highly selective sensing of explosive TNT by Guo et al. [231]. The IL $[C_4mim][PF_6]$ was combined with three-dimensional graphene to make an IL-graphene paste electrode with a large surface area, low background current, and pronounced mesoporosity. A linear relationship was observed between peak current using absorptive stripping voltammetry and concentration from 2 to 1,000 ppb, with a low detection limit of 0.5 ppb for TNT. This performance was superior to that demonstrated by IL-CNT and IL-graphite composites. We have also shown for many of explosive targets and employing electrochemical [204], piezoelectric [176], and EQCM platforms that by using IL materials, certain performance parameters can be achieved which are not usually possible with conventional materials.

These interesting works have shown that it is possible to selectively detect highly dangerous explosive and toxic species using an IL as an electrolyte and/or preconcentration medium. In many cases, the IL has been combined with other materials

(e.g., nanomaterials), or the electrochemical technique has been combined with a complementary technique. It seems that the high viscosity of ILs compared to conventional solvent/electrolyte systems (resulting in slower mass transport, smaller diffusion coefficients, and therefore lower currents) may prevent the detection of trace quantities of explosives that are required for a viable real-world sensor. However, perhaps one of their most useful applications could be as electrolytes in sensors that can be deployed directly after an explosion in an enclosed area where temperature could still be high and other electrolytes would volatilize. This would allow for the fast identification of "hot," "warm," and "cold" zones, allowing forensic personnel to determine the areas that are safe to enter for postexplosion analysis.

2.5 Future Directions and Concluding Remarks

This chapter gives a brief highlight of the current state of knowledge of IL-electrode interface study and the notable contributions to the sensor fields using IL materials from our laboratories and others. ILs bring in several benefits as nonvolatile and stable electrolytes and solvents for electrochemical sensor as well as sensing materials for adsorption-based mass sensor developments. By synergistically utilizing IL interface electrochemistry as well as molecular design and control of IL composites, ILs-based electrochemical and mass sensors are shown to enable multiple gas detections with multiple modes detection principles that can address many gas sensors challenges, especially for sensors that can operate in unconventional and hostile environments (i.e., elevated temperature, low pressure) or in the presence of typically interfering substances (e.g., high humidity, pyrophorics) as well as for sensor miniaturization and robustness. However, in order to further the developments of ILs for the sensor applications discussed here, many aspects of the behavior of ILs need urgent investigation as well: the fundamental electrochemical issues such as the structure of the double layer and diffusion layer at electrode/ionic liquid interface; the speciation of solute ions such as metal ions and polymerized ions; transference numbers and how these are influenced by speciation; dielectric properties and how these merge with conduction properties as a function of surface chemistry and the wetting phenomena of ILs at gas/liquid/solid interfaces; the thermodynamic quantities such as chemical potentials of solutes in ILs, and how these influence redox potentials and redox reversibility; ion association and its effect on thermodynamic and transport properties; and interactions of ILs with solutes and interfaces. Additionally, ILs have been shown as promising alternative solvents in a variety of applications. However, only a few processes are commercialized due to the relatively high cost of ILs. The recovery and reuse of ILs play an important role in the commercialization of processes employing ILs. The understanding of recyclability of ILs based on the available literature in various application fields is still in its infancy stage which was recognized by ILs' research communities. With ever flourishing research and applications of ILs in the future, the study toward thermal stability of ionic liquids for engineering applications should analyze the ILs with thoughts

on evaporation or temperatures at which evaporation kinetics are known. The temperature-dependent properties and the high dependency of the results on the experimental factors need to be investigated in the comparison of different conditions. In summary, many fundamental aspects of the physical chemistry and electrochemistry of ILs need to be thoroughly investigated, and they promise to further improve the potential of their various electrochemical and chemical applications.

Acknowledgement We like to thank the support from NIOSH R21, NIOSH R01, ONR, and MIIE. We also like to thank Professor Naifei Hu for helpful comments and suggestions.

References

1. Lu W, Fadeev AG, Qi BH, Smela E, Mattes BR, Ding J, Spinks GM, Mazurkiewicz J, Zhou DZ, Wallace GG, MacFarlane DR, Forsyth SA, Forsyth M (2002) Use of ionic liquids for pi-conjugated polymer electrochemical devices. Science 297(5583):983–987
2. Plechkova NV, Seddon KR (2008) Applications of ionic liquids in the chemical industry. Chem Soc Rev 37(1):123–150. doi:10.1039/B006677j
3. Blanchard LA, Brennecke JF (2001) Recovery of organic products from ionic liquids using supercritical carbon dioxide (vol 40, pg 289, 2001). Ind Eng Chem Res 40(11):2550
4. Endres F (2001) Electrodeposition of a thin germanium film on gold from a room temperature ionic liquid. Phys Chem Chem Phys 3(15):3165–3174
5. Handy ST (2003) Greener solvents: room temperature ionic liquids from biorenewable sources. Chemistry 9(13):2938–2944
6. Jensen MP, Neuefeind J, Beitz JV, Skanthakumar S, Soderholm L (2003) Mechanisms of metal ion transfer into room-temperature ionic liquids: the role of anion exchange. J Am Chem Soc 125(50):15466–15473
7. Yang CH, Sun QJ, Qiao J, Li YF (2003) Ionic liquid doped polymer light-emitting electrochemical cells. J Phys Chem B 107(47):12981–12988
8. Buzzeo MC, Evans RG, Compton RG (2004) Non-haloaluminate room-temperature ionic liquids in electrochemistry – a review. ChemPhysChem 5(8):1106–1120
9. Wei D, Ivaska A (2008) Applications of ionic liquids in electrochemical sensors. Anal Chim Acta 607(2):126–135
10. Rogers EI, Sljukic B, Hardacre C, Compton RG (2009) Electrochemistry in room-temperature ionic liquids: potential windows at mercury electrodes. J Chem Eng Data 54(7):2049–2053. doi:10.1021/Je800898z
11. Earle MJ, Esperança JMSS, Gilea MA, Lopes JNC, Rebelo LPN, Magee JW, Seddon KR, Widegren JA (2006) The distillation and volatility of ionic liquids. Nature 439:831. doi:10.1038/nature04451
12. Mays DE, Hussam A (2009) Voltammetric methods for determination and speciation of inorganic arsenic in the environment–a review. Anal Chim Acta 646(1–2):6–16. doi:10.1016/j.aca.2009.05.006
13. Macpherson JV, Marcar S, Unwin PR (1994) Microjet electrode – a hydrodynamic ultramicroelectrode with high mass-transfer rates. Anal Chem 66(13):2175–2179
14. Drummond TG, Hill MG, Barton JK (2003) Electrochemical DNA sensors. Nat Biotechnol 21(10):1192–1199. doi:10.1038/nbt873
15. Gallagher JJ, Svenson RH, Kasell JH, German LD, Bardy GH, Broughton A, Critelli G (1982) Catheter technique for closed-chest ablation of the atrioventricular-conduction system – a therapeutic alternative for the treatment of refractory supra-ventricular tachycardia. N Engl J Med 306(4):194–200

16. Wang J (2005) Carbon-nanotube based electrochemical biosensors: a review. Electroanal 17(1):7–14. doi:10.1002/elan.200403113
17. Laviron E (1974) Adsorption, autoinhibition and autocatalysis in polarography and in linear potential sweep voltammetry. Electroanal Chem Interracial Electrochem 52:355–393
18. Hayes R, Borisenko N, Tam MK, Howlett PC, Endres F, Atkin R (2011) Double layer structure of ionic liquids at the Au(111) electrode interface: an atomic force microscopy investigation. J Phys Chem C 115(14):6855–6863. doi:10.1021/Jp200544b
19. Baldelli S (2008) Surface structure at the ionic liquid-electrified metal interface. Acc Chem Res 41(3):421–431. doi:10.1021/ar700185h
20. Lockett V, Horne M, Sedev R, Rodopoulos T, Ralston J (2010) Differential capacitance of the double layer at the electrode/ionic liquids interface. Phys Chem Chem Phys 12(39):12499–12512. doi:10.1039/c0cp00170h
21. Hayes R, El Abedin SZ, Atkin R (2009) Pronounced structure in confined aprotic room-temperature ionic liquids. J Phys Chem B 113(20):7049–7052. doi:10.1021/Jp902837s
22. Stetter JR, Li J (2008) Amperometric gas sensors – a review. Chem Rev 108(2):352–366. doi:10.1021/Cr0681039
23. Tuantranont A, Wisitsora-at A, Sritongkham P, Jaruwongrungsee K (2011) A review of monolithic multichannel quartz crystal microbalance: a review. Anal Chim Acta 687(2):114–128. doi:10.1016/j.aca.2010.12.022
24. Rheaume JM, Pisano AP (2011) A review of recent progress in sensing of gas concentration by impedance change. Ionics 17(2):99–108. doi:10.1007/s11581-010-0515-1
25. Santos PS, Ando RA, Siqueira LJA, Bazito FC, Torresi RM (2007) The sulfur dioxide-1-butyl-3-methylimidazolium bromide interaction: drastic changes in structural and physical properties. J Phys Chem B 111(30):8717–8719. doi:10.1021/jp0743572
26. Sanchez LMG, Meindersma GW, de Haan AB (2007) Solvent properties of functionalized ionic liquids for CO2 absorption. Chem Eng Res Des 85(A1):31–39. doi:10.1205/cherd06124
27. Feng GA, Qiao R, Huang JS, Dai S, Sumpter BG, Meunier V (2011) The importance of ion size and electrode curvature on electrical double layers in ionic liquids. Phys Chem Chem Phys 13(3):1152–1161. doi:10.1039/C0cp02077j
28. Yuan HT, Shimotani H, Tsukazaki A, Ohtomo A, Kawasaki M, Iwasa Y (2010) Hydrogenation-induced surface polarity recognition and proton memory behavior at protic-ionic-liquid/oxide electric-double-layer interfaces. J Am Chem Soc 132(19):6672–6678. doi:10.1021/ja909110s
29. Sun J, Forsyth M, MacFarlane DR (1998) Room-temperature molten salts based on the quaternary ammonium ion. J Phys Chem B 102(44):8858–8864. doi:10.1021/jp981159p
30. MacFarlane DR, Meakin P, Sun J, Amini N, Forsyth M (1999) Pyrrolidinium imides: a new family of molten salts and conductive plastic crystal phases. J Phys Chem B 103(20):4164–4170. doi:10.1021/jp984145s
31. Bockris JOM, Swinkels DAJ (1964) Adsorption of n-decylamine on solid metal electrodes. J Electrochem Soc 111(6):736–743. doi:10.1149/1.2426222
32. Ryan JP, Kunz RJ, Shepard JW (1960) A radioactive tracer study of the adsorption of fluorinated compounds on solid planar surfaces. II. C8F17SO2N(C2H5)CH2COOH. J Phys Chem 64(5):525–529. doi:10.1021/j100834a003
33. Granese SL (1988) Study of the inhibitory-action of nitrogen-containing compounds. Corrosion 44(6):322–327
34. Vázquez CI, Lacconi GI (2013) Nucleation and growth of silver nanostructures onto HOPG electrodes in the presence of picolinic acid. J Electroanal Chem 691:42–50. doi:10.1016/j.jelechem.2012.12.017
35. Capon A, Parson R (1973) The oxidation of formic acid at noble metal electrodes: I. Review of previous work. J Electroanal Chem Interfacial Electrochem 44(1):1–7. doi:10.1016/S0022-0728(73)80508-X
36. Jeanmaire DL, Van Duyne RP (1977) Surface Raman spectroelectrochemistry: Part I. Heterocyclic, aromatic, and aliphatic amines adsorbed on the anodized silver electrode. J Electroanal Chem Interfacial Electrochem 84(1):1–20. doi:10.1016/S0022-0728(77)80224-6

37. Sandroff CJ, Herschbach DR (1982) Surface-enhanced Raman study of organic sulfides adsorbed on silver: facile cleavage of sulfur-sulfur and carbon-sulfur bonds. J Phys Chem 86(17):3277–3279. doi:10.1021/j100214a002
38. Rupprechter G, Dellwig T, Unterhalt H, Freund HJ (2001) High-pressure carbon monoxide adsorption on Pt(111) revisited: a sum frequency generation study. J Phys Chem B 105(18):3797–3802. doi:10.1021/jp003585s
39. Liu D, Ma G, Allen HC (2005) Adsorption of 4-picoline and piperidine to the hydrated SiO2 surface: probing the surface acidity with vibrational sum frequency generation spectroscopy. Environ Sci Technol 39(7):2025–2032. doi:10.1021/es0482280
40. Wang J, Buck SM, Chen Z (2002) Sum frequency generation vibrational spectroscopy studies on protein adsorption. J Phys Chem B 106(44):11666–11672. doi:10.1021/jp021363j
41. Bockris JOM, Jeng KT (1992) In-situ studies of adsorption of organic compounds on platinum electrodes. J Electroanal Chem 330(1–2):541–581. doi:10.1016/0022-0728(92)80330-7
42. Carlos-Cuellar S, Li P, Christensen AP, Krueger BJ, Burrichter C, Grassian VH (2003) Heterogeneous uptake kinetics of volatile organic compounds on oxide surfaces using a Knudsen cell reactor: adsorption of acetic acid, formaldehyde, and methanol on α-Fe2O3, α-Al2O3, and SiO2. J Phys Chem A 107(21):4250–4261. doi:10.1021/jp0267609
43. Bewick A, Kunimatsu K (1980) Infra red spectroscopy of the electrode-electrolyte interphase. Surf Sci 101(1–3):131–138. doi:10.1016/0039-6028(80)90604-4
44. Péré E, Cardy H, Cairon O, Simon M, Lacombe S (2001) Quantitative assessment of organic compounds adsorbed on silica gel by FTIR and UV–VIS spectroscopies: the contribution of diffuse reflectance spectroscopy. Vib Spectrosc 25(2):163–175. doi:10.1016/S0924-2031(00)00113-2
45. Park H, Choi W (2005) Photocatalytic reactivities of nafion-coated TiO2 for the degradation of charged organic compounds under UV or visible light. J Phys Chem B 109(23):11667–11674. doi:10.1021/jp051222s
46. Heinz TF, Chen CK, Ricard D, Shen YR (1982) Spectroscopy of molecular monolayers by resonant second-harmonic generation. Phys Rev Lett 48:478–481
47. Sagara T, Kawamura H, Nakashima N (1996) Electrode reaction of methylene blue at an alkanethiol-modified gold electrode as characterized by electroreflectance spectroscopy. Langmuir 12(17):4253–4259. doi:10.1021/la951530p
48. Chang J-K, Lee M-T, Tsai W-T, Deng M-J, Sun IW (2009) X-ray photoelectron spectroscopy and in situ X-ray absorption spectroscopy studies on reversible insertion/desertion of dicyanamide anions into/from manganese oxide in ionic liquid. Chem Mater 21(13):2688–2695. doi:10.1021/cm9000569
49. Gaillard C, Chaumont A, Billard I, Hennig C, Ouadi A, Wipff G (2007) Uranyl coordination in ionic liquids: the competition between ionic liquid anions, uranyl counterions, and Cl- anions investigated by extended X-ray absorption fine structure and UV–visible spectroscopies and molecular dynamics simulations. Inorg Chem 46(12):4815–4826. doi:10.1021/ic061864+
50. Del Pópolo MG, Lynden-Bell RM, Kohanoff J (2005) Ab initio molecular dynamics simulation of a room temperature ionic liquid. J Phys Chem B 109(12):5895–5902. doi:10.1021/jp044414g
51. Emel'yanenko VN, Verevkin SP, Heintz A (2007) The gaseous enthalpy of formation of the ionic liquid 1-butyl-3-methylimidazolium dicyanamide from combustion calorimetry, vapor pressure measurements, and ab initio calculations. J Am Chem Soc 129(13):3930–3937. doi:10.1021/ja0679174
52. De Feyter S, De Schryver FC (2003) Two-dimensional supramolecular self-assembly probed by scanning tunneling microscopy. Chem Soc Rev 32(3):139–150. doi:10.1039/b206566p
53. Hansma P, Elings V, Marti O, Bracker C (1988) Scanning tunneling microscopy and atomic force microscopy: application to biology and technology. Science 242(4876):209–216. doi:10.1126/science.3051380
54. De Feyter S, Gesquière A, Abdel-Mottaleb MM, Grim PCM, De Schryver FC, Meiners C, Sieffert M, Valiyaveettil S, Müllen K (2000) Scanning tunneling microscopy: a unique tool in

the study of chirality, dynamics, and reactivity in physisorbed organic monolayers. Acc Chem Res 33(8):520–531. doi:10.1021/ar970040g
55. Wilkinson KJ, Balnois E, Leppard GG, Buffle J (1999) Characteristic features of the major components of freshwater colloidal organic matter revealed by transmission electron and atomic force microscopy. Colloids Surf A Physicochem Eng Asp 155(2–3):287–310. doi:10.1016/S0927-7757(98)00874-7
56. Baldelli S, Bao JM, Wu W, Pei SS (2011) Sum frequency generation study on the orientation of room-temperature ionic liquid at the graphene-ionic liquid interface. Chem Phys Lett 516(4–6):171–173. doi:10.1016/j.cplett.2011.09.084
57. Santos CS, Baldelli S (2010) Gas-liquid interface of room-temperature ionic liquids. Chem Soc Rev 39(6):2136–2145. doi:10.1039/b921580h
58. Aliaga C, Baldelli S (2008) A sum frequency generation study of the room-temperature ionic liquid-titanium dioxide interface. J Phys Chem C 112(8):3064–3072. doi:10.1021/jp709753r
59. Endres F (2012) Interfaces of ionic liquids. Phys Chem Chem Phys 14(15):5008–5009. doi:10.1039/C2cp90031a
60. Endres F, Borisenko N, El Abedin SZ, Hayes R, Atkin R (2012) The interface ionic liquid(s)/electrode(s): in situ STM and AFM measurements. Faraday Discuss 154:221–233. doi:10.1039/C1fd00050k
61. Zhang SJ, Sun N, He XZ, Lu XM, Zhang XP (2006) Physical properties of ionic liquids: database and evaluation. J Phys Chem Ref Data 35(4):1475–1517. doi:10.1063/1.2204959
62. Rooney D, Jacquemin J, Gardas R (2010) Thermophysical properties of ionic liquids. In: Kirchner B (ed) Ionic liquids, vol 290, Topics in current chemistry. Springer, Berlin, pp 185–212. doi:10.1007/128_2008_32
63. Endres F, El Abedin SZ (2006) Air and water stable ionic liquids in physical chemistry. Phys Chem Chem Phys 8(18):2101–2116. doi:10.1039/B600519p
64. O'Mahony AM, Silvester DS, Aldous L, Hardacre C, Compton RG (2008) Effect of water on the electrochemical window and potential limits of room-temperature ionic liquids. J Chem Eng Data 53(12):2884–2891. doi:10.1021/je800678e
65. Dzyuba SV, Bartsch RA (2002) Influence of structural variations in 1-alkyl(aralkyl)-3-methylimidazolium hexafluorophosphates and bis(trifluorormethyl-sulfonyl)imides on physical properties of the ionic liquids. ChemPhysChem 3(2):161. doi:10.1002/1439-7641(20020215)3:2<161::Aid-Cphc161>3.0.Co;2-3
66. McEwen AB, Ngo HL, LeCompte K, Goldman JL (1999) Electrochemical properties of imidazolium salt electrolytes for electrochemical capacitor applications. J Electrochem Soc 146(5):1687–1695. doi:10.1149/1.1391827
67. Suarez PAZ, Einloft S, Dullius JEL, de Souza RF, Dupont J (1998) Synthesis and physical-chemical properties of ionic liquids based on 1-n-butyl-3-methylimidazolium cation. J Chim Phys Pcb 95(7):1626–1639
68. Wang HP, Liu WW, Cheng LY, Zhang YM, Yu MF (2008) The physical properties of aqueous solution of room-temperature ionic liquids based on imidazolium: database and evaluation. J Mol Liq 140(1–3):68–72. doi:10.1016/j.molliq.2008.01.008
69. Schroder C, Neumayr G, Steinhauser O (2009) On the collective network of ionic liquid/water mixtures. III. Structural analysis of ionic liquids on the basis of Voronoi decomposition. J Chem Phys 130(19), 194503. doi:10.1063/1.3127782
70. Schroder C, Rudas T, Neumayr G, Benkner S, Steinhauser O (2007) On the collective network of ionic liquid/water mixtures. I. Orientational structure. J Chem Phys 127(23), 234503. doi:10.1063/1.2805074
71. Schroder C, Rudas T, Neumayr G, Gansterer W, Steinhauser O (2007) Impact of anisotropy on the structure and dynamics of ionic liquids: a computational study of 1-butyl-3-methylimidazolium trifluoroacetate. J Chem Phys 127(4), 044505. doi:10.1063/1.2754690
72. Silvester DS, Compton RG (2006) Electrochemistry in room temperature ionic liquids: a review and some possible applications. Z Phys Chem 220(10–11):1247–1274. doi:10.1524/zpch.2006.220.10.1247

73. Ho TD, Zhang C, Hantao LW, Anderson JL (2014) Ionic Liquids in Analytical Chemistry: Fundamentals, Advances, and Perspectives. Analytical Chemistry 86 (1):262-285. doi:10.1021/Ac4035554
74. Soukup-Hein RJ, Warnke MM, Armstrong DW (2009) Ionic liquids in analytical chemistry. Annu Rev Anal Chem 2:145–168. doi:10.1146/annurev-anchem-060908-155150
75. Anderson JL, Armstrong DW, Wei GT (2006) Ionic liquids in analytical chemistry. Anal Chem 78(9):2892–2902. doi:10.1021/Ac069394o
76. Delahay P, Turner DR (1955) New instrumental methods in electrochemistry. J Electrochem Soc 102(2):46C–47C. doi:10.1149/1.2429993
77. Bard A, Faulkner L (2001) Electrochemical methods: fundamentals and applications. Wiley. citeulike-article-id:8415288. New York
78. Schroder U, Wadhawan JD, Compton RG, Marken F, Suarez PAZ, Consorti CS, de Souza RF, Dupont J (2000) Water-induced accelerated ion diffusion: voltammetric studies in 1-methyl-3-[2,6-(S)-dimethylocten-2-yl]imidazolium tetrafluoroborate, 1-butyl-3-methylimidazolium tetrafluoroborate and hexafluorophosphate ionic liquids. New J Chem 24(12):1009–1015. doi:10.1039/B007172M
79. Tang YJ, Zeng XQ (2008) Poly(vinyl ferrocene) redox behavior in ionic liquids. J Electrochem Soc 155(5):F82–F90. doi:10.1149/1.2868797
80. Wang Z, Mu X, Guo M, Huang Y, Mason AJ, Zeng X (2013) Methane recognition and quantification by differential capacitance at the hydrophobic ionic liquid-electrified metal electrode interface. J Electrochem Soc 160(6):B83–B89. doi:10.1149/2.138306jes
81. Taylor AW, Qiu FL, Hu JP, Licence P, Walsh DA (2008) Heterogeneous electron transfer kinetics at the ionic liquid/metal interface studied using cyclic voltammetry and scanning electrochemical microscopy. J Phys Chem B 112(42):13292–13299. doi:10.1021/Jp8024717
82. Muller EA, Strader ML, Johns JE, Yang A, Caplins BW, Shearer AJ, Suich DE, Harris CB (2013) Femtosecond electron solvation at the ionic liquid/metal electrode interface. J Am Chem Soc 135(29):10646–10653. doi:10.1021/ja3108593
83. Cremer T (2013) Ionic liquid/metal interfaces. Ionic liquid bulk and interface properties. Springer Theses. Springer International Publishing, pp 69–122. doi:10.1007/978-3-319-00380-1_4
84. Wu P, Huang JS, Meunier V, Sumpter BG, Qiao R (2011) Complex capacitance scaling in ionic liquids-filled nanopores. ACS Nano 5(11):9044–9051. doi:10.1021/Nn203260w
85. Kondrat S, Georgi N, Fedorov MV, Kornyshev AA (2011) A superionic state in nano-porous double-layer capacitors: insights from Monte Carlo simulations. Phys Chem Chem Phys 13(23):11359–11366. doi:10.1039/c1cp20798a
86. Druschler M, Huber B, Passerini S, Roling B (2010) Hysteresis effects in the potential-dependent double layer capacitance of room temperature ionic liquids at a polycrystalline platinum interface. J Phys Chem C 114(8):3614–3617. doi:10.1021/Jp911513k
87. Lau VWH, Masters AF, Bond AM, Maschmeyer T (2012) Ionic-liquid-mediated active-site control of MoS2 for the electrocatalytic hydrogen evolution reaction. Chemistry 18(26):8230–8239. doi:10.1002/chem.201200255
88. Kilic MS, Bazant MZ, Ajdari A (2007) Steric effects in the dynamics of electrolytes at large applied voltages. I. Double-layer charging. Phys Rev E 75(2), 021502. doi:10.1103/Physreve.75.021502
89. Gore TR, Bond T, Zhang WB, Scott RWJ, Burgess IJ (2010) Hysteresis in the measurement of double-layer capacitance at the gold-ionic liquid interface. Electrochem Commun 12(10):1340–1343. doi:10.1016/j.elecom.2010.07.015
90. Wang Z, Lin P, Baker GA, Stetter J, Zeng X (2011) Ionic liquids as electrolytes for the development of a robust amperometric oxygen sensor. Anal Chem 83(18):7066–7073. doi:10.1021/ac201235w
91. Galinski M, Lewandowski A, Stepniak I (2006) Ionic liquids as electrolytes. Electrochim Acta 51(26):5567–5580. doi:10.1016/j.electacta.2006.03.016
92. Sun P, Armstrong DW (2010) Ionic liquids in analytical chemistry. Anal Chim Acta 661(1):1–16. doi:10.1016/j.aca.2009.12.007
93. Hagiwara R, Lee JS (2007) Ionic liquids for electrochemical devices. Electrochemistry 75(1):23–34

94. Wang Z, Zeng X (2013) Bis(trifluoromethylsulfonyl)imide (NTf2)-based ionic liquids for facile methane electro-oxidation on Pt. J Electrochem Soc 160(9):H604–H611. doi:10.1149/2.039309jes
95. Seo DM, Borodin O, Balogh D, O'Connell M, Ly Q, Han SD, Passerini S, Henderson WA (2013) Electrolyte solvation and ionic association III. Acetonitrile-lithium salt mixtures-transport properties. J Electrochem Soc 160(8):A1061–A1070. doi:10.1149/2.018308jes
96. Frank HS, Wen W-Y (1957) Ion-solvent interaction. Structural aspects of ion-solvent interaction in aqueous solutions: a suggested picture of water structure. Discuss Faraday Soc 24:133–140. doi:10.1039/df9572400133
97. Kaminsky M (1957) Ion-solvent interaction and the viscosity of strong-electrolyte solutions. Discuss Faraday Soc 24:171–179. doi:10.1039/df9572400171
98. Visser AE, Rogers RD (2003) Room-temperature ionic liquids: new solvents for f-element separations and associated solution chemistry. J Solid State Chem 171(1–2):109–113. doi:10.1016/S0022-4596(02)00193-7
99. Bonhôte P, Dias A-P, Papageorgiou N, Kalyanasundaram K, Grätzel M (1996) Hydrophobic, highly conductive ambient-temperature molten salts. Inorg Chem 35(5):1168–1178. doi:10.1021/ic951325x
100. Lee PC, Han TH, Hwang T, Oh JS, Kim SJ, Kim BW, Lee Y, Choi HR, Jeoung SK, Yoo SE, Nam JD (2012) Electrochemical double layer capacitor performance of electrospun polymer fiber-electrolyte membrane fabricated by solvent-assisted and thermally induced compression molding processes. J Membr Sci 409:365–370. doi:10.1016/j.memsci.2012.04.007
101. Han XX, Zhou LX (2011) Optimization of process variables in the synthesis of butyl butyrate using acid ionic liquid as catalyst. Chem Eng J 172(1):459–466. doi:10.1016/j.cej.2011.06.025
102. Belding SR, Rees NV, Aldous L, Hardacre C, Compton RG (2008) Behavior of the heterogeneous electron-transfer rate constants of arenes and substituted anthracenes in room-temperature ionic liquids. J Phys Chem C 112(5):1650–1657. doi:10.1021/jp7103598
103. Law CS, Nodder SD, Mountjoy JJ, Marriner A, Orpin A, Pilditch CA, Franz P, Thompson K (2010) Geological, hydrodynamic and biogeochemical variability of a New Zealand deep-water methane cold seep during an integrated three-year time-series study. Mar Geol 272(1–4): 189–208. doi:10.1016/j.margeo.2009.06.018
104. Mirkin MV, Bard AJ (1992) Simple analysis of quasi-reversible steady-state voltammograms. Anal Chem 64(19):2293–2302. doi:10.1021/Ac00043a020
105. Wang Y, Kakiuchi T, Yasui Y, Mirkin MV (2010) Kinetics of ion transfer at the ionic liquid/water nanointerface. J Am Chem Soc 132(47):16945–16952. doi:10.1021/ja1066948
106. Barnes AS, Rogers EI, Streeter I, Aldous L, Hardacre C, Compton RG (2008) Extraction of electrode kinetic parameters from microdisc voltammetric data measured under transport conditions intermediate between steady-state convergent and transient linear diffusion as typically applies to room temperature ionic liquids. J Phys Chem B 112(25):7560–7565. doi:10.1021/jp711897b
107. Rogers EI, Huang X-J, Dickinson EJF, Hardacre C, Compton RG (2009) Investigating the mechanism and electrode kinetics of the oxygen|superoxide (O2|O2•–) couple in various room-temperature ionic liquids at gold and platinum electrodes in the temperature range 298–318 K. J Phys Chem C 113(41):17811–17823. doi:10.1021/jp9064054
108. Janek RP, Fawcett WR, Ulman A (1997) Impedance spectroscopy of self-assembled monolayers on Au(111): evidence for complex double-layer structure in aqueous NaClO4 at the potential of zero charge. J Phys Chem B 101(42):8550–8558. doi:10.1021/jp971698e
109. Wang ZW, Wu PY (2011) Spectral insights into gelation microdynamics of PNIPAM in an ionic liquid. J Phys Chem B 115(36):10604–10614. doi:10.1021/Jp205650h
110. Pasilis SP, Blumenfeld A (2011) Effect of nitrate, perchlorate, and water on uranyl(VI) speciation in a room-temperature ionic liquid: a spectroscopic investigation. Inorg Chem 50(17):8302–8307. doi:10.1021/Ic2008232
111. Gao Y, Li N, Zheng LQ, Zhao XY, Zhang J, Cao Q, Zhao MW, Li Z, Zhang GY (2007) The effect of water on the microstructure of 1-butyl-3-methylimidazolium tetrafluoroborate/TX-100/benzene ionic liquid microemulsions. Chemistry 13(9):2661–2670. doi:10.1002/chem.200600939

112. Roth C, Appelhagen A, Jobst N, Ludwig R (2012) Microheterogeneities in ionic-liquid-methanol solutions studied by FTIR spectroscopy, DFT calculations and molecular dynamics simulations. ChemPhysChem 13(7):1708–1717. doi:10.1002/cphc.201101022
113. Kortenbruck K, Pohrer B, Schluecker E, Friedel F, Ivanovic-Burmazovic I (2012) Determination of the diffusion coefficient of CO2 in the ionic liquid EMIM NTf2 using online FTIR measurements. J Chem Thermodyn 47:76–80. doi:10.1016/j.jct.2011.09.025
114. Zhang QH, Liu SM, Li ZP, Li J, Chen ZJ, Wang RF, Lu LJ, Deng YQ (2009) Novel cyclic sulfonium-based ionic liquids: synthesis, characterization, and physicochemical properties. Chemistry 15(3):765–778. doi:10.1002/chem.200800610
115. Tao GH, Zou M, Wang XH, Chen ZY, Evans DG, Kou Y (2005) Comparison of polarities of room-temperature ionic liquids using FT-IR spectroscopic probes. Aust J Chem 58(5):327–331. doi:10.1071/Ch05025
116. Shalu, Chaurasia SK, Singh RK, Chandra S (2013) Thermal stability, complexing behavior, and ionic transport of polymeric gel membranes based on polymer PVdF-HFP and ionic liquid, [BMIM][BF4]. J Phys Chem B 117(3):897–906. doi:10.1021/Jp307694q
117. Zhou D, Zhou R, Chen CX, Yee WA, Kong JH, Ding GQ, Lu XH (2013) Non-volatile polymer electrolyte based on poly(propylene carbonate), ionic liquid, and lithium perchlorate for electrochromic devices. J Phys Chem B 117(25):7783–7789. doi:10.1021/Jp4021678
118. Dobbelin M, Pozo-Gonzalo C, Marcilla R, Blanco R, Segura JL, Pomposo JA, Mecerreyes D (2009) Electrochemical synthesis of PEDOT derivatives bearing imidazolium-ionic liquid moieties. J Polym Sci Pol Chem 47(12):3010–3021. doi:10.1002/Pola.23384
119. Pieniazek PA, Stangret J (2005) Hydration of tetraethylammonium tetrafluoroborate derived from FTIR spectroscopy. Vib Spectrosc 39(1):81–87. doi:10.1016/j.vibspec.2004.11.004
120. Shamsuri AA, Daik R (2013) Utilization of an ionic liquid/urea mixture as a physical coupling agent for agarose/talc composite films. Materials 6(2):682–698. doi:10.3390/Ma6020682
121. Xie WL, Wang YB (2011) Synthesis of high fatty acid starch esters with 1-butyl-3-methylimidazolium chloride as a reaction medium. Starch-Starke 63 (4):190-197. doi:10.1002/star.201000126
122. Zadegan S, Hossainalipour M, Ghassai H, Rezaie HR, Naimi-Jamal MR (2010) Synthesis of cellulose-nanohydroxyapatite composite in 1-n-butyl-3-methylimidazolium chloride. Ceram Int 36(8):2375–2381. doi:10.1016/j.ceramint.2010.07.019
123. Du Z, Yu YL, Wang JH (2007) Extraction of proteins from biological fluids by use of an ionic liquid/aqueous two-phase system. Chemistry 13(7):2130–2137. doi:10.1002/chem.200601234
124. Atkin R, Abedin SZE, Hayes R, Gasparotto LHS, Borisenko N, Endres F (2009) AFM and STM studies on the surface interaction of [BMP]TFSA and [EMIm]TFSA ionic liquids with Au(111). J Phys Chem C 113(30):13266–13272. doi:10.1021/jp9026755
125. Hasib-ur-Rahman M, Larachi F (2012) CO2 Capture in alkanolamine-RTIL blends via carbamate crystallization: route to efficient regeneration. Environ Sci Technol 46(20):11443–11450. doi:10.1021/Es302513j
126. Rai R, Pandey S, Baker SN, Vora S, Behera K, Baker GA, Pandey S (2012) Ethanol-Assisted, Few Nanometer, Water-In-Ionic-Liquid Reverse Micelle Formation by a Zwitterionic Surfactant. Chemistry-a European Journal 18 (39):12213-12217. doi:10.1002/chem.201200682
127. Andanson JM, Jutz F, Baiker A (2009) Supercritical CO2/ionic liquid systems: what can we extract from infrared and Raman spectra? J Phys Chem B 113(30):10249–10254. doi:10.1021/Jp904440x
128. Chambreau SD, Schneider S, Rosander M, Hawkins T, Gallegos CJ, Pastewait MF, Vaghjiani GL (2008) Fourier transform infrared studies in hypergolic ignition of ionic liquids. J Phys Chem A 112(34):7816–7824. doi:10.1021/Jp8038175
129. Xue ZM, Zhang ZF, Han J, Chen Y, Mu TC (2011) Carbon dioxide capture by a dual amino ionic liquid with amino-functionalized imidazolium cation and taurine anion. Int J Greenh Gas Con 5(4):628–633. doi:10.1016/j.ijggc.2011.05.014
130. Sakellarlos NI, Kazarian SG (2005) Solute partitioning between an ionic liquid and high-pressure CO2 studied with in situ FTIR spectroscopy. J Chem Thermodyn 37(6):621–626. doi:10.1016/j.jct.2005.03.022

131. Du XZ, Miao W, Liang YQ (2005) IRRAS studies on chain orientation in the monolayers of amino acid amphiphiles at the air-water interface depending on metal complex and hydrogen bond formation with the headgroups. J Phys Chem B 109(15):7428–7434. doi:10.1021/Jp0441700
132. Andanson JM, Jutz F, Baiker A (2010) Purification of ionic liquids by supercritical CO2 monitored by infrared spectroscopy. J Supercrit Fluid 55(1):395–400. doi:10.1016/j.supflu.2010.08.012
133. Du XZ, Liang YQ (2000) Roles of metal complex and hydrogen bond in molecular structures and phase behaviors of metal N-octadecanoyl-L-alaninate Langmuir-Blodgett films. J Phys Chem B 104(43):10047–10052. doi:10.1021/Jp002016h
134. Xing DY, Peng N, Chung TS (2011) Investigation of unique interactions between cellulose acetate and ionic liquid [EMIM]SCN, and their influences on hollow fiber ultrafiltration membranes. J Membr Sci 380(1–2):87–97. doi:10.1016/j.memsci.2011.06.032
135. Dahl K, Sando GM, Fox DM, Sutto TE, Owrutsky JC (2005) Vibrational spectroscopy and dynamics of small anions in ionic liquid solutions. J Chem Phys 123(8), 084504. doi:10.1063/1.2000229
136. Siddiqui KA, Mehrotra GK, Mrozinski J, Butcher RJ (2008) H-bonded porous supramolecular network of a Cu-II complex assisted by assembled 2D sheet of chair form hexameric water cluster. Eur J Inorg Chem 26:4166–4172. doi:10.1002/ejic.200800463
137. Zhang MJ, Zhao PP, Leng Y, Chen GJ, Wang J, Huang J (2012) Schiff base structured acid-base cooperative dual sites in an ionic solid catalyst lead to efficient heterogeneous knoevenagel condensations. Chemistry 18 (40):12773-12782. doi:10.1002/chem.201201338
138. He HY, Chen H, Zheng YZ, Zhang XC, Yao XQ, Yu ZW, Zhang SJ (2013) The hydrogen-bonding interactions between 1-ethyl-3-methylimidazolium lactate ionic liquid and methanol. Aust J Chem 66(1):50–59. doi:10.1071/Ch12308
139. Liu M, Li LS, Da SL, Feng YQ (2004) Preparation of p-tert-butyl-calix[8]arene bonded silica stationary phase and separation for steroid hormone medicines. Anal Lett 37(14):3017–3031. doi:10.1081/Al-200035899
140. Soll S, Zhao Q, Weber J, Yuan JY (2013) Activated CO2 sorption in mesoporous imidazolium-type poly(ionic liquid)-based polyampholytes. Chem Mater 25(15):3003–3010. doi:10.1021/Cm4009128
141. Tadjeddine A, Peremans A, Guyotsionnest P (1995) Vibrational spectroscopy of the electrochemical interface by visible-infrared sum-frequency generation. Surf Sci 335(1–3):210–220. doi:10.1016/0039-6028(95)00419-X
142. Busson B, Tadjeddine A (2010) Chiral specificity of doubly resonant sum-frequency generation in an anisotropic thin film (vol 112C, pg 11813, 2008). J Phys Chem C 114(49):21891. doi:10.1021/Jp110099k
143. Bozzini B, Busson B, Humbert C, Mele C, Raffa P, Tadjeddine A (2011) Investigation of Au electrodeposition from [BMP][TFSA] room-temperature ionic liquid containing K[Au(CN)(2)] by in situ two-dimensional sum frequency generation spectroscopy. J Electroanal Chem 661(1):20–24. doi:10.1016/j.jelechem.2011.07.004
144. Guyotsionnest P, Tadjeddine A (1990) Spectroscopic investigations of adsorbates at the metal electrolyte interface using sum frequency generation. Chem Phys Lett 172(5):341–345. doi:10.1016/S0009-2614(90)87124-A
145. Tadjeddine A, Guyotsionnest P (1991) Spectroscopic investigation of adsorbed cyanide and thiocyanate on platinum using sum frequency generation. Electrochim Acta 36(11–12):1839–1847
146. Tadjeddine A, Guyotsionnest P (1993) Spectroscopic investigation of adsorbed cyanide and thiocyanate ions on platinum by sum-frequency generation. Sov Electrochem 29(1):94–101
147. Rollins JB, Fitchett BD, Conboy JC (2007) Structure and orientation of the imidazolium cation at the room-temperature ionic liquid/SiO2 interface measured by sum-frequency vibrational spectroscopy. J Phys Chem B 111(18):4990–4999. doi:10.1021/Jp0671906
148. Fitchett BA, Conboy JC (2004) Structure of the room-temperature ionic liquid/SiO2 interface studied by sum-frequency vibrational spectroscopy. J Phys Chem B 108(52):20255–20262. doi:10.1021/Jp0471251

149. Conboy JC, Messmer MC, Richmond GL (1997) Dependence of alkyl chain conformation of simple ionic surfactants on head group functionality as studied by vibrational sum-frequency spectroscopy. J Phys Chem B 101(34):6724–6733. doi:10.1021/Jp971867v
150. Baldelli S (2003) Influence of water on the orientation of cations at the surface of a room-temperature ionic liquid: a sum frequency generation vibrational spectroscopic study. J Phys Chem B 107(25):6148–6152. doi:10.1021/jp027753n
151. Roling B, Druschler M, Huber B (2012) Slow and fast capacitive process taking place at the ionic liquid/electrode interface. Faraday Discuss 154:303–311. doi:10.1039/C1fd00088h
152. Baldelli S (2005) Probing electric fields at the ionic liquid-electrode interface using sum frequency generation spectroscopy and electrochemistry. J Phys Chem B 109(27):13049–13051. doi:10.1021/Jp052913r
153. Hillman AR (2011) The EQCM: electrogravimetry with a light touch. J Solid State Electrochem 15(7–8):1647–1660. doi:10.1007/s10008-011-1371-2
154. Xiao CH, Zeng XQ (2013) In situ EQCM evaluation of the reaction between carbon dioxide and electrogenerated superoxide in ionic liquids. J Electrochem Soc 160(10):H749–H756. doi:10.1149/2.073310jes
155. Tang Y, Baker GA, Zeng X (2010) Ionic liquid conditioning of poly(vinylferrocene) for the doping/undoping of glycylglycylglycine tripeptide. J Phys Chem C 114(32):13709–13715. doi:10.1021/jp1030202
156. Levi MD, Sigalov S, Aurbach D, Daikhin L (2013) In situ electrochemical quartz crystal admittance methodology for tracking compositional and mechanical changes in porous carbon electrodes. J Phys Chem C 117(29):14876–14889. doi:10.1021/jp403065y
157. Levi MD, Salitra G, Levy N, Aurbach D, Maier J (2009) Application of a quartz-crystal microbalance to measure ionic fluxes in microporous carbons for energy storage. Nat Mater 8(11):872–875. doi:10.1038/nmat2559
158. Sigalov S, Levi MD, Salitra G, Aurbach D, Maier J (2010) EQCM as a unique tool for determination of ionic fluxes in microporous carbons as a function of surface charge distribution. Electrochem Commun 12(12):1718–1721. doi:10.1016/j.elecom.2010.10.005
159. Oyama T, Yamaguchi S, Rahman MR, Okajima T, Ohsaka T, Oyama N (2010) EQCM study of the [Au(III)Cl4](-)-[Au(I)Cl2](-)-Au(0) redox system in 1-ethyl-3-methylimidazolium tetrafluoroborate room-temperature ionic liquid. Langmuir 26(11):9069–9075. doi:10.1021/la904483y
160. Giessibl FJ (2003) Advances in atomic force microscopy. Rev Mod Phys 75(3):949–983
161. Batchelor-McAuley C, Dickinson EJF, Rees NV, Toghill KE, Compton RG (2011) New electrochemical methods. Anal Chem 84(2):669–684. doi:10.1021/ac2026767
162. Valtiner M, Ankah GN, Bashir A, Renner FU (2011) Atomic force microscope imaging and force measurements at electrified and actively corroding interfaces: challenges and novel cell design. Rev Sci Instrum 82(2):023703. doi:10.1063/1.3541650
163. Guriyanova S, Mairanovsky VG, Bonaccurso E (2011) Superviscosity and electroviscous effects at an electrode/aqueous electrolyte interface: an atomic force microscope study. J Colloid Interface Sci 360(2):800–804. doi:10.1016/j.jcis.2011.04.072
164. Fedorov MV, Kornyshev AA (2008) Ionic liquid near a charged wall: structure and capacitance of electrical double layer. J Phys Chem B 112(38):11868–11872. doi:10.1021/jp803440q
165. Atkin R, Warr GG (2007) Structure in confined room-temperature ionic liquids. J Phys Chem C 111(13):5162–5168. doi:10.1021/jp067420g
166. Mezger M, Schroder H, Reichert H, Schramm S, Okasinski JS, Schoder S, Honkimaki V, Deutsch M, Ocko BM, Ralston J, Rohwerder M, Stratmann M, Dosch H (2008) Molecular layering of fluorinated ionic liquids at a charged sapphire (0001) surface. Science 322(5900):424–428. doi:10.1126/science.1164502
167. Fedorov MV, Georgi N, Kornyshev AA (2010) Double layer in ionic liquids: the nature of the camel shape of capacitance. Electrochem Commun 12(2):296–299. doi:10.1016/j.elecom.2009.12.019
168. Bazant MZ, Storey BD, Kornyshev AA (2011) Double layer in ionic liquids: overscreening versus crowding. Phys Rev Lett 106(4):046102

169. Lim RYH, O'Shea SJ (2004) Discrete solvation layering in confined binary liquids. Langmuir 20(12):4916–4919. doi:10.1021/la036200g
170. Endres F, Hofft O, Borisenko N, Gasparotto LH, Prowald A, Al-Salman R, Carstens T, Atkin R, Bund A, Zein El Abedin S (2010) Do solvation layers of ionic liquids influence electrochemical reactions? Phys Chem Chem Phys 12(8):1724–1732. doi:10.1039/b923527m
171. Atkin R, Borisenko N, Druschler M, el-Abedin SZ, Endres F, Hayes R, Huber B, Roling B (2011) An in situ STM/AFM and impedance spectroscopy study of the extremely pure 1-butyl-1-methylpyrrolidinium tris(pentafluoroethyl)trifluorophosphate/Au(111) interface: potential dependent solvation layers and the herringbone reconstruction. Phys Chem Chem Phys 13(15):6849–6857. doi:10.1039/c0cp02846k
172. Singh PR, Zeng X (2011) Size-dependent intercalation of ions into highly oriented pyrolytic graphite in ionic liquids: an electrochemical atomic force microscopy study. J Phys Chem C 115(35):17429–17439. doi:10.1021/jp203833v
173. K-I U, K-I F (2010) Observation of redox-state-dependent reversible local structural change of ferrocenyl-terminated molecular island by electrochemical frequency modulation AFM. Langmuir 26(11):9104–9110. doi:10.1021/la904797h
174. Rehman A, Zeng X (2012) Ionic liquids as green solvents and electrolytes for robust chemical sensor development. Acc Chem Res 45(10):1667–1677. doi:10.1021/ar200330v
175. Shiddiky MJA, Torriero AAJ (2011) Application of ionic liquids in electrochemical sensing systems. Biosens Bioelectron 26(5):1775–1787. doi:10.1016/j.bios.2010.08.064
176. Rehman A, Hamilton A, Chung A, Baker GA, Wang Z, Zeng XQ (2011) Differential solute gas response in ionic-liquid-based QCM arrays: elucidating design factors responsible for discriminative explosive gas sensing. Anal Chem 83(20):7823–7833. doi:10.1021/ac201583c
177. Zevenbergen MAG, Wouters D, Dam V-AT, Brongersma SH, Crego-Calama M (2011) Electrochemical sensing of ethylene employing a thin ionic-liquid layer. Anal Chem 83(16):6300–6307. doi:10.1021/ac2009756
178. Aguilar AD, Forzani ES, Leright M, Tsow F, Cagan A, Iglesias RA, Nagahara LA, Amlani I, Tsui R, Tao NJ (2010) A hybrid nanosensor for TNT vapor detection. Nano Lett 10(2):380–384. doi:10.1021/nl902382s
179. Huang X-J, Aldous L, O'Mahony AM, Javier del Campo F, Compton RG (2010) Toward membrane-free amperometric gas sensors: a microelectrode array approach. Anal Chem 82(12):5238–5245. doi:10.1021/ac1006359
180. Torriero AAJ, Bond AM (2009) Critical evaluation of dynamic electrochemistry in ionic liquids. In: Electroanalytical chemistry research trend. Nova Science, New York, NY, pp 1–63
181. Turner MB, Spear SK, Holbrey JD, Rogers RD (2004) Production of bioactive cellulose films reconstituted from ionic liquids. Biomacromolecules 5(4):1379–1384. doi:10.1021/bm049748q
182. Liu Y, Wang M, Li J, Li Z, He P, Liu H, Li J (2005) Highly active horseradish peroxidase immobilized in 1-butyl-3-methylimidazolium tetrafluoroborate room-temperature ionic liquid based sol-gel host materials. Chem Commun 13:1778–1780. doi:10.1039/b417680d
183. Bontempelli G, Comisso N, Toniolo R, Schiavon G (1997) Electroanalytical sensors for nonconducting media based on electrodes supported on perfluorinated ion-exchange membranes. Electroanalysis 9(6):433–443
184. Cox JA, Alber KS, Brockway CA, Tess ME, Gorski W (1995) Solid-phase extraction in conjunction with solution or solid-state voltammetry as a strategy for the determination of neutral organic-compounds. Anal Chem 67(5):993–998
185. Barroso-Fernandez B, Lee-Alvarez MT, Seliskar CJ, Heineman WR (1998) Electrochemical behavior of methyl viologen at graphite electrodes modified with Nafion sol-gel composite. Anal Chim Acta 370(2–3):221–230
186. Otsuki S, Adachi K (1995) Characterization of Nafion solutions and films and observation of the casting process using basic-dyes as optical probes. J Appl Polym Sci 56(6):697–705
187. Rehman A, Xiao C, Zeng X (2012) Dynamics of redox process in ionic liquids and their interplay for discriminative electrochemical sensing. Anal Chem 84(3):1416–1424
188. Stetter JR, Korotcenkov G, Zeng X, Tang Y, Liu Y (2011) Electrochemical gas sensors: fundamentals, fabrication, and parameters. In: Korotcenkov G (ed) Chemical sensors comprehensive

sensor technologies, vol 5, Sensors technology series. Momentum Press, LLC, New York, NY, pp 1–89
189. Samec Z, Langmaier J, Kakiuchi T (2009) Charge-transfer processes at the interface between hydrophobic ionic liquid and water. Pure Appl Chem 81(8):1473–1488. doi:10.1351/Pac-Con-08-08-36
190. Yasui Y, Kitazumi Y, Ishimatsu R, Nishi N, Kakiuchi T (2009) Ultraslow response of interfacial tension to the change in the phase-boundary potential at the interface between water and a room-temperature ionic liquid, trioctylmethylammonium bis(nonafluorobutanesulfonyl) amide. J Phys Chem B 113(11):3273–3276. doi:10.1021/jp9006312
191. Morf WE (1981) The principles of ion-selective electrodes and of membrane transport. Elsevier, Amsterdam
192. Peng B, Zhu J, Liu X, Qin Y (2008) Potentiometric response of ion-selective membranes with ionic liquids as ion-exchanger and plasticizer. Sensors Actuators B Chem 133(1):308–314. doi:10.1016/j.snb.2008.02.027
193. Liu H, Liu Y, Li J (2010) Ionic liquids in surface electrochemistry. Phys Chem Chem Phys 12(8):1685–1697
194. Zhu J, Qin Y, Zhang Y (2009) Preparation of all solid-state potentiometric ion sensors with polymer-CNT composites. Electrochem Commun 11(8):1684–1687. doi:10.1016/j.elecom.2009.06.025
195. Nishi N, Murakami H, Yasui Y, Kakiuchi T (2008) Use of highly hydrophobic ionic liquids for ion-selective electrodes of the liquid membrane type. Anal Sci 24(10):1315–1320. doi:10.2116/analsci.24.1315
196. Bakker E, Pretsch E (2007) Modern potentiometry. Angew Chem Int Ed 46(30):5660–5668. doi:10.1002/anie.200605068
197. Langmaier J, Samec Z (2009) Voltammetry of ion transfer across a polarized room-temperature ionic liquid membrane facilitated by valinomycin: theoretical aspects and application. Anal Chem 81(15):6382–6389. doi:10.1021/ac9008258
198. Silvester DS, Arrigan DWM (2011) Array of water vertical bar room temperature ionic liquid micro-interfaces. Electrochem Commun 13(5):477–479. doi:10.1016/j.elecom.2011.02.025
199. Buzzeo MC, Hardacre C, Compton RG (2004) Use of room temperature ionic liquids in gas sensor design. Anal Chem 76(15):4583–4588. doi:10.1021/ac040042w
200. Barrosse-Antle LE, Bond AM, Compton RG, O'Mahony AM, Rogers EI, Silvester DS (2010) Voltammetry in room temperature ionic liquids: comparisons and contrasts with conventional electrochemical solvents. Chemistry 5(2):202–230. doi:10.1002/asia.200900191
201. Huang X-J, Silvester DS, Streeter I, Aldous L, Hardacre C, Compton RG (2008) Electroreduction of chlorine gas at platinum electrodes in several room temperature ionic liquids: evidence of strong adsorption on the electrode surface revealed by unusual voltammetry in which currents decrease with increasing voltage scan rates. J Phys Chem C 112(49):19477–19483. doi:10.1021/jp8082437
202. Wang Z, Guo M, Baker GA, Stetter J, Lin L, Mason AJ, Zeng X (2014) Methane–oxygen electrochemical coupling in an ionic liquid: a robust sensor for simultaneous quantification. Analyst, 139, 5140–5147
203. Ohsaka T, Alam MT, Islam MM, Okajima T (2007) Measurements of differential capacitance in room temperature ionic liquid at mercury, glassy carbon and gold electrode interfaces. Electrochem Commun 9(9):2370–2374. doi:10.1016/j.elecom.2007.07.009
204. Xiao CH, Rehman A, Zeng XQ (2012) Dynamics of redox processes in ionic liquids and their interplay for discriminative electrochemical sensing. Anal Chem 84(3):1416–1424. doi:10.1021/ac2024798
205. Schienle M, Paulus C, Frey A, Hofmann F, Holzapfl B, Schindler-Bauer P, Thewes R (2004) A fully electronic DNA sensor with 128 positions and in-pixel A/D conversion. J Solid-State Circuits 39(12):2438–2445
206. Zhu X, Ahn CH (2006) On-chip electrochemical analysis system using nanoelectrodes and bioelectronic CMOS chip. IEEE Sensors J 6(5):1280–1286

207. Jin X, Huang Y, Mason A, Zeng X (2009) Multichannel monolithic quartz crystal microbalance gas sensor array. Anal Chem 81(2):595–603
208. Li L, Liu X, Qureshi WA, Mason AJ (2011) CMOS amperometric instrumentation and packaging for biosensor array applications. IEEE Trans Biomed Circuits Syst 5(5):439–448
209. Trombly N, Mason A (2008) Post-CMOS electrode formation and isolation for on-chip temperature-controlled electrochemical sensors. IET Electron Lett 44(1):29–30
210. Yang C, Huang Y, Hassler BL, Worden RM, Mason AJ (2009) Amperometric electrochemical microsystem for a miniaturized protein biosensor array. IEEE Trans Biomed Circuits Syst 3(3):160–168
211. Niedziolka J, Rozniecka E, Stafiej J, Sirieix-Plenet J, Gaillon L, di Caprio D, Opallo M (2005) Ion transfer processes at ionic liquid based redox active drop deposited on an electrode surface. Chem Commun 23:2954–2956. doi:10.1039/b502194d
212. Wadhawan JD, Schröder U, Neudeck A, Wilkins SJ, Compton RG, Marken F, Consorti CS, de Souza RF, Dupont J (2000) Ionic liquid modified electrodes. Unusual partitioning and diffusion effects of Fe(CN)64–/3– in droplet and thin layer deposits of 1-methyl-3-(2,6-(S)-dimethylocten-2-yl)-imidazolium tetrafluoroborate. J Electroanal Chem 493(1–2):75–83. doi:10.1016/S0022-0728(00)00308-9
213. Yu P, Lin Y, Xiang L, Su L, Zhang J, Mao L (2005) Molecular films of water-miscible ionic liquids formed on glassy carbon electrodes: characterization and electrochemical applications. Langmuir 21(20):9000–9006. doi:10.1021/la051089v
214. Ng SR, Guo CX, Li CM (2011) Highly sensitive nitric oxide sensing using three-dimensional graphene/ionic liquid nanocomposite. Electroanalysis 23(2):442–448. doi:10.1002/elan.201000344
215. Lu D, Shomali N, Shen A (2010) Task specific ionic liquid for direct electrochemistry of metal oxides. Electrochem Commun 12(9):1214–1217. doi:10.1016/j.elecom.2010.06.022
216. Liang C, Yuan C-Y, Warmack RJ, Barnes CE, Dai S (2002) Ionic liquids: a new class of sensing materials for detection of organic vapors based on the use of a quartz crystal microbalance. Anal Chem 74(9):2172–2176. doi:10.1021/ac011007h
217. Yu L, Garcia D, Rex RB, Zeng XQ (2005) Ionic liquid high temperature gas sensors. Chem Commun 17:2277–2279
218. Goubaidoulline I, Vidrich G, Johannsmann D (2004) Organic vapor sensing with ionic liquids entrapped in alumina nanopores on quartz crystal resonators. Anal Chem 77(2):615–619. doi:10.1021/ac048436a
219. Jin X, Yu L, Zeng X (2008) Enhancing the sensitivity of ionic liquid sensors for methane detection with polyaniline template. Sens Actuators B 133(2):526–532. doi:10.1016/j.snb.2008.03.022
220. Yu L, Jin X, Zeng X (2008) Methane interactions with polyaniline/butylmethylimidazolium camphorsulfonate ionic liquid composite. Langmuir 24(20):11631–11636. doi:10.1021/la8018327
221. Zeng X, Li X, Xing L, Liu X, Luo S, Wei W, Kong B, Li Y (2009) Electrodeposition of chitosan–ionic liquid–glucose oxidase biocomposite onto nano-gold electrode for amperometric glucose sensing. Biosens Bioelectron 24(9):2898–2903. doi:10.1016/j.bios.2009.02.027
222. Xi F, Liu L, Wu Q, Lin X (2008) One-step construction of biosensor based on chitosan–ionic liquid–horseradish peroxidase biocomposite formed by electrodeposition. Biosensors and Bioelectronics 24 (1):29-34. doi:10.1016/j.bios.2008.03.023
223. Gao R, Zheng J (2009) Amine-terminated ionic liquid functionalized carbon nanotube-gold nanoparticles for investigating the direct electron transfer of glucose oxidase. Electrochem Commun 11(3):608–611. doi:10.1016/j.elecom.2008.12.060
224. Liu Y, Shi L, Wang M, Li Z, Liu H, Li J (2005) A novel room temperature ionic liquid sol-gel matrix for amperometric biosensor application. Green Chem 7(9):655–658. doi:10.1039/b504689k
225. Wu X, Zhao B, Wu P, Zhang H, Cai C (2009) Effects of ionic liquids on enzymatic catalysis of the glucose oxidase toward the oxidation of glucose. J Phys Chem B 113(40):13365–13373. doi:10.1021/jp905632k

226. Jin X, Yu L, Garcia D, Ren RX, Zeng X (2006) Ionic liquid high-temperature gas sensor array. Anal Chem 78(19):6980–6989. doi:10.1021/ac0608669
227. Oter O, Ertekin K, Topkaya D, Alp S (2006) Emission-based optical carbon dioxide sensing with HPTS in green chemistry reagents: room-temperature ionic liquids. Anal Bioanal Chem 386(5):1225–1234. doi:10.1007/s00216-006-0659-z
228. Oter O, Ertekin K, Derinkuyu S (2008) Ratiometric sensing of CO2 in ionic liquid modified ethyl cellulose matrix. Talanta 76(3):557–563. doi:10.1016/j.talanta.2008.03.047
229. Kan T, Aoki H, Binh-Khiem N, Matsumoto K, Shimoyama I (2013) Ratiometric optical temperature sensor using two fluorescent dyes dissolved in an ionic liquid encapsulated by parylene film. Sensors 13(4):4138–4145
230. Forzani ES, Lu D, Leright MJ, Aguilar AD, Tsow F, Iglesias RA, Zhang Q, Lu J, Li J, Tao N (2009) A hybrid electrochemical – colorimetric sensing platform for detection of explosives. J Am Chem Soc 131(4):1390–1391. doi:10.1021/ja809104h
231. Guo CX, Lu ZS, Lei Y, Li CM (2010) Ionic liquid-graphene composite for ultratrace explosive trinitrotoluene detection. Electrochem Commun 12(9):1237–1240. doi:10.1016/j.elecom.2010.06.028

Angel A.J. Torriero
Editor

Electrochemistry in Ionic Liquids

Volume 1: Fundamentals

Springer

Editor
Angel A.J. Torriero
Centre for Chemistry and Biotechnology
School of Life and Environmental Sciences
Faculty of Science, Engineering and Built Environment
Deakin University, Melbourne Burwood Campus
Burwood, VIC, Australia

ISBN 978-3-319-13484-0 ISBN 978-3-319-13485-7 (eBook)
DOI 10.1007/978-3-319-13485-7

Library of Congress Control Number: 2015937618

Springer Cham Heidelberg New York Dordrecht London

Printed on acid-free paper

Springer International Publishing AG Switzerland is part of Springer Science+Business Media (www.springer.com)